



universität
wien

MASTERARBEIT / MASTER'S THESIS

Titel der Masterarbeit / Title of the Master's Thesis

„Norm conserving pseudo-potentials
for the Coulomb interaction“

verfasst von / submitted by

Stefan Riemelmoser, BSc

angestrebter akademischer Grad / in partial fulfilment of the requirements for the degree of
Master of Science (MSc)

Wien, 2017 / Vienna 2017

Studienkennzahl lt. Studienblatt /
degree programme code as it appears on
the student record sheet:

A 066 876

Studienrichtung lt. Studienblatt /
degree programme as it appears on
the student record sheet:

Masterstudium Physik

Betreut von / Supervisor:

Univ.-Prof. Dipl.-Ing. Dr. Georg Kresse

Acknowledgments

My sincere thanks go to my supervisor Georg Kresse for fruitful discussions and all around great support during my thesis. Also, I want to thank Tobias Schäfer for advise and guidance through the VASP code. Furthermore, thanks to all the nice colleagues at the CMP group for providing helpful advice and a great working environment. Last but not least, I want to thank my parents for continuing moral and financial support.

Abstract

In recent years, there has been a continuing surge of interest in more and more accurate descriptions for the correlation energy in *ab initio* electronic structure calculations. The correlation energies obtained from second order Møller-Plesset perturbation theory and the random phase approximation both converge very slowly w.r.t. the cutoff energy. This is caused by the singularity of the Coulomb potential which determines the $1/q^2$ high frequency behavior in Fourier space. In this work, we investigate whether the convergence can be improved by replacing the repulsive Coulomb potential by a norm conserving pseudo-potential. In the pseudization of the electron-electron interaction, we follow a revised version of the RRKJ method. We study the convergence of the pseudized correlation energies and the errors due to the pseudization for the case of the homogeneous electron gas.

Zusammenfassung

In den letzten Jahren gab es ein stetig wachsendes Interesse an einer immer genaueren Beschreibung von Korrelations-Energien im Zuge von *ab initio* Berechnungen elektronischer Strukturen. Die Korrelations-Energien innerhalb von Møller-Plesset Störungstheorie zweiter Ordnung und der sogenannten random phase approximation konvergieren nur langsam in Bezug auf die Basissätze, die wiederum durch eine Energie ("cutoff energy") parametrisiert werden. Der Grund liegt in der Singularität des Coulomb Potentials, welche ein $1/q^2$ Hochfrequenz-Verhalten im Fourierraum verursacht. In dieser Arbeit untersuchen wir, ob die Konvergenz verbessert werden kann, indem das repulsive Coulomb Potential durch ein normerhaltendes Pseudopotential ersetzt wird. Die Pseudisierung der Elektron-Elektron Wechselwirkung führen wir mithilfe einer verbesserten Version der RRKJ-Methode durch. Wir untersuchen die Konvergenz der pseudisierten Korrelations-Energien und die Fehler, die durch die Pseudisierung gemacht werden für das homogene Elektronengases.

Contents

| | | |
|----------|---|-----------|
| 1 | Introduction | 1 |
| 1.1 | Organization of this work | 2 |
| 2 | The theory of pseudo-potentials | 3 |
| 2.1 | The Bloch theorem | 3 |
| 2.1.1 | Proof | 4 |
| 2.1.2 | Structure factor | 6 |
| 2.2 | Nearly free electron approximation | 7 |
| 2.2.1 | Non-degenerate case | 7 |
| 2.2.2 | Degenerate case | 8 |
| 2.2.3 | Problems of the NFE approximation | 9 |
| 2.3 | Augmented plane wave method | 10 |
| 2.4 | Orthogonalized plane wave method | 12 |
| 2.4.1 | The PKA pseudo-potential transformation | 14 |
| 2.4.2 | Non-local operators | 16 |
| 2.5 | Definition of pseudo-potentials | 17 |
| 2.6 | Norm conserving pseudo-potentials | 18 |
| 2.6.1 | Norm-conservation condition for scattering states | 20 |
| 2.6.2 | The Topp-Hopfield pseudo-potential | 20 |
| 2.6.3 | The HSC pseudo-potential | 21 |
| 2.6.4 | The Kerker method | 21 |
| 2.7 | The RRKJ pseudo-potential | 22 |
| 2.7.1 | Revised RRKJ method | 23 |
| 3 | Møller-Plesset perturbation theory | 24 |
| 3.1 | Hartree-Fock approximation | 24 |
| 3.1.1 | Koopmans' theorem | 26 |
| 3.2 | MP2 approximation | 27 |
| 3.3 | Spin restriction | 29 |
| 3.4 | MP2 for periodic systems | 30 |
| 3.5 | Goldstone diagrams | 32 |
| 3.5.1 | Linked-cluster theorem | 33 |
| 3.6 | Random phase approximation | 33 |
| 4 | Pseudization of the $e^- - e^-$ interaction | 38 |
| 4.1 | Two-particle interaction | 38 |
| 4.2 | Numerov algorithm | 39 |
| 4.2.1 | Boundary conditions | 40 |
| 4.3 | Construction of the pseudo-potential | 40 |
| 4.4 | Analysis of the scaling behavior | 41 |
| 4.5 | Fourier space representation | 42 |
| 4.5.1 | Local approximation | 46 |
| 4.5.2 | Analysis of the asymptotic behavior | 48 |

| | | |
|----------|--|-----------|
| 4.6 | Maximum reference energy rule | 51 |
| 5 | Correlation energies for Jellium | 55 |
| 5.1 | Simple cubic lattice | 56 |
| 5.2 | Electron - nucleus scattering | 56 |
| 5.3 | Pseudization of MP perturbation theory | 57 |
| 5.3.1 | Hartree-Fock groundstate energies | 59 |
| 5.3.2 | MP2 correlation energies | 61 |
| 5.4 | Pseudization of ACFDT-RPA | 64 |
| 6 | Summary and conclusion | 67 |
| A | Spherical Bessel functions | 68 |
| A.1 | Spherical Bessel transform | 69 |
| B | Scattering theory | 71 |
| B.1 | Finite range potentials | 71 |
| B.1.1 | Phase shifts | 73 |
| B.1.2 | Born approximation | 74 |
| B.1.3 | Scattering approach to pseudo-potentials | 76 |
| B.2 | Coulomb potential | 76 |
| C | Hartree-Fock approximation | 78 |
| C.1 | Slater-Condon rules | 78 |
| C.2 | Derivation of the Hartree-Fock equations | 79 |
| C.3 | Brillouin's theorem | 81 |
| | Bibliography | 83 |

Chapter 1

Introduction

Since the 1930s, the electron-nucleus interaction in electronic structure calculations has been successfully described via the pseudo-potential method. Formally, this method can be expressed as a transformation of the Schrödinger equation that changes the potential and the wave function inside a core region, but retains the eigenvalues and the scattering properties of the potential. The fact that the transformation is not unique can be used to give the “pseudo-potential” any convenient shape. This fact can be used to achieve that both the pseudo-potential and the “pseudo wave function” are smoother than their original counterparts. Therefore, they can be expanded in a smaller number of plane waves, hence improving the convergence in Fourier space. In the 1970s, it was discovered that if the pseudo charge density is distributed correctly between the core and the outer region, the energy range for which the pseudo-potential is correct can be greatly improved. Since then, the pseudo-potential method in combination with density functional theory (DFT) has enjoyed high popularity and is nowadays a prevalent electronic structure method.

The pseudo-potential concept goes beyond the description of electron-nucleus interactions and can be applied more generally. Prendergast *et al.* [1] and Lloyd-Williams *et al.* [2] have used pseudo-potentials to describe the electron-electron interaction within diffusion Monte Carlo (DMC) and truncated Configuration Interaction (CI) calculations.

In the present work, we apply this concept to obtain correlation energies via second order Møller-Plesset perturbation theory (MP2) and the random phase approximation (RPA). In both cases, the singular nature of the Coulomb interaction causes very slow convergence of the correlation energies w.r.t. the energy cutoff. Whereas the Coulomb potential falls off slowly as $1/q^2$, the pseudo-potentials cut off at some point in Fourier space. The fact that the spectrum of the repulsive Coulomb potential is continuous suggests that the pseudo-potentials should be norm conserving. In the construction of our pseudo-potentials we follow a method developed by Rappe *et al.* [3] (RRKJ) and improved on by Kresse [4]. The pseudo wave function is expanded in spherical Bessel functions with suitable boundary conditions. Thereafter, the pseudo-potential is obtained through inversion of the Schrödinger equation.

1.1 Organization of this work

The thesis is structured in a theoretical and practical part. In chapter 2, we discuss how studies of the nearly free electron approximation (NFE) laid the foundation for the development of pseudo-potential theory. We examine early pseudo-potential methods to explore general themes and thereafter discuss the proper theoretical frame work as developed by Phillips and others [5][6]. We derive the norm conservation identity and discuss the construction of various norm conserving pseudo-potentials. In chapter 3, we provide the theoretical background for the MP2 and RPA theories. We discuss the Hartree-Fock approximation for the electronic ground state and show how we can obtain correlation energies through Møller-Plesset perturbation theory. We derive the respective expressions for the correlation energies within MP2 and RPA.

In chapter 4, we describe the construction of the pseudo-potentials via the revised RKKJ method in detail. We discuss the choice of the reference energy at which the pseudization is performed and the representation of the pseudo-potentials in Fourier space. In chapter 5, we show how the electron-electron interaction can be pseudized within Møller-Plesset perturbation theory. We discuss the implementation of the MP2 and RPA expressions in the Vienna Ab-Initio Simulation Package (VASP) and calculate correlation energies for the homogeneous electron gas. We compare the converge of the pseudized correlation energies and Coulomb correlation energies and examine the errors that stem from the pseudization.

Appendix A briefly discusses properties of the spherical Bessel functions that we use in the construction of our pseudo-potentials. In appendix B, we provide a short summary of basic scattering theory and apply its concepts to gain further insight on the pseudo-potential method. Finally, in appendix C we discuss theorems for the Hartree-Fock approximation that we use in chapter 3.

Chapter 2

The theory of pseudo-potentials

The Bloch theorem, formulated by Bloch [7] at the end of the 1920s, is a key stone in the development of modern solid state physics and a starting point for the development of many electronic structure methods. In its derivation and the subsequent discussion of the nearly free electron approximation we will follow closely Ashcroft and Mermin [8, chapters 8-9].

2.1 The Bloch theorem

We consider independent electrons in a periodic solid, i.e. the electrons each obey a time independent one-particle Schrödinger equation

$$H\psi = \left(-\frac{1}{2}\nabla^2 + V(\mathbf{r}) \right) \psi = E\psi, \quad (2.1)$$

where we have introduced Hartree atomic units where $m_e = \hbar = e = 1$, which we will use throughout the thesis. The effective one-electron potential V has the symmetry of the solid

$$V(\mathbf{r} + \mathbf{R}) = V(\mathbf{r}), \quad (2.2)$$

where \mathbf{R} is a lattice vector of the underlying Bravais lattice. The Bloch theorem states that the eigenstates ψ can be written as a product of a plane wave and a function that has the periodicity of the lattice

$$\begin{aligned} \psi_{n\mathbf{k}}(\mathbf{r}) &= e^{i\mathbf{k}\cdot\mathbf{r}} u_{n\mathbf{k}}(\mathbf{r}) \\ u_{n\mathbf{k}}(\mathbf{r}) &= u_{n\mathbf{k}}(\mathbf{r} + \mathbf{R}), \end{aligned} \quad (2.3)$$

where n is a band index.

2.1.1 Proof

Since we are interested in the bulk of the solid only, we are free to impose convenient boundary conditions. A usual choice are the Born-von Karman conditions

$$\psi(\mathbf{r} + N_i \mathbf{a}_i) = \psi(\mathbf{r}), \quad i = 1, 2, 3 \quad (2.4)$$

where the a_i are primitive lattice vectors, the N_i are integers and $N_{\text{cell}} = N_1 N_2 N_3$ is the number of unit cells in the solid. To describe a proper 3D bulk, the N_i should all be large numbers of order $\mathcal{O}(N_{\text{cell}}^{1/3})$. We expand the wave function in a plane wave basis

$$\psi(\mathbf{r}) = \sum_{\mathbf{q}} c_{\mathbf{q}} e^{i\mathbf{q}\cdot\mathbf{r}}, \quad (2.5)$$

where summation is over all \mathbf{q} that are compatible with the boundary condition, i.e.

$$\mathbf{q} = \sum_{i=1}^3 \frac{m_i}{N_i} \mathbf{b}_i, \quad m_i \text{ integer}, \quad (2.6)$$

as one can see by inserting equation (2.4) into the expansion (2.5). The \mathbf{b}_i are the primitive reciprocal lattice vectors with normalization

$$a_i b_j = 2\pi \delta_{ij}. \quad (2.7)$$

Since the potential $V(r)$ has the symmetry of the lattice (2.2), only reciprocal lattice vectors \mathbf{G} can contribute in its Fourier expansion

$$\begin{aligned} V(\mathbf{r}) &= \sum_{\mathbf{G}} V_{\mathbf{G}} e^{i\mathbf{G}\cdot\mathbf{r}} \\ V_{\mathbf{G}} &= \frac{1}{\Omega} \int_{\Omega} d\mathbf{r} e^{-i\mathbf{G}\cdot\mathbf{r}} V(\mathbf{r}), \end{aligned} \quad (2.8)$$

where Ω is the lattice volume. By inserting both expansions into the Schrödinger equation (2.1), we obtain

$$\begin{aligned} \sum_{\mathbf{q}} -\frac{1}{2} \nabla^2 c_{\mathbf{q}} e^{i\mathbf{q}\cdot\mathbf{r}} + \sum_{\mathbf{G}} V_{\mathbf{G}} e^{i\mathbf{G}\cdot\mathbf{r}} \sum_{\mathbf{q}} c_{\mathbf{q}} e^{i\mathbf{q}\cdot\mathbf{r}} &= E \sum_{\mathbf{q}} c_{\mathbf{q}} e^{i\mathbf{q}\cdot\mathbf{r}} \\ \sum_{\mathbf{q}} \left(\frac{1}{2} q^2 - E \right) c_{\mathbf{q}} e^{i\mathbf{q}\cdot\mathbf{r}} + \sum_{\mathbf{G}, \mathbf{q}} V_{\mathbf{G}} c_{\mathbf{q}} e^{i(\mathbf{G}+\mathbf{q})\cdot\mathbf{r}} &= 0 \\ \sum_{\mathbf{q}} e^{i\mathbf{q}\cdot\mathbf{r}} \left[\left(\frac{1}{2} q^2 - E \right) c_{\mathbf{q}} + \sum_{\mathbf{G}'} V_{\mathbf{G}'} c_{\mathbf{q}-\mathbf{G}'} \right] &= 0. \end{aligned} \quad (2.9)$$

In the last step, we have renamed \mathbf{G} to \mathbf{G}' and used that summation over \mathbf{q} and $\mathbf{q}+\mathbf{G}'$ are equivalent, since \mathbf{G}' is a reciprocal lattice vector and \mathbf{q} obeys equation (2.6). Since plane waves with wave vectors of the form (2.6) are orthonormal [see 8, Appendix D]

$$\langle e^{i(\mathbf{k}-\mathbf{G})\cdot\mathbf{r}}, e^{i(\mathbf{k}-\mathbf{G}')\cdot\mathbf{r}} \rangle := \frac{1}{\Omega} \int_{\Omega} d\mathbf{r} e^{i(\mathbf{k}-\mathbf{G})\cdot\mathbf{r}*} e^{i(\mathbf{k}-\mathbf{G}')\cdot\mathbf{r}} = \delta_{\mathbf{G}\mathbf{G}'} \quad (2.10)$$

we obtain a system of linear equations for the coefficients $c_{\mathbf{q}}$

$$\left(\frac{1}{2}q^2 - E \right) c_{\mathbf{q}} + \sum_{\mathbf{G}'} V_{\mathbf{G}'} c_{\mathbf{q}-\mathbf{G}'} = 0, \quad (2.11)$$

We rewrite this equation as

$$\left(\frac{1}{2}(\mathbf{k} - \mathbf{G})^2 - E \right) c_{\mathbf{k}-\mathbf{G}} + \sum_{\mathbf{G}'} V_{\mathbf{G}'-\mathbf{G}} c_{\mathbf{k}-\mathbf{G}'} = 0, \quad (2.12)$$

by introducing $\mathbf{k}=\mathbf{q}+\mathbf{G}$ with \mathbf{G} chosen such that \mathbf{k} is in the first Brillouin zone and thereafter replacing \mathbf{G}' by $\mathbf{G}' - \mathbf{G}$. From this expression we find that the problem decays into N_{cell} independent problems for the possible values of \mathbf{k} , where the $c_{\mathbf{k}}$ for each \mathbf{k} couple only with wave vectors that differ from them by a reciprocal lattice vector, thus the wave function must be of the form

$$\psi_{\mathbf{k}} = \sum_{\mathbf{k}} c_{\mathbf{k}-\mathbf{G}} e^{i(\mathbf{k}-\mathbf{G})\cdot\mathbf{r}} = e^{i\mathbf{k}\cdot\mathbf{r}} \left(\sum_{\mathbf{k}} c_{\mathbf{k}-\mathbf{G}} e^{-i\mathbf{G}\cdot\mathbf{r}} \right), \quad (2.13)$$

which proves the Bloch theorem (2.3) since the term in the brackets is translation invariant.

There are infinitely many solutions to equation (2.12) that are labeled by the band index n . The Bloch theorem can also be stated as

$$\psi(\mathbf{r} + \mathbf{R}) = e^{i\mathbf{k}\cdot\mathbf{R}} \psi(\mathbf{r}), \quad (2.14)$$

which follows immediately from (2.3). On the other side, the original theorem can be recovered by proving that it implies the translation invariance of $u(\mathbf{r})$

$$\begin{aligned} \psi(\mathbf{r}) &= e^{i\mathbf{k}\cdot\mathbf{r}} u(\mathbf{r}) \\ \psi(\mathbf{r} + \mathbf{R}) &= e^{i\mathbf{k}\cdot(\mathbf{r}+\mathbf{R})} u(\mathbf{r} + \mathbf{R}) = e^{i\mathbf{k}\cdot\mathbf{R}} \psi(\mathbf{r}) \\ &\Rightarrow u(\mathbf{r} + \mathbf{R}) = u(\mathbf{r}). \end{aligned} \quad (2.15)$$

Ashcroft and Mermin also provide an elegant alternative proof that uses only fundamental quantum mechanics [see 8, pp. 167-169].

2.1.2 Structure factor

Let us consider total potentials V that can be written as a superposition of atomic potentials v

$$V(\mathbf{r}) = \sum_n v(\mathbf{r} - \mathbf{R}_n), \quad (2.16)$$

where the R_n are atomic centers (not necessarily lattice vectors). We can decompose the matrix elements $V_{\mathbf{G}\mathbf{G}'}$ into a structure factor and a form factor

$$\begin{aligned} V_{\mathbf{G}\mathbf{G}'} &= \frac{1}{\Omega} \int_{\Omega} d\mathbf{r} e^{-i(\mathbf{k}-\mathbf{G})\cdot\mathbf{r}} \sum_n v(\mathbf{r} - \mathbf{R}_n) e^{i(\mathbf{k}-\mathbf{G}')\cdot\mathbf{r}} \\ &= \sum_n e^{-i(\mathbf{k}-\mathbf{G})\cdot\mathbf{R}_n} e^{i(\mathbf{k}-\mathbf{G}')\cdot\mathbf{R}_n} \\ &\quad \times \frac{1}{\Omega} \int_{\Omega} e^{-i(\mathbf{k}-\mathbf{G})\cdot(\mathbf{r}-\mathbf{R}_n)} v(\mathbf{r} - \mathbf{R}_n) e^{i(\mathbf{k}-\mathbf{G}')\cdot(\mathbf{r}-\mathbf{R}_n)} \\ &= S(\mathbf{G} - \mathbf{G}') \times v_{\mathbf{G}\mathbf{G}'}, \end{aligned} \quad (2.17)$$

where S is the structure factor

$$S(\mathbf{G} - \mathbf{G}') := \frac{1}{N_{\text{cell}}} \sum_n e^{i(\mathbf{G}-\mathbf{G}')\cdot\mathbf{R}_n}, \quad (2.18)$$

and $v_{\mathbf{G}\mathbf{G}'}$ the form factor

$$\begin{aligned} v_{\mathbf{G}\mathbf{G}'} &:= \frac{1}{\Omega_{\text{cell}}} \int_{\mathbb{R}^3} d\mathbf{r} e^{-i(\mathbf{k}-\mathbf{G})\cdot\mathbf{r}} v(r) e^{i(\mathbf{k}-\mathbf{G}')\cdot\mathbf{r}} \\ &= \frac{1}{\Omega_{\text{cell}}} \int_{\mathbb{R}^3} d\mathbf{r} e^{-i(\mathbf{G}'-\mathbf{G})\cdot\mathbf{r}} v(r), \end{aligned} \quad (2.19)$$

where the second of these expressions is valid only if the potential is “local”, see section 2.4.2. The normalizations are distributed such as to achieve scale invariance, and the integration domain in equation (2.19) is usually extended from Ω to the entire space [9, chapter 2]. For an ideal lattice with one atom per unit cell the \mathbf{R}_n are lattice vectors, we can show that the structure factor vanishes unless its argument is a reciprocal lattice vector

$$\begin{aligned} S(\mathbf{k} - \mathbf{G}) &= \frac{1}{N_{\text{cell}}} \sum_{\mathbf{R}} e^{i(\mathbf{k}-\mathbf{G})\cdot\mathbf{R}} = \frac{1}{N_{\text{cell}}} \sum_{\mathbf{R}} e^{i\mathbf{k}\cdot\mathbf{R}} \\ &\stackrel{!}{=} \frac{1}{N_{\text{cell}}} \sum_{\mathbf{R}} e^{i\mathbf{k}\cdot(\mathbf{R}+\mathbf{R}_0)} = \frac{1}{N_{\text{cell}}} e^{i\mathbf{k}\cdot\mathbf{R}_0} \sum_{\mathbf{R}} e^{i\mathbf{k}\cdot\mathbf{R}} \\ \Rightarrow S(\mathbf{k} - \mathbf{G}) &= \delta_{\mathbf{k}\mathbf{0}}, \end{aligned} \quad (2.20)$$

where we have shifted all lattice vectors by an arbitrary lattice vector \mathbf{R}_0 in the second step [8, appendix F].

2.2 Nearly free electron approximation

The starting point for the nearly free electron (NFE) approximation is the Fourier space representation of the Schrödinger equation (2.12). We consider the limiting case of a weak potential and treat the electron energies as a perturbation series on free electron states

$$\begin{aligned}\Psi_{\mathbf{k}}^{(0)} &\propto e^{i\mathbf{k}\cdot\mathbf{r}} \\ E_{\mathbf{k}}^{(0)} &= \frac{1}{2}k^2.\end{aligned}\tag{2.21}$$

2.2.1 Non-degenerate case

For \mathbf{k} far from a Brillouin border, the free energy states are non-degenerate in the sense of

$$|E_{\mathbf{k}}^{(0)} - E_{\mathbf{k}-\mathbf{G}}^{(0)}| \gg V \quad \forall \mathbf{G} \neq \mathbf{0},\tag{2.22}$$

where V is a typical Fourier component of the potential. We use Schrödinger equation (2.12) to express the expansion coefficients $c_{\mathbf{k}-\mathbf{G}}$. For the $\mathbf{G} = \mathbf{0}$ coefficient, we obtain

$$(E - E_{\mathbf{k}}^{(0)})c_{\mathbf{k}} = \sum_{\mathbf{G}'} V_{\mathbf{G}'} c_{\mathbf{k}-\mathbf{G}'} = \sum_{\mathbf{G} \neq \mathbf{0}} V_{\mathbf{G}} c_{\mathbf{k}-\mathbf{G}},\tag{2.23}$$

where we have shifted the energy by V_0 and changed the summation index. For the other coefficients, the Schrödinger equation yields

$$\begin{aligned}c_{\mathbf{k}-\mathbf{G}} &= \frac{V_{-\mathbf{G}} c_{\mathbf{k}}}{E - E_{\mathbf{k}-\mathbf{G}}^{(0)}} + \sum_{\mathbf{G}' \neq \mathbf{0}} \frac{V_{\mathbf{G}'-\mathbf{G}} c_{\mathbf{k}-\mathbf{G}'}}{E - E_{\mathbf{k}-\mathbf{G}}^{(0)}} \\ &= \frac{V_{-\mathbf{G}} c_{\mathbf{k}}}{E - E_{\mathbf{k}-\mathbf{G}}^{(0)}} + \mathcal{O}(V^2),\end{aligned}\tag{2.24}$$

where we have used that the terms with $\mathbf{G}' \neq \mathbf{0}$ are of higher order as they contain coefficients that vanish as $V \rightarrow 0$. By inserting this result in equation (2.23), we find that the leading correction for non-degenerate energy states is of second order in V

$$\begin{aligned}(E - E_{\mathbf{k}}^{(0)})c_{\mathbf{k}} &= \sum_{\mathbf{G} \neq \mathbf{0}} \frac{V_{\mathbf{G}} V_{-\mathbf{G}}}{E - E_{\mathbf{k}-\mathbf{G}}^{(0)}} c_{\mathbf{k}} + \mathcal{O}(V^3) \\ E &= E_{\mathbf{k}}^{(0)} + \sum_{\mathbf{G} \neq \mathbf{0}} \frac{|V_{\mathbf{G}}|^2}{E_{\mathbf{k}}^{(0)} - E_{\mathbf{k}-\mathbf{G}}^{(0)}} + \mathcal{O}(V^3).\end{aligned}\tag{2.25}$$

In the second step we have used $V_{-\mathbf{G}} = V_{\mathbf{G}^*}$ (see equation (2.8)) and replaced E by $E_{\mathbf{k}}^{(0)}$ in the denominator to get an explicit expression for E (which is valid within our approximation). By inspecting the sign of the denominator,

we find that that non-degenerate bands repel each other under perturbation from a weak potential.

2.2.2 Degenerate case

For \mathbf{k} near a Brillouin border where we have mixing from m reciprocal lattice vectors \mathbf{G}_i (including $\mathbf{0}$), the energy states are degenerate in the sense of

$$|E_{\mathbf{k}-\mathbf{G}}^{(0)} - E_{\mathbf{k}-\mathbf{G}_i}^{(0)}| \gg V \quad \forall \mathbf{G} \notin \{\mathbf{G}_i\}, \quad (2.26)$$

compare equation (2.22). The free electron solution for the degenerate case, to which the perturbation series must reduce for $V \rightarrow 0$, is now a linear combination of plane waves

$$\psi_{\mathbf{k}}^{(0)}(\mathbf{r}) = \sum_{\mathbf{G}_i} c_{\mathbf{k}-\mathbf{G}_i} e^{i(\mathbf{k}-\mathbf{G}_i)\cdot\mathbf{r}}. \quad (2.27)$$

We proceed analog to the non-degenerate case and distinguish between components $c_{\mathbf{k}-\mathbf{G}}$ with $\mathbf{G} = \mathbf{G}_i$ and $\mathbf{G} \neq \mathbf{G}_i$ to obtain

$$\begin{aligned} (E - E_{\mathbf{k}-\mathbf{G}_i}^{(0)})c_{\mathbf{k}-\mathbf{G}_i} &= \sum_{j=1}^m V_{\mathbf{G}_j-\mathbf{G}_i} c_{\mathbf{k}-\mathbf{G}_j} \\ &+ \sum_{j=1}^m \left(\sum_{\mathbf{G} \notin \{\mathbf{G}_i\}} \frac{V_{\mathbf{G}-\mathbf{G}_i} V_{\mathbf{G}_j-\mathbf{G}}}{E - E_{\mathbf{k}-\mathbf{G}}^{(0)}} \right) c_{\mathbf{k}-\mathbf{G}_j} + \mathcal{O}(V^3). \end{aligned} \quad (2.28)$$

This system of coupled equations for the $c_{\mathbf{k}-\mathbf{G}_i}$ reduces to the non-degenerate result (equation (2.25)) for $m = 1$. The leading corrections to the degenerate energy states are first order in V

$$(E - E_{\mathbf{k}-\mathbf{G}_i}^{(0)})c_{\mathbf{k}-\mathbf{G}_i} = \sum_{j=1}^m V_{\mathbf{G}_j-\mathbf{G}_i} c_{\mathbf{k}-\mathbf{G}_j} + \mathcal{O}(V^2), \quad (2.29)$$

meaning that the effect of a weak potential on the free electron bands is significant near a Brillouin border only. It is instructive to consider the simple case of $m = 2$, i.e.

$$\begin{aligned} (E - E_{\mathbf{k}}^{(0)})c_{\mathbf{k}} &= V_{\mathbf{G}} c_{\mathbf{k}-\mathbf{G}} \\ (E - E_{\mathbf{k}}^{(0)})c_{\mathbf{k}-\mathbf{G}} &= V_{-\mathbf{G}} c_{\mathbf{k}}. \end{aligned} \quad (2.30)$$

Solutions exist if the secular determinant vanishes

$$\begin{vmatrix} E - E_{\mathbf{k}}^{(0)} & -V_{\mathbf{G}} \\ -V_{-\mathbf{G}} & E - E_{\mathbf{k}-\mathbf{G}}^{(0)} \end{vmatrix} = 0, \quad (2.31)$$

resulting in an energy gap of size $|2V_{\mathbf{G}}|$ at the Brillouin border. In general, we truncate the plane wave expansion after a cut-off E_{\max} and replace

$$\sum_{\mathbf{G}} \rightarrow \sum_{\mathbf{G}} \quad |\mathbf{k} - \mathbf{G}|^2 < 2E_{\max}. \quad (2.32)$$

This yields the NFE secular equation

$$\left| \left[\frac{1}{2}(\mathbf{k} - \mathbf{G})^2 - E \right] \delta_{\mathbf{G}\mathbf{G}'} + V_{\mathbf{G}\mathbf{G}'} \right| = 0, \quad (2.33)$$

which we can also write as

$$\begin{aligned} H\mathbf{c} &= E\mathbf{c} \\ H_{\mathbf{G}\mathbf{G}'} &= \langle e^{i(\mathbf{k}-\mathbf{G})\cdot\mathbf{r}} | (T + V) | e^{i(\mathbf{k}-\mathbf{G}')\cdot\mathbf{r}} \rangle. \end{aligned} \quad (2.34)$$

For the NFE approximation to be useful, the potential must be weak (i.e. it has a rapidly converging Fourier expansion) to ensure that the secular equation (2.33) is of manageable size. The development of the NFE approximation in the 1930s was crucial in the understanding of electronic band structures of metals and solids in general. X-ray experiments at that time showed that many materials, such as (sp)-bonded metals, possess valence bands that are NFE-like. Mott and Jones successfully applied the NFE approximation to treat metals and also nonmetals like diamond (see Heine and Weaire [10, pp. 252-255] and references cited therein).

2.2.3 Problems of the NFE approximation

It seems at first glance paradoxical that although the measured valence bands for metals and semiconductors have NFE form, the NFE approximation leads to a secular equation of unreasonably high dimension ($10^6 \times 10^6$ for aluminum) and to band gaps that are too large when applied to real atomic potentials (except H, He and to a lesser extent Li, Be) [11].

To resolve the paradox, we note that all atomic potentials beyond He possess tightly bound core states. The problem can be located at the atomic core: there, all atomic potentials that are “strong” in the aforementioned sense are dominated by the barely screened nuclear charge, leading to valence states that closely resemble outer atomic states. The corresponding wave functions are highly oscillatory, as they have to fulfill the orthogonality requirement. Both the strong nuclear potential and the oscillating wave functions need to be represented by many Fourier components, leading to a large secular equation [11]. Although a weak potential and the corresponding smooth wave function lead to an NFE-like band structure, the reverse conclusion does not hold.

Outside the core region, the potential is flat and unproblematic for the NFE approximation. By the end of the 1930s it was realized that this fact can be taken advantage of, if the wave function is properly modified in the core region. Such is the spirit of Slater’s augmented plane wave (APW) method

[see 12] and Herring's orthogonal plane wave (OPW) method [see 13]. We will discuss the APW and OPW methods mainly along the lines of Heine [11], Ziman [9, chapter 3] and Martin [14, chapters 11,16].

2.3 Augmented plane wave method

Motivated by the discussion above, we cut out spheres around each atom with sphere radius r_{cn} chosen such that we can assume the potential is spherically symmetric inside the spheres and constant in the interstitial regions (this is called "muffin-tin approximation", see figure 2.1).

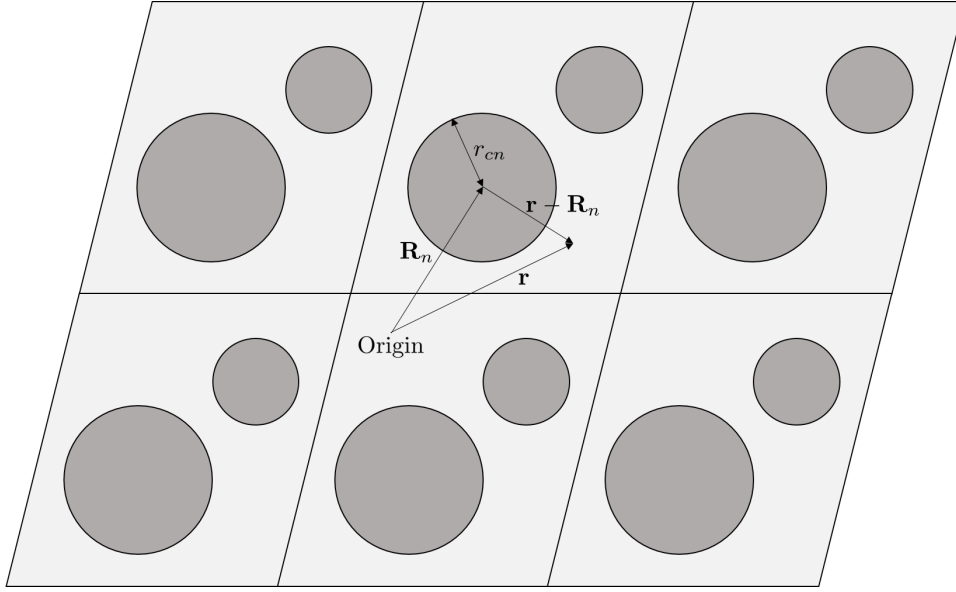


FIGURE 2.1: The units cells are divided into muffin-tin spheres and interstitial regions. The muffin-tin radii r_{cn} must be chosen small enough so as to prevent the spheres from intersecting.

Inside the spheres, the wave function can be expanded into spherical coordinates $|\mathbf{r} - \mathbf{R}_n|, \theta, \phi$ about each nucleus located at $\mathbf{r} = \mathbf{R}_n$

$$\psi(\mathbf{r}) = \sum_{l=0}^{\infty} \sum_{m=-l}^l C_l^m R_l(|\mathbf{r} - \mathbf{R}_n|) Y_l^m(\theta, \phi), \quad (2.35)$$

where the Y_l^m are spherical harmonics and the $R_l(r)$ obey the radial Schrödinger equation

$$\left[-\frac{1}{2r^2} \frac{d}{dr} \left(r^2 \frac{d}{dr} \right) + \frac{l(l+1)}{2r^2} + V(r) \right] R_l(r) = ER_l(r). \quad (2.36)$$

In the interstitial regions, the solutions are plane waves. Hence, we construct an "augmented plane wave" by matching equation (2.35) to a single plane wave at the sphere surfaces. From the spherical harmonic expansion of a plane wave [see 15, p. 421]

$$e^{i\mathbf{k}\cdot\mathbf{r}} = 4\pi e^{i\mathbf{k}\cdot\mathbf{R}_n} \sum_{l=0}^{\infty} \sum_{m=-l}^l i^l j_l(k|\mathbf{r} - \mathbf{R}_n|) Y_l^{m*}(\theta_k, \phi_k) Y_l^m(\theta, \phi), \quad (2.37)$$

where the j_l are spherical Bessel functions (see appendix A), we can read off the components C_l^m , yielding

$$\chi_{\mathbf{k}}^{\text{APW}}(\mathbf{r}) = \begin{cases} 4\pi e^{i\mathbf{k}\cdot\mathbf{R}_n} \sum_{l,m} [j_l(kr_{cn})/R_l(r_{cn})] i^l R_l(|\mathbf{r} - \mathbf{R}_n|) \\ \times Y_l^{m*}(\theta_k, \phi_k) Y_l^m(\theta, \phi) & \text{for } r \leq r_{cn} \\ e^{i\mathbf{k}\cdot\mathbf{r}} & \text{for } r > r_{cn}. \end{cases} \quad (2.38)$$

From this expression we immediately obtain that $\chi_{\mathbf{k}}^{\text{APW}}$ fulfills the Bloch theorem (equation (2.14)), therefore the full wave function can be written as

$$\psi_{\mathbf{k}} = \sum_{\mathbf{G}} c_{\mathbf{k}-\mathbf{G}} \chi_{\mathbf{k}-\mathbf{G}}^{\text{APW}}. \quad (2.39)$$

Although the $\chi_{\mathbf{k}}^{\text{APW}}$ are continuous at the sphere boundary per definition, their slopes in general are not. It was pointed out by Slater [12] that since the augmented plane wave expansion (equation (2.39)) is exact, convergence of the secular problem can be interpreted as finding a wave function with a continuous slope. To obtain a secular equation analog to the NFE case, we need to evaluate the matrix elements

$$\langle \chi_{\mathbf{k}-\mathbf{G}}^{\text{APW}} | (H - E) | \chi_{\mathbf{k}-\mathbf{G}'}^{\text{APW}} \rangle = \frac{1}{\Omega} \int_{\Omega} d\mathbf{r} \chi_{\mathbf{k}-\mathbf{G}}^{\text{APW}*}(\mathbf{r}) [H(\mathbf{r}) - E] \chi_{\mathbf{k}-\mathbf{G}'}^{\text{APW}}(\mathbf{r}). \quad (2.40)$$

The integral can be split into integrals over a sphere and over the interstitial regions plus surface terms that result from the fact that the slope of the $\chi_{\mathbf{k}-\mathbf{G}}^{\text{APW}}$ is discontinuous at the sphere surfaces. The former integrals vanish, since the $\chi_{\mathbf{k}-\mathbf{G}}^{\text{APW}}$, per definition, obey the Schrödinger equation inside the spheres at energy E . Thus, the form of the atomic potential inside the core appears only through the boundary term. After some calculation (see [14, chapter 16][16, chapter 2]), the secular equation can be written as

$$\left| \left[\frac{1}{2}(\mathbf{k} - \mathbf{G})^2 - E \right] \delta_{\mathbf{G}\mathbf{G}'} + V_{\mathbf{G}\mathbf{G}'}^{\text{APW}} \right| = 0, \quad (2.41)$$

This looks like the NFE expression (equation (2.33)), where we have replaced the Fourier components of the real atomic potential with those of an effective potential

$$\begin{aligned}
V_{\mathbf{G}\mathbf{G}'}^{\text{APW}} = & -4\pi \sum_n r_{cn}^2 \frac{1}{\Omega} \left\{ \left(\frac{1}{2} |\mathbf{k} - \mathbf{G}'|^2 - E \right) \frac{j_1(|\mathbf{G} - \mathbf{G}'| r_{cn})}{|\mathbf{G} - \mathbf{G}'|} \right. \\
& - \frac{1}{2} \sum_{l=0}^{\infty} (2l+1) P_l(\cos(\gamma)) j_l(|\mathbf{k} - \mathbf{G}| r_{cn}) j_l(|\mathbf{k} - \mathbf{G}'| r_{cn}) \quad (2.42) \\
& \left. \times \left[\frac{R_l'(r_{cn})}{R_l(r_{cn})} - \frac{|\mathbf{k} - \mathbf{G}'| j_l'(|\mathbf{k} - \mathbf{G}'| r_{cn})}{j_l(|\mathbf{k} - \mathbf{G}'| r_{cn})} \right] \right\},
\end{aligned}$$

where P_l is a Legendre polynomial and γ is the angle between $\mathbf{k} - \mathbf{G}$ and $\mathbf{k} - \mathbf{G}'$.

The first term subtracts the plane wave kinetic energy inside the muffin-tin spheres and the second term accounts for differences between the boundary contributions of the atomic potential and an empty sphere. In the limiting case of free electrons, obtained by setting the potential inside the spheres equal to its constant value in the interstitial region, the spherical Bessel functions are now exact solutions for the whole space. Thus, the difference of the logarithmic derivatives in equation (2.42) vanishes from which we can reproduce the free electron parabolas immediately. We expect that since the $\chi_{\mathbf{k}-\mathbf{G}}^{\text{APW}}$ already obey the Schrödinger equation exactly inside the muffin-tin spheres, only a few Fourier components should suffice to approximate the wave function. And in fact, good results are usually achieved with secular equations of size 20×20 . This requires the components of V^{APW} to be NFE-like, hence we can conclude that the logarithmic derivatives at $r = r_{cn}$ in equation (2.42) should resemble those of a weak potential (since all other terms are independent of the actual form of the atomic potential).

However, the original formulation of the APW method as presented comes with a severe drawback and is therefore not used in today's electronic structure calculations: Since the matrix elements in equation (2.41) are implicitly energy-dependent through the logarithmic derivatives, the energy eigenstates cannot be obtained with a single diagonalization. Instead, we would have to perform an expensive search for roots of the secular determinant. This has led to the development of very popular linearized methods, such as the LAWP method. Furthermore, the muffin-tin approximation can be dropped, resulting in so called "full potential" methods [see 14, chapter 17].

2.4 Orthogonalized plane wave method

Another problem of the NFE approximation is the fact that even if we are interested only in the valence states, the orthogonality requirement ties their convergence to that of the lowest energy eigenstate (which is the tightly bound first core state). To directly tackle this issue, we construct an orthogonal plane wave

$$\chi_{\mathbf{k}}^{\text{OPW}}(\mathbf{r}) = e^{i\mathbf{k}\cdot\mathbf{r}} - \sum_c b_{c\mathbf{k}} \psi_c(\mathbf{r}), \quad (2.43)$$

where the coefficients $b_{c\mathbf{k}}$ are chosen such that $\chi_{\mathbf{k}}^{\text{OPW}}$ is orthogonal to all core states ψ_c per definition, i.e.

$$\langle \psi_c, \chi_{\mathbf{k}}^{\text{OPW}} \rangle = \langle \psi_c, e^{i\mathbf{k}\cdot\mathbf{r}} \rangle - \sum_{c'} \langle \psi_c, b_{c'\mathbf{k}} \psi_{c'} \rangle \stackrel{!}{=} 0. \quad (2.44)$$

From the orthonormality of the core functions we immediately obtain

$$b_{c\mathbf{k}} = \langle \psi_c, e^{i\mathbf{k}\cdot\mathbf{r}} \rangle. \quad (2.45)$$

The fact, that we need the core states for this construction, seems to lead the motivation above *ad absurdum*, but for many materials the ψ_c can be replaced by the atomic core functions (“frozen core approximation”). Furthermore, the oscillations of the valence wave function are already built in due to the nodal structure of the ψ_c , at least approximately. The validity of this approximation determines the size of the secular equation. Once again, the expansion of the ψ in orthogonal plane waves

$$\psi_{\mathbf{k}} = \sum_{\mathbf{G}} c_{\mathbf{k}-\mathbf{G}} \chi_{\mathbf{k}-\mathbf{G}}^{\text{OPW}} \quad (2.46)$$

is exact, since the $\chi_{\mathbf{k}-\mathbf{G}}^{\text{OPW}}$ fulfill the Bloch theorem (as both the plane waves and the ψ_c do so separately [see 8, p. 261]). In the derivation of the OPW secular equation, we can take advantage of the fact that the ψ_c are eigenfunctions of H

$$\begin{aligned} (H - E) \chi_{\mathbf{k}-\mathbf{G}'}^{\text{OPW}} &= (H - E) e^{i(\mathbf{k}-\mathbf{G}')\cdot\mathbf{r}} + \sum_c (E_c - E) b_{c\mathbf{k}-\mathbf{G}'} \psi_c \\ \langle \chi_{\mathbf{k}-\mathbf{G}}^{\text{OPW}} | (H - E) | \chi_{\mathbf{k}-\mathbf{G}'}^{\text{OPW}} \rangle &= \\ \langle e^{i(\mathbf{k}-\mathbf{G})\cdot\mathbf{r}} | (H - E) | e^{i(\mathbf{k}-\mathbf{G}')\cdot\mathbf{r}} \rangle &+ \sum_c (E_c - E) b_{c\mathbf{k}-\mathbf{G}'} \langle e^{i(\mathbf{k}-\mathbf{G})\cdot\mathbf{r}}, \psi_c \rangle \\ + \sum_c (E_c - E) b_{c\mathbf{k}-\mathbf{G}} \langle \psi_c, e^{i(\mathbf{k}-\mathbf{G}')\cdot\mathbf{r}} \rangle &+ \sum_{cc'} (E - E_c) b_{c'\mathbf{k}-\mathbf{G}}^* b_{c\mathbf{k}-\mathbf{G}'} \langle \psi_{c'}, \psi_c \rangle. \end{aligned} \quad (2.47)$$

We find that the first term is the familiar plane wave Hamiltonian (equation (2.33)) and that the last three terms differ only by sign due to the orthonormality of the ψ_c and by equation (2.45), thus

$$\left| \left[\frac{1}{2}(\mathbf{k} - \mathbf{G})^2 - E \right] \delta_{\mathbf{G}\mathbf{G}'} + V_{\mathbf{G}\mathbf{G}'} + \sum_c (E - E_c) b_{c\mathbf{k}-\mathbf{G}}^* b_{c\mathbf{k}-\mathbf{G}'} \right| = 0. \quad (2.48)$$

As in the APW case, we can formally write this as

$$\left| \left[\frac{1}{2}(\mathbf{k} - \mathbf{G})^2 - E \right] \delta_{\mathbf{G}\mathbf{G}'} + V_{\mathbf{G}\mathbf{G}'}^{\text{OPW}} \right| = 0. \quad (2.49)$$

$V_{\mathbf{G}\mathbf{G}'}^{\text{OPW}}$ is also energy-dependent, however this problem is less severe than it was for the APW potential, as the energy dependence of $V_{\mathbf{G}\mathbf{G}'}^{\text{OPW}}$ originates only from the fact that the $\chi_{\mathbf{k}-\mathbf{G}}^{\text{OPW}}$ are not orthonormal

$$S_{\mathbf{G}\mathbf{G}'} := \langle \chi_{\mathbf{k}-\mathbf{G}}^{\text{OPW}}, \chi_{\mathbf{k}-\mathbf{G}'}^{\text{OPW}} \rangle = \delta_{\mathbf{G}\mathbf{G}'} - \sum_c b_{c\mathbf{k}-\mathbf{G}}^* b_{c\mathbf{k}-\mathbf{G}'}, \quad (2.50)$$

where we have used equation (2.45) and introduced the overlap matrix S . If we bring all terms in equation (2.48) that contain E to the right, the secular equation can be written as a generalized eigenvalue problem

$$\begin{aligned} \tilde{H}\mathbf{c} &= E S \mathbf{c} \\ \tilde{H}_{\mathbf{G}\mathbf{G}'} &= \frac{1}{2}(\mathbf{k} - \mathbf{G})^2 \delta_{\mathbf{G}\mathbf{G}'} + V_{\mathbf{G}\mathbf{G}'} - \sum_c E_c b_{c\mathbf{k}-\mathbf{G}}^* b_{c\mathbf{k}-\mathbf{G}'}, \end{aligned} \quad (2.51)$$

that can be reduced to an ordinary eigenvalue problem via basis transformation [see 17, pp. 36-37].

The OPW method typically requires secular equations that are comparable to the APW case in size. In the 1940s and 1950s, the OPW method was applied to a number of metals and semiconductors, amongst others were calculations that lead to the understanding of the band structures of Ge and Si.

2.4.1 The PKA pseudo-potential transformation

At the end of the 1950s, the OPW method was investigated from a theoretical standpoint by Phillips and Kleinman [5] and Antončík [6] (PKA) in order to address some of its problems and to broaden its scope of application. They were able to show that the rapid convergence of equation (2.46) can be explained by a formal transformation of the OPW Hamiltonian. This yields a Schrödinger equation for the “smooth” part of the valence wave function that is governed by a weak potential.

We start by formally separating the smooth part ψ^{ps} (by this notation we anticipate its interpretation as pseudo wave function) from the exact valence wave function

$$\psi_{\mathbf{k}}^{\text{ps}} = \sum_{\mathbf{G}} c_{\mathbf{k}-\mathbf{G}} e^{i(\mathbf{k}-\mathbf{G})\cdot\mathbf{r}}, \quad (2.52)$$

where the coefficients $c_{\mathbf{k}-\mathbf{G}}$ are the same as in equation (2.46), thus

$$\begin{aligned} \psi_{\mathbf{k}} &= \sum_{\mathbf{G}} c_{\mathbf{k}-\mathbf{G}} \left[e^{i(\mathbf{k}-\mathbf{G})\cdot\mathbf{r}} - \sum_c b_{c\mathbf{k}-\mathbf{G}} \psi_c(\mathbf{r}) \right] \\ &= \psi_{\mathbf{k}}^{\text{ps}} - \sum_c \langle \psi_c, \psi_{\mathbf{k}}^{\text{ps}} \rangle \psi_c. \end{aligned} \quad (2.53)$$

We insert this expression directly into the Schrödinger equation to obtain

$$\begin{aligned}
H\psi_{\mathbf{k}}^{\text{ps}} &= E\psi_{\mathbf{k}}^{\text{ps}} \\
H\psi_{\mathbf{k}}^{\text{ps}} - \sum_c \langle \psi_c, \psi_{\mathbf{k}}^{\text{ps}} \rangle H\psi_c &= E\psi_{\mathbf{k}}^{\text{ps}} - E \sum_c \langle \psi_c, \psi_{\mathbf{k}}^{\text{ps}} \rangle \psi_c \\
H\psi_{\mathbf{k}}^{\text{ps}} + \sum_c (E - E_c) \langle \psi_c, \psi_{\mathbf{k}}^{\text{ps}} \rangle \psi_c &= E\psi_{\mathbf{k}}^{\text{ps}}.
\end{aligned} \tag{2.54}$$

This can be interpreted as a generalized eigenvalue problem, where a pseudo-Hamiltonian H^{ps} acts on the pseudo wave function ψ^{ps}

$$\begin{aligned}
H^{\text{ps}}\psi^{\text{ps}} &= ES^{\text{ps}}\psi^{\text{ps}} \\
S^{\text{ps}}\psi^{\text{ps}} &= \psi^{\text{ps}} - \sum_c \langle \Psi_c, \psi^{\text{ps}} \rangle \psi_c \\
H^{\text{ps}} &= T + V + V_R \\
V_R\psi^{\text{ps}} &= - \sum_c E_c \langle \psi_c, \psi^{\text{ps}} \rangle \psi_c,
\end{aligned} \tag{2.55}$$

Since this is just the real space representation of equation (2.51), the ‘‘pseudo-potential’’

$$V^{\text{ps}} = V + V_R \tag{2.56}$$

is related to V^{OPW} by

$$\begin{aligned}
V^{\text{OPW}}\psi^{\text{ps}} &= V^{\text{ps}}\psi^{\text{ps}} + E \sum_c \langle \psi_c, \psi^{\text{ps}} \rangle \psi_c \\
&= V\psi^{\text{ps}} + \sum_c (E - E_c) \langle \psi_c, \psi^{\text{ps}} \rangle \psi_c.
\end{aligned} \tag{2.57}$$

Since $E - E_c$ is always positive, the strong attractive potential V gets weaker through the addition of the core part (this is stated more rigorously by the cancellation theorem, see [11]), whereas the pseudo wave function is smooth by definition. Therefore, the small size of the OPW secular equation is explained by equivalence to an NFE problem by a transformation of the Schrödinger equation which alters the potential and wave function but retains the energy eigenvalue.

The physical interpretation is convincing: Although the valence electrons are bound by a strong atomic potential, for a number of materials they behave like nearly free electrons, resulting in NFE-like valence bands. This is due to the Pauli principle keeping them away from the core region and due to screening by the core electrons [see 8, p. 190].

The OPW pseudo-potential is not unique, as a more generalized pseudo-Hamiltonian

$$\begin{aligned}
H^{\text{ps}} &= T + V + V_R \\
V_R\psi^{\text{ps}} &= \sum_c \langle F_c, \psi^{\text{ps}} \rangle \psi_c,
\end{aligned} \tag{2.58}$$

where the F_c are completely arbitrary functions, still has the correct energy eigenvalues, since ψ^{ps} is orthogonal to the core state subspace.

2.4.2 Non-local operators

The repulsive potential V_R is termed non-local, since its action on a general state $|\varphi\rangle$ involves the value of φ at all positions in space

$$V_R\varphi(\mathbf{r}) := \int d\mathbf{r}' V_R(\mathbf{r}, \mathbf{r}')\varphi(\mathbf{r}') \quad (2.59)$$

In general, a non-local operator acts differently on the different angular momentum components φ_l

$$\begin{aligned} \varphi &= \sum_l \varphi_l(\mathbf{r}) \\ \varphi_l(\mathbf{r}) &:= \sum_m \chi_l^m(r) Y_l^m(\theta, \phi). \end{aligned} \quad (2.60)$$

We can pick out the l -th component of φ by introducing a non-local projection operator \mathcal{P}_l

$$\begin{aligned} \mathcal{P}_l(\mathbf{r}, \mathbf{r}') &:= \sum_m Y_l^m(\theta, \phi) Y_l^{m*}(\theta', \phi') \frac{\delta(r - r')}{r^2} \\ \mathcal{P}_l\varphi(\mathbf{r}) &= \sum_m \left[\int d\mathbf{r}' Y_l^{m*}(\theta', \phi') \varphi(\mathbf{r}') \right] Y_l^m(\theta, \phi) = \varphi_l(\mathbf{r}), \end{aligned} \quad (2.61)$$

where we have used equation (2.60) and the orthogonality relation of the Y_l^m [see 18, p. 757]

$$\int_0^{2\pi} d\phi \int_{-\pi}^{\pi} \sin\theta d\theta Y_l^{m*}(\theta, \phi) Y_{l'}^{m'}(\theta, \phi) = \delta_{ll'} \delta_{mm'} \quad (2.62)$$

Additionally, from this result we verify the completeness relation

$$\sum_l \mathcal{P}_l = 1. \quad (2.63)$$

We can also use the \mathcal{P}_l to decompose any operator Q

$$Q = \sum_l Q_l \mathcal{P}_l, \quad (2.64)$$

where the Q_l are in general also non-local operators. A “semi-local” operator has merely functions as components Q_l and thus acts directly on the φ_l by multiplication

$$Q\varphi = \sum_l f_l(\mathbf{r})\varphi_l = \sum_{lm} Q_l(\mathbf{r})\chi_l^m(r)Y_l^m(\theta, \phi), \quad (2.65)$$

where in particular the angular momentum components stay decomposed if the Q_l are spherically symmetric [19, appendix A].

2.5 Definition of pseudo-potentials

The general concept of transforming the Schrödinger equation to find the smooth part of ψ is not restricted to the OPW method. For instance, we can construct such a pseudo wave function for the APW method by extending the plane wave solution in the interstitial regions to the muffin-tin spheres. In section 2.3, we also found that the energy eigenvalues are completely determined by the logarithmic derivatives at the sphere surfaces and the potential outside the spheres. The logarithmic derivatives

$$L_l(r, E) := \frac{\partial}{\partial r} \ln(R_l(r, E)) = \frac{R_l'(r, E)}{R_l(r, E)} \quad (2.66)$$

are related to the scattering properties of the potential V (see appendix B). Motivated by our discussion of the APW and the OPW method, we define a pseudo-potential by demanding that i) it yields the correct logarithmic derivatives at the surface of a core sphere with radius r_c and ii) it is equal to the original potential outside the sphere

$$L_l^{\text{ps}}(r_c, E_{\text{ref}}) = L_l(r_c, E_{\text{ref}}) \quad (2.67)$$

$$V^{\text{ps}}(r) = V(r) \quad \text{for } r \geq r_c, \quad (2.68)$$

where the reference energy E_{ref} is usually the valence energy. Although we assume that the original potential is spherically symmetric, it is possible to drop this requirement [19, part I].

The pseudo-potential is in general energy dependent, non-local and not unique, which we have already demonstrated in sections 2.3 and 2.4.

The pseudo wave function obeys the radial Schrödinger equation

$$\left[-\frac{1}{2r^2} \frac{d}{dr} \left(r^2 \frac{d}{dr} \right) + \frac{l(l+1)}{2r^2} + V_l^{\text{ps}}(r) \right] R_l^{\text{ps}}(r) = E_{\text{ref}} R_l^{\text{ps}}(r), \quad (2.69)$$

with equation (2.67) as boundary condition. It equals the original wave function outside the spheres and joins smoothly at $r = r_c$, as the continuous logarithmic derivatives ensure continuity in the function value and the first derivative. Scattering theory tells us that we can always choose a pseudo-potential such that the R_l^{ps} are node free inside the core region (see appendix B).

We can exploit the fact that V^{ps} is not unique to give it any convenient parametrized form. Natural candidates are potentials of the form

$$V^{\text{ps}} = \sum_l V_l(r) \mathcal{P}_l, \quad (2.70)$$

see section 2.4. In particular, simple choices for the V_l are delta functions and square wells. The former leads to the KKRZ pseudo-potential of Ziman and Lloyd

$$V^{\text{ps}} = \sum_l B_l \delta(r - r_c) \mathcal{P}_l \quad \text{for } r \leq r_c, \quad (2.71)$$

the latter to the “model potential” of Abarenkov and Heine

$$V_l^{\text{ps}}(r) = A_l(E) \quad \text{for } r \leq r_{cl}. \quad (2.72)$$

The parameters are either obtained through *ab initio* calculations or fitted to experimental data [11]. The great usability and universality of the pseudo-potential method stems from the fact that we can pseudize the atomic potentials and thereafter bring them together to build up different solids (the validity of this approximation generally depends on the chemical properties of the atoms and the geometry of the solid). Furthermore, pseudo-potential calculations are not limited to band structures: Inspired by the theoretical studies of PKA, a variety of material properties were obtained by calculations from Cohen, Harrison and others. These calculations encompass *inter alia* electron phonon-interaction and frequency of lattice vibrations, resistivity of liquid (molten) metals and self-consistent screening in solids as well as cohesion of metals (see Heine [11] and references cited therein).

2.6 Norm conserving pseudo-potentials

These early pseudo-potentials all suffered from a quite severe drawback: The calculations could not be used to predict excited states, as E is in general only correctly reproduced at $E = E_{\text{ref}}$ (per definition). This is due to the fact that the logarithmic matching condition fixes the pseudo wave function inside the core only up to a constant, thus the charge density is not correctly distributed between the core and the outer region. There exists an important identity, which we will derive below following Kresse [4], that relates the integrated core charge to the energy derivatives of the L_l .

For the sake of convenience, we substitute

$$R_l(r) =: \frac{\phi_l(r)}{r} \quad (2.73)$$

in the radial Schrödinger equation to obtain

$$\left[-\frac{1}{2} \frac{d^2}{dr^2} + \frac{l(l+1)}{2r^2} + V(r) \right] \phi_l(r) = E \phi_l(r). \quad (2.74)$$

The logarithmic derivatives of ϕ_l differ only by a constant factor from the L_l

$$x_l(r, E) := \frac{\partial}{\partial r} (\ln \phi_l(r, E)) = L_l(r, E) + \frac{1}{r}, \quad (2.75)$$

hence the boundary condition (2.67) can also be written as

$$x_l^{\text{PS}}(r_c, E_{\text{ref}}) = x_l(r_c, E_{\text{ref}}). \quad (2.76)$$

We start the derivation by differentiating the identity

$$\int_0^{r_c} dr \phi_l(r) \left[-\frac{1}{2} \frac{d^2}{dr^2} + \frac{l(l+1)}{2r^2} + V(r) - E \right] \phi_l(r) = 0 \quad (2.77)$$

with respect to the energy. The assumption of a energy independent potential yields

$$\begin{aligned} & \int_0^{r_c} dr \left\{ \dot{\phi}_l(r) \left[-\frac{1}{2} \frac{d^2}{dr^2} + \frac{l(l+1)}{2r^2} + V(r) - E \right] \phi_l(r) - \phi_l(r)^2 \right. \\ & \left. + \phi_l(r) \left[-\frac{1}{2} \frac{d^2}{dr^2} \right] \dot{\phi}_l(r) + \phi_l(r) \left[\frac{l(l+1)}{2r^2} + V(r) - E \right] \dot{\phi}_l(r) \right\} = 0 \quad (2.78) \\ & \int_0^{r_c} dr \left\{ \frac{1}{2} \left(\dot{\phi}_l(r) \frac{d^2}{dr^2} \phi_l(r) - \phi_l(r) \frac{d^2}{dr^2} \dot{\phi}_l(r) \right) - \phi_l(r)^2 \right\} = 0, \end{aligned}$$

where we have used that ϕ obeys the radial Schrödinger equation (2.74) and where the dot signifies an energy derivative. For a regular potential V (see section 4.2), the $r = 0$ boundary term vanishes after integration

$$\begin{aligned} & \frac{d}{dr} \left[\dot{\phi}_l(r) \frac{d}{dr} \phi_l(r) - \phi_l(r) \frac{d}{dr} \dot{\phi}_l(r) \right] = \frac{d}{dr} \dot{\phi}_l(r) \frac{d}{dr} \phi_l(r) + \dot{\phi}_l(r) \frac{d^2}{dr^2} \phi_l(r) \\ & - \frac{d}{dr} \phi_l(r) \frac{d}{dr} \dot{\phi}_l(r) - \phi_l(r) \frac{d^2}{dr^2} \dot{\phi}_l(r) = \dot{\phi}_l(r) \frac{d^2}{dr^2} \phi_l(r) - \phi_l(r) \frac{d^2}{dr^2} \dot{\phi}_l(r) \quad (2.79) \\ & \frac{1}{2} \left(\dot{\phi}_l(r) \frac{d}{dr} \phi_l(r) - \phi_l(r) \frac{d}{dr} \dot{\phi}_l(r) \right) \Big|_{r=r_c} = \int_0^{r_c} dr \phi_l(r)^2. \end{aligned}$$

The right side is just the charge inside the core sphere, whereas the left side contains the energy derivative of the x_l

$$\begin{aligned} -\frac{1}{2} \phi_l(r)^2 \dot{x}_l(r) &= -\frac{1}{2} \left(\phi_l(r)^2 \frac{\dot{\phi}_l'(r)}{\phi_l(r)} - \frac{\phi_l'(r)}{\phi_l(r)^2} \dot{\phi}_l(r) \right) \\ &= \frac{1}{2} \left(\dot{\phi}_l(r) \frac{d}{dr} \phi_l(r) - \phi_l(r) \frac{d}{dr} \dot{\phi}_l(r) \right), \quad (2.80) \end{aligned}$$

hence we obtain

$$-\frac{1}{2}\phi_l(r)^2\dot{x}_l(r)\Big|_{r=r_c} = \int_0^{r_c} dr\phi_l(r)^2. \quad (2.81)$$

If we assume that V^{ps} is also energy-independent and regular, this identity is valid for ϕ_l^{ps} as well. Therefore, the logarithmic derivatives are reproduced correctly up to first order in E (around $E = E_{\text{ref}}$) at $r = r_c$ (and thus for $r > r_c$), if the pseudo wave function fulfills the “norm-conservation condition”

$$\begin{aligned} \int_0^{r_c} dr\phi_l^{\text{ps}}(r)^2 &= \int_0^{r_c} dr\phi_l(r)^2 \\ 4\pi \int_0^\infty dr\phi_l^{\text{ps}}(r)^2 &= 4\pi \int_0^\infty dr\phi_l(r)^2 = 1 \end{aligned} \quad (2.82)$$

ensuring that the pseudo-charge is correctly distributed and that the pseudo wave function is correctly normalized. Thus, we define a norm conserving pseudo-potential by demanding that it fulfills the norm-conservation condition in addition to (2.67) and (2.68). Since we require ϕ^{ps} to be normalized, we can also write the logarithmic boundary condition as [4]

$$\begin{aligned} \phi_l^{\text{ps}}(r_c, E_{\text{ref}}) &= \phi_l(r_c, E_{\text{ref}}) \\ \phi_l^{\text{ps}'}(r_c, E_{\text{ref}}) &= \phi_l'(r_c, E_{\text{ref}}). \end{aligned} \quad (2.83)$$

2.6.1 Norm-conservation condition for scattering states

At first glance, the norm conservation condition seems to be inapplicable to scattering states, as they are not normalizable. However, the relevant condition is only the correct charge distribution between the core and the outer region, not an overall normalization. Therefore, we alter the condition (2.82) for scattering states by imposing normalization some cutoff radius r_c [20]

$$4\pi \int_0^{r_c} dr\phi_l^{\text{ps}}(r)^2 = 4\pi \int_0^{r_c} dr\phi_l(r)^2 = 1. \quad (2.84)$$

2.6.2 The Topp-Hopfield pseudo-potential

The first norm conserving pseudo-potential was used by Topp and Hopfield [21], who were motivated by the physical meaning of the pseudo-charge in chemical bondings. They used an empirical pseudo-potential for Na of the form

$$V^{\text{ps}}(r) = \begin{cases} V_0 \cos(kr) + C & \text{for } r \leq r_c \\ -\frac{1}{r} & \text{for } r \geq r_c, \end{cases} \quad (2.85)$$

where the parameters were fitted so that the potential is smooth and reproduces the experimental atomic $3s$ energy. They observed approximately coinciding energy eigenvalues for the lowest excited states, which they correctly attributed to the identity (2.81).

2.6.3 The HSC pseudo-potential

The term “norm conserving pseudo-potential” was coined by Hamann, Schlüter, and Chiang [22] (HSC), who developed an influential method that was used to construct and tabulate pseudo-potentials for all elements from H to Pu [see 23] and therefore has often been used as a reference for comparison. The HSC method consists of three steps: (i) an auxiliary pseudo-potential is created by cutting off the singularity at $r = 0$,

$$V_{1l}^{\text{ps}} = [1 - f(r/r_{cl})] V(r) + c_l f(r/r_{cl}), \quad (2.86)$$

where $f(x)$ is a smooth function that approaches 0 as $x \rightarrow \infty$, approaches 1 at least as fast as x^3 as $x \rightarrow 0$ and cuts off around $x \sim 1$, so that V_{1l}^{ps} converges to $V(r)$ for $r \geq r_{cl}$ and where c_l is adjusted so that the V_{1l}^{ps} reproduces the reference energy eigenvalue. (ii) the pseudo wave function is altered inside the core region by another cutoff function g that is of the same type as f

$$\phi_{2l}^{\text{ps}} = \gamma_l \left[\phi_{1l}^{\text{ps}} + \delta_l r^{l+1} g(r/r_{cl}) \right], \quad (2.87)$$

where the parameters γ_l and δ_l are chosen such that ψ_{2l}^{ps} fulfills the norm conservation condition. (iii) the final pseudo-potential is obtained by inversion of the radial Schrödinger equation at the reference energy

$$V_{l2}(r) = E_{\text{ref}} - \frac{1}{2} \left[\frac{l(l+1)}{r^2} - \frac{\phi_{2l}^{\text{ps}''}(r)}{\phi_{2l}^{\text{ps}}(r)} \right]. \quad (2.88)$$

The choice of the cutoff radii r_{cl} is a compromise between smooth and rather l -independent pseudo-potentials obtained for large r_{cl} and maximally accurate pseudo-potentials for small r_{cl} (this is a general theme in pseudo-potential theory). The cutoff functions were chosen to be Gaussians

$$f(x) = g(x) = \exp(-x^\lambda), \quad (2.89)$$

with $\lambda = 4$ by HSC and $\lambda = 3.5$ in reference [23] respectively.

2.6.4 The Kerker method

It was pointed out by Kerker [24] that it is simpler to skip the first step of the HSC method and directly assess the ϕ_l^{ps} inside the core as parametrized analytic functions of convenient form that fulfill the normalization condition and have the correct logarithmic derivative at $r = r_c$. The pseudo-potential is again obtained via equation (2.88). From this expression we also see that

V^{PS} is continuous at $r = r_c$ if the ϕ_l^{PS} additionally have the correct second derivatives

$$\left. \frac{d^n}{dr^n} \phi_l^{\text{PS}}(r) \right|_{r=r_c} = \left. \frac{d^n}{dr^n} \phi_l(r) \right|_{r=r_c}, \quad n = 0, 1, 2. \quad (2.90)$$

The form chosen by Kerker is

$$\phi_l^{\text{PS}}(r) = r^{l+1} e^{p(r)}, \quad (2.91)$$

where $p(r)$ is a polynomial

$$p(r) = \alpha r^4 + \beta r^3 + \gamma r^2 + \delta, \quad (2.92)$$

whose linear term is absent so as to avoid a singularity at $r = 0$.

2.7 The RRKJ pseudo-potential

Rappe, Rabe, Kaxiras, and Joannopoulos [3] (RRKJ) proposed a pseudization scheme based on the Kerker method that directly optimizes the convergence of the total energy of the solid in a plane wave basis. They argued that the convergence of the total energy of the isolated pseudoatoms is sufficient for this purpose, since the solid valence states either resemble their atomic counterparts (molecular and ionic solids), are NFE-like and therefore unproblematic for a plane wave basis (metal bonded materials) or a mixture of these two (transition metals). Covalent bonded materials are exempt from these categories, but since the covalent bonding region is comparable in size to the volume assigned to the atomic states, the approximation is still justifiable. Furthermore, using scaling arguments RRKJ proved that in the limit of large cutoff energies, the total energy convergence is similar to the kinetic energy convergence. The assumption of a continuous potential downs the lower bound for the cutoff energy that is necessary for this second approximation.

The construction of the original RRKJ pseudo-potential consists of two steps: (i) the pseudo wave function is expanded in a series of spherical Bessel functions

$$\phi_{1l}^{\text{PS}}(r) = \sum_{i=1}^{3(4)} \alpha_i j_l(q_i r) r, \quad (2.93)$$

where the wave vectors q_i are chosen such that their logarithmic derivatives match the L_l at $r = r_c$

$$\left. \frac{d}{dr} (\ln(j_l(q_i r) r)) \right|_{r=r_c} = \left. \frac{d}{dr} (\ln(\phi_l(r))) \right|_{r=r_c}. \quad (2.94)$$

The j_l are a natural basis for ϕ_l^{ps} as they are regular solutions to the radial Schrödinger equation for a free particle (see appendix A). Due to the form of the q_i , it is sufficient if the pseudo wave function fulfills

$$\begin{aligned}\phi_{1l}^{\text{ps}}(r_c) &= \phi_l(r_c) \\ \phi_{1l}^{\text{ps}''}(r_c) &= \phi_l''(r_c) \\ \int_0^{r_c} dr \phi_l^{\text{ps}}(r)^2 &= \int_0^{r_c} dr \phi_l(r)^2,\end{aligned}\tag{2.95}$$

in order to ensure a continuous norm conserving pseudo-potential. Since the latter is a quadratic constraint on the α_i , it is in general necessary to include a fourth j_l with α_4 fixed. (ii) additional j_l with nodes at $r = r_c$ are added to the pseudo wave function

$$\phi_{2l}^{\text{ps}}(r) = \phi_{1l}^{\text{ps}}(r) + \sum_{i=1}^m \beta_i j_l(\tilde{q}_i r), \quad j(\tilde{q}_i r) = 0,\tag{2.96}$$

where the β_i are chosen to minimize the kinetic energy beyond the cutoff q_c

$$\Delta E_l^{\text{kin}}(q_c) = \frac{1}{2} \int_0^{q_c} dq q^2 \bar{\phi}_{2l}^{\text{ps}}(q)^2 \rightarrow \min,\tag{2.97}$$

where $\bar{\phi}^{\text{ps}}(q)$ denotes the spherical Bessel transform of the pseudo wave function (see appendix A). For a given r_c , the cutoff wave vector q_c is iterated until ΔE_l^{kin} is smaller than tolerance error.

RRKJ verified that the kinetic energy criterion indicates total energy convergence for fcc-Cu. This result was confirmed by Kresse [4] and Kresse and Hafner [25], who also showed this for a number of other materials.

2.7.1 Revised RRKJ method

It is simpler to use only Bessel functions with wave vectors of the type (2.94)

$$\phi_l^{\text{ps}}(r) = \sum_{i=1}^n \alpha_i j_l(q_i r),\tag{2.98}$$

and directly vary the α_i to minimize the kinetic energy (the α_i are still constrained by equation (2.95)). It was pointed out by Lin *et al.* [26] that q_c cannot be reduced arbitrarily, since q_c is essentially determined by q_n . Therefore, choosing n too large for a set q_c means a surplus of degrees of freedom that lead to large high-frequency oscillations. Furthermore, Kresse and Hafner [25] found that this barely improves the ΔE_l at the cutoff energy $E_c = q_c^2/2$, but leads to slow convergence beyond q_c . Thus, Lin *et al.* suggested to use only the minimum number of j_l that allows for optimization of the kinetic energy ($n = 4$) and set $q_c = q_4$. The convergence is then achieved by reducing r_c until $\Delta E_l^{\text{kin}}(q_4)$ is underneath the tolerance limit. Kresse [4] and Kresse and Hafner [25] found that even the fourth j_l is unnecessary and it is best to use only $n = 3$, if possible.

Chapter 3

Møller-Plesset perturbation theory

In Møller-Plesset (MP) perturbation theory, the correlation energy

$$E_{\text{corr}} := E_{\text{MB}} - E_{\text{HF}} \quad (3.1)$$

is obtained by a perturbation series that arises from partitioning the full many-body (MB) Hamiltonian into a zeroth order term, namely the Hartree-Fock (HF) Hamiltonian, and a perturbation term

$$H_{\text{MB}} = H_0 + (H_{\text{MB}} - H_0) \quad (3.2)$$

Following Szabo and Ostlund [27, chapters 2-3,6], we will begin this chapter with a short review of the Hartree-Fock approximation and thereafter derive the second order contribution to E_{corr} . At first, we will discuss the general theory and then specialize to the spin restricted approximation.

3.1 Hartree-Fock approximation

Within the Born-Oppenheimer approximation, the many-body Hamiltonian for a system of N electrons at positions \mathbf{r}_i in the field of M nuclei with charges Z_A at positions \mathbf{R}_A reads

$$H_{\text{MB}} = \sum_{i=1}^N -\frac{1}{2} \nabla_i^2 - \sum_{i=1}^N \sum_{A=1}^M \frac{Z_A}{|\mathbf{r}_i - \mathbf{R}_A|} + \sum_{i<j}^N \frac{1}{|\mathbf{r}_i - \mathbf{r}_j|} + \sum_{A<B}^M \frac{Z_A Z_B}{|\mathbf{R}_A - \mathbf{R}_B|}. \quad (3.3)$$

The electrostatic interaction energy between nuclei, which constitutes the last term, is constant and will be neglected from now on. Furthermore, it is convenient to introduce a core Hamiltonian $h(\mathbf{r}_1)$ that collects all one-electron operators

$$h(\mathbf{r}_1) = -\frac{1}{2}\nabla_1^2 - \sum_A \frac{Z_A}{|\mathbf{r}_1 - \mathbf{R}_A|} \quad (3.4)$$

In the HF approximation, the N -electron wave function is assessed as a Slater determinant, i.e. an antisymmetrized product of one-particle spin orbitals χ_i

$$\Psi_0(\mathbf{x}_1, \dots, \mathbf{x}_N) := \frac{1}{\sqrt{N!}} \sum_{\sigma} (-1)^{\sigma} \chi_1(\mathbf{x}_{\sigma(1)}) \dots \chi_N(\mathbf{x}_{\sigma(N)}), \quad (3.5)$$

where \mathbf{x} is a combined coordinate that describes position and spin. The determinant is properly normalized, as we demand that the χ_i are orthonormal

$$\langle \chi_i | \chi_j \rangle = \delta_{ij}. \quad (3.6)$$

It is convenient to introduce the following short hand notations for one- and two-electron integrals

$$\begin{aligned} \langle i|h|j \rangle &:= \frac{1}{\Omega} \int d\mathbf{x}_1 \chi_i^*(\mathbf{x}_1) h(\mathbf{r}_1) \chi_j(\mathbf{x}_1) \\ \langle ij|kl \rangle &:= \frac{1}{\Omega^2} \int d\mathbf{x}_1 d\mathbf{x}_2 \chi_i^*(\mathbf{x}_1) \chi_j^*(\mathbf{x}_2) \frac{1}{|\mathbf{r}_1 - \mathbf{r}_2|} \chi_k(\mathbf{x}_1) \chi_l(\mathbf{x}_2) \\ \langle ij||kl \rangle &:= \langle ij|kl \rangle - \langle ij|lk \rangle. \end{aligned} \quad (3.7)$$

As we can easily see, the two-electron integrals $\langle ij|kl \rangle$ fulfill per definition the identity

$$\langle ij|kl \rangle = \langle ji|lk \rangle = \langle kl|ij \rangle^*, \quad (3.8)$$

which they pass on to the antisymmetrized two-electron integrals $\langle ij||kl \rangle$

$$\langle ij||kl \rangle = \langle ji||lk \rangle = \langle kl||ij \rangle^*. \quad (3.9)$$

Furthermore, the $\langle ij||kl \rangle$ vanish per definition if the first two or last two indices are equal

$$\langle ij||kk \rangle = \langle ii||kl \rangle = 0. \quad (3.10)$$

In appendix C, we show that the HF energy of the ground state determinant can be expressed as

$$E_{\text{HF}} = \langle \Psi_0 | H_{\text{MB}} | \Psi_0 \rangle = \sum_{a=1}^N \langle a|h|a \rangle + \frac{1}{2} \sum_{a=1}^N \sum_{b=1}^N \langle ab||ab \rangle. \quad (3.11)$$

Furthermore, we prove that the optimal spin orbitals which minimize E_{HF} fulfill the (canonical) Hartree-Fock equation

$$f |\chi_a\rangle = \varepsilon_a |\chi_a\rangle, \quad (3.12)$$

where the Fock operator f consists of the core Hamiltonian and an effective one-electron potential, that is the sum of a “Coulomb term” (or “Hartree term”), which describes a classical mean field interaction and a non-local “exchange term”, that results from the fermionic antisymmetry.

$$\begin{aligned} f &:= h + \sum_{b=1}^N J_b - K_b \\ J_j(\mathbf{x}_1)\chi_i(\mathbf{x}_1) &:= \frac{1}{\Omega} \int d\mathbf{x}_2 \chi_j^*(\mathbf{x}_2) \frac{1}{|\mathbf{r}_1 - \mathbf{r}_2|} \chi_j(\mathbf{x}_2) \chi_i(\mathbf{x}_1) \\ K_j(\mathbf{x}_1)\chi_i(\mathbf{x}_1) &:= \frac{1}{\Omega} \int d\mathbf{x}_2 \chi_j^*(\mathbf{x}_2) \frac{1}{|\mathbf{r}_1 - \mathbf{r}_2|} \chi_i(\mathbf{x}_2) \chi_j(\mathbf{x}_1). \end{aligned} \quad (3.13)$$

The Coulomb term seems to include an unphysical self-interaction term, but it is exactly canceled by the exchange term, hence we could replace $\sum_b \rightarrow \sum_{b \neq a}$ in equation (3.13). After introducing a basis, the nonlinear eigenvalue problem (3.12) is usually solved iteratively. Then, the ground state determinant is built up from the N orbitals with the lowest spin orbital energies ε_a , which we thus call occupied orbitals. The remaining orbitals are unoccupied, but will contribute to the ground state energy via the perturbation series.

By exciting one electron from an occupied spin orbital χ_a to an unoccupied spin orbital χ_r , we can define singly excited determinants $|\Psi_a^r\rangle$

$$\begin{aligned} \Psi_a^r(\mathbf{x}_1, \dots, \mathbf{x}_N) &:= \frac{1}{\sqrt{N!}} \sum_{\sigma} (-1)^{\sigma} \chi_1(\mathbf{x}_{\sigma(1)}) \dots \\ &\quad \chi_{a-1}(\mathbf{x}_{\sigma(a-1)}) \chi_r(\mathbf{x}_{\sigma(a)}) \chi_{a+1}(\mathbf{x}_{\sigma(a+1)}) \dots \chi_N(\mathbf{x}_{\sigma(N)}), \end{aligned} \quad (3.14)$$

and furthermore doubly excited determinants $|\Psi_{ab}^{rs}\rangle$, triply excited determinants $|\Psi_{abc}^{rst}\rangle$ etc. in an analogous way. Due to the orthonormality of the χ_i , the determinants are orthonormal as well.

3.1.1 Koopmans' theorem

Under the assumption that the spin orbitals do not change, Koopmans' theorem states that if we add or remove an electron, the ε_i can be interpreted as ionization potentials and electron affinities

$$\begin{aligned} E_{\text{HF}}^{N-1} - E_{\text{HF}}^N &= -\varepsilon_c, & c \in \text{occ} \\ E_{\text{HF}}^{N+1} - E_{\text{HF}}^N &= -\varepsilon_r, & r \in \text{unocc}. \end{aligned} \quad (3.15)$$

To prove this, we need to calculate the HF energy of a determinant $|\Psi_0^{N-1}\rangle$ created by removing orbital c from the N electron ground state, i.e.

$$E_{\text{HF}}^{N-1} = \langle \Psi_0^{N-1} | H_{\text{MB}} | \Psi_0^{N-1} \rangle = \sum_{a \neq c}^{\text{occ}} \langle a | h | a \rangle + \frac{1}{2} \sum_{a \neq c}^{\text{occ}} \sum_{b \neq c}^{\text{occ}} \langle ab || ab \rangle, \quad (3.16)$$

ie. which yields for the ionization potential

$$\begin{aligned} E_{\text{HF}}^{N-1} - E_{\text{HF}}^N &= -\langle c | h | c \rangle - \sum_a^{\text{occ}} \frac{1}{2} \langle ac || ac \rangle - \frac{1}{2} \sum_b^{\text{occ}} \langle cb || cb \rangle \\ &= -\langle c | h | c \rangle - \sum_b^{\text{occ}} \langle cb || cb \rangle, \end{aligned} \quad (3.17)$$

as $\langle cc || cc \rangle = 0$. On the other hand, we can obtain ε_c as

$$\varepsilon_c = \langle \chi_c | f | \chi_c \rangle = \langle \chi_c | h + \sum_b J_b - K_b | \chi_c \rangle = \langle c | h | c \rangle + \sum_b^{\text{occ}} \langle cb || cb \rangle, \quad (3.18)$$

to complete the prove (the argument is analog for the electron affinities).

3.2 MP2 approximation

We have constructed the HF ground state $|\Psi_0\rangle$ as an approximation to the exact N electron wave function that minimizes the HF energy. On the other hand, we can use the Fock operator f to construct an approximate Hamiltonian H_0 , called Hartree-Fock Hamiltonian, whose ground state is exactly $|\Psi_0\rangle$

$$\begin{aligned} H_0 |\Psi_0\rangle &= E^{(0)} |\Psi_0\rangle \\ H_0 &= \sum_a^{\text{occ}} f(\mathbf{x}_a) \\ E^{(0)} &= \sum_a^{\text{occ}} \varepsilon_a. \end{aligned} \quad (3.19)$$

To prove this, we use equations (3.5) and (3.12) as well as the fact that H_0 is invariant under permutation of the electron indices

$$\begin{aligned} H_0 |\Psi_0\rangle &= \sum_a^{\text{occ}} f(\mathbf{x}_a) \frac{1}{\sqrt{N!}} \sum_{\sigma} (-1)^{\sigma} \chi_1(\mathbf{x}_{\sigma(1)}) \dots \chi_N(\mathbf{x}_{\sigma(N)}) \\ &= \sum_a^{\text{occ}} \varepsilon_a \frac{1}{\sqrt{N!}} \sum_{\sigma} (-1)^{\sigma} \chi_1(\mathbf{x}_{\sigma(1)}) \dots \chi_N(\mathbf{x}_{\sigma(N)}). \end{aligned} \quad (3.20)$$

In the same way, excited determinants are eigenstates of H_0 with eigenvalues equal to the sum of ε_i included in the determinant, e.g.

$$\begin{aligned}\langle \Psi_a^r | H_0 | \Psi_a^r \rangle &= \sum_b^{\text{occ}} \varepsilon_b - \varepsilon_a + \varepsilon_r \\ \langle \Psi_{ab}^{rs} | H_0 | \Psi_{ab}^{rs} \rangle &= \sum_c^{\text{occ}} \varepsilon_c - \varepsilon_a - \varepsilon_b + \varepsilon_r + \varepsilon_s.\end{aligned}\tag{3.21}$$

In chapter 2, we have already encountered the second order result of the Rayleigh-Schrödinger perturbation series for the special case where the unperturbed states are plane waves (equation (2.25)). Now, we expand the exact ground state energy E_{MB} , where our unperturbed Hamiltonian is H_0 with unperturbed eigenstates $|\Psi_0\rangle$, $|\Psi_a^r\rangle$, $|\Psi_{ab}^{rs}\rangle$ etc. and where our perturbation potential is $H_{\text{MB}} - H_0$. This yields

$$\begin{aligned}E_{\text{MB}} &= E^{(0)} + E^{(1)} + E^{(2)} + \dots \\ &= \langle \Psi_0 | H_0 | \Psi_0 \rangle + \langle \Psi_0 | H_{\text{MB}} - H_0 | \Psi_0 \rangle \\ &\quad + \sum_L \frac{|\langle \Psi_0 | H_{\text{MB}} - H_0 | L \rangle|^2}{E^{(0)} - E_L} + \dots,\end{aligned}\tag{3.22}$$

where the sum over L indicates summation over all unique excited determinants $|L\rangle$ and the E_L are the unperturbed eigenvalues, see equation (3.21). The sum of the zero and first order terms reproduces the HF energy

$$\begin{aligned}E^{(0)} + E^{(1)} &= \sum_a^{\text{occ}} \varepsilon_a + \sum_a^{\text{occ}} \langle a | h | a \rangle + \frac{1}{2} \sum_{ab}^{\text{occ}} \langle ab || ab \rangle \\ &\quad - \sum_a^{\text{occ}} \langle a | h | a \rangle - \sum_{ab} \langle ab || ab \rangle \\ &= \sum_a^{\text{occ}} \varepsilon_a - \frac{1}{2} \sum_{ab}^{\text{occ}} \langle ab || ab \rangle = E_{\text{HF}},\end{aligned}\tag{3.23}$$

hence the HF energy can be seen as sum over the occupied spin orbital energies minus double counting corrections. The leading term in the perturbation series for E_{corr} is thus the MP2 energy $E^{(2)}$

$$E_{\text{corr}} = E_{\text{MB}} - E_{\text{HF}} \approx E^{(2)} = \sum_L \frac{|\langle \Psi_0 | H_{\text{MB}} - H_0 | L \rangle|^2}{E^{(0)} - E_L}\tag{3.24}$$

We can use the fact that the $|L\rangle$ are eigenstates of H_0 , as well as Brillouin's theorem and the Slater-Condon rules (see appendix C) to show that only doubly excited determinants contribute

$$\begin{aligned}\langle \Psi_0 | H_{\text{MB}} - H_0 | L \rangle &= E_L \langle \Psi_0 | L \rangle + \langle \Psi_0 | H_{\text{MB}} | L \rangle \\ &= \langle \Psi_0 | H_{\text{MB}} | \Psi_{ab}^{rs} \rangle = \langle ab || rs \rangle.\end{aligned}\tag{3.25}$$

Thus, we obtain for the MP2 energy

$$\begin{aligned}
E^{(2)} &= \sum_{a<b}^{\text{occ}} \sum_{r<s}^{\text{unocc}} \frac{|\langle ab||rs \rangle|^2}{\varepsilon_a + \varepsilon_b - \varepsilon_r - \varepsilon_s} = \frac{1}{4} \sum_{ab}^{\text{occ}} \sum_{rs}^{\text{unocc}} \frac{|\langle ab||rs \rangle|^2}{\varepsilon_a + \varepsilon_b - \varepsilon_r - \varepsilon_s} \\
&= \frac{1}{4} \sum_{ab}^{\text{occ}} \sum_{rs}^{\text{unocc}} \frac{[\langle rs|ab \rangle - \langle sr|ab \rangle][\langle ab|rs \rangle - \langle ab|sr \rangle]}{\varepsilon_a + \varepsilon_b - \varepsilon_r - \varepsilon_s} \\
&= \frac{1}{2} \sum_{ab}^{\text{occ}} \sum_{rs}^{\text{unocc}} \frac{\langle ab|rs \rangle \langle rs|ab \rangle}{\varepsilon_a + \varepsilon_b - \varepsilon_r - \varepsilon_s} - \frac{1}{2} \sum_{ab}^{\text{occ}} \sum_{rs}^{\text{unocc}} \frac{\langle ab|rs \rangle \langle rs|ba \rangle}{\varepsilon_a + \varepsilon_b - \varepsilon_r - \varepsilon_s},
\end{aligned} \tag{3.26}$$

where we have used the identities (3.9) and (3.10) as well as the symmetry of $E^{(2)}$ under exchange of a and b and r and s respectively. The first term is called direct MP2 energy $E_d^{(2)}$, the second term exchange MP2 energy $E_x^{(2)}$.

3.3 Spin restriction

So far, we have made no assumptions for the form of the spin orbitals χ_i . At this point, we will introduce an approximation that allows us to handle the electron spin in an easy manner. For closed shell systems, i.e. systems with an even number of electrons, one often constricts the χ_i to be spin-degenerate

$$\begin{aligned}
\chi_{2i-1}(\mathbf{x}) &= \varphi_i(\mathbf{r})\alpha(\omega) \\
\chi_{2i}(\mathbf{x}) &= \varphi_i(\mathbf{r})\beta(\omega),
\end{aligned} \tag{3.27}$$

where $\alpha(\omega)$ and $\beta(\omega)$ are the usual orthonormal “up” and “down” spin functions. One can show that as we would expect, the spin restricted ground state determinant is in fact a pure singlet state. This is also true for excited determinants where no spatial orbital φ_i is singly occupied [see 27, chapter 2]. Now that we have made specifications for the spin, we are able to simplify the one- and two-electron integrals by integrating out the spin part. We will indicate the β spin function by barred indices, for example

$$\langle \varphi_i \alpha | h | \varphi_j \beta \rangle =: \langle i | h | \bar{j} \rangle. \tag{3.28}$$

Furthermore, we will denote spatial integrals by round brackets

$$\begin{aligned}
(i|h|j) &:= \frac{1}{\Omega} \int d\mathbf{r}_1 \varphi_i^*(\mathbf{r}_1) h(\mathbf{r}_1) \varphi_j(\mathbf{r}_1) \\
(ij|kl) &:= \frac{1}{\Omega^2} \int d\mathbf{r}_1 d\mathbf{r}_2 \varphi_i^*(\mathbf{r}_1) \varphi_j^*(\mathbf{r}_2) \frac{1}{|\mathbf{r}_1 - \mathbf{r}_2|} \varphi_j(\mathbf{r}_1) \varphi_k(\mathbf{r}_2).
\end{aligned} \tag{3.29}$$

By using the orthonormality of the spin functions we immediately obtain

$$\begin{aligned}
\langle i|h|j\rangle &= \langle \bar{i}|h|\bar{j}\rangle = \langle i|h|j\rangle \\
\langle i|h|\bar{j}\rangle &= \langle \bar{i}|h|j\rangle = 0 \\
\langle ij|kl\rangle &= \langle \bar{i}\bar{j}|\bar{k}\bar{l}\rangle = \langle \bar{i}\bar{j}|\bar{k}l\rangle = \langle i\bar{j}|k\bar{l}\rangle = \langle ij|kl\rangle \\
&\text{all other two-electron integrals} = 0.
\end{aligned} \tag{3.30}$$

This yields for the HF ground state energy

$$\begin{aligned}
E_{\text{HF}} &= \sum_a^{N/2} \langle a|h|a\rangle + \sum_{\bar{a}}^{N/2} \langle \bar{a}|h|\bar{a}\rangle \\
&+ \frac{1}{2} \sum_a^{N/2} \sum_b^{N/2} \langle ab|ab\rangle - \langle ab|ba\rangle + \frac{1}{2} \sum_{\bar{a}}^{N/2} \sum_b^{N/2} \langle \bar{a}\bar{b}|\bar{a}\bar{b}\rangle - \langle \bar{a}\bar{b}|\bar{b}\bar{a}\rangle \\
&+ \frac{1}{2} \sum_a^{N/2} \sum_{\bar{b}}^{N/2} \langle a\bar{b}|a\bar{b}\rangle - \langle a\bar{b}|\bar{b}a\rangle + \frac{1}{2} \sum_{\bar{a}}^{N/2} \sum_b^{N/2} \langle \bar{a}\bar{b}|\bar{a}\bar{b}\rangle - \langle \bar{a}\bar{b}|\bar{b}\bar{a}\rangle \\
&= 2 \sum_a^{\text{occ}} \langle a|h|a\rangle + \sum_{ab}^{\text{occ}} 2 \langle ab|ab\rangle - \langle ab|ba\rangle.
\end{aligned} \tag{3.31}$$

We find that all electrons interact via the Coulomb term, whereas only electrons with like spin feel the exchange interaction. Thus, we can immediately write down the spin restricted HF equations

$$\begin{aligned}
f(\mathbf{r}_1)\varphi_i(\mathbf{r}_1) &= \varepsilon_i\varphi_i(\mathbf{r}_1) \\
f(\mathbf{r}_1) &= h(\mathbf{r}_1) + \sum_b^{\text{occ}} 2J_b(\mathbf{r}_1) - K_b(\mathbf{r}_1) \\
\varepsilon_i &= \langle i|h|i\rangle + \sum_b^{\text{occ}} 2\langle ib|ib\rangle - \langle ib|bi\rangle.
\end{aligned} \tag{3.32}$$

Analogously, the spin restricted MP2 energy is given by

$$E^{(2)} = 2 \sum_{ab}^{\text{occ}} \sum_{rs}^{\text{unocc}} \frac{\langle ab|rs\rangle\langle rs|ab\rangle}{\varepsilon_a + \varepsilon_b - \varepsilon_r - \varepsilon_s} - \sum_{ab}^{\text{occ}} \sum_{rs}^{\text{unocc}} \frac{\langle ab|rs\rangle\langle rs|ba\rangle}{\varepsilon_a + \varepsilon_b - \varepsilon_r - \varepsilon_s}. \tag{3.33}$$

3.4 MP2 for periodic systems

For a periodic system, the spatial orbitals have to fulfill the Bloch theorem as discussed previously. Thus, the eigenstates of the HF-Hamiltonian can be labeled by the band indices i and quasimomentum indices \mathbf{k} of the orbitals occupied in that determinant. Since we need to sum over all unique determinants (see equation (3.22)), the MP2 energy per unit cell is [28],[29]

$$\begin{aligned}
E^{(2)} = & \frac{2}{N_{\text{cell}}} \sum_{\mathbf{k}_1 \dots \mathbf{k}_4}^{\text{BZ}} \sum_{ab}^{\text{occ}} \sum_{rs}^{\text{unocc}} \frac{(a\mathbf{k}_1, b\mathbf{k}_2 | r\mathbf{k}_3, s\mathbf{k}_4)(r\mathbf{k}_3, s\mathbf{k}_4 | a\mathbf{k}_1, b\mathbf{k}_2)}{\varepsilon_{a\mathbf{k}_1} + \varepsilon_{b\mathbf{k}_2} - \varepsilon_{r\mathbf{k}_3} - \varepsilon_{s\mathbf{k}_4}} \\
& - \frac{1}{N_{\text{cell}}} \sum_{\mathbf{k}_1 \dots \mathbf{k}_4}^{\text{BZ}} \sum_{ab}^{\text{occ}} \sum_{rs}^{\text{unocc}} \frac{(a\mathbf{k}_1, b\mathbf{k}_2 | r\mathbf{k}_3, s\mathbf{k}_4)(r\mathbf{k}_3, s\mathbf{k}_4 | b\mathbf{k}_2, a\mathbf{k}_1)}{\varepsilon_{a\mathbf{k}_1} + \varepsilon_{b\mathbf{k}_2} - \varepsilon_{r\mathbf{k}_3} - \varepsilon_{s\mathbf{k}_4}}.
\end{aligned} \tag{3.34}$$

Recently, Schäfer *et al.* [29] have implemented a plane wave based MP2 method in VASP, that uses the Laplace transformed MP2 (LTMP2) formulation [30]. To obtain the Fourier space representation of the two-electron integrals, we use

$$\frac{1}{|\mathbf{r}_1 - \mathbf{r}_2|} = \frac{1}{\Omega} \sum_{\mathbf{G}} \sum_{\mathbf{k}}^{\text{BZ}} \frac{4\pi}{(\mathbf{k} - \mathbf{G})^2} e^{i(\mathbf{k} - \mathbf{G}) \cdot (\mathbf{r}_1 - \mathbf{r}_2)}, \tag{3.35}$$

which is the discretized version of an expression that we will derive later on (equation (4.34)), i.e. we replace

$$\int \frac{d\mathbf{q}}{(2\pi)^3} \rightarrow \frac{1}{\Omega} \sum_{\mathbf{G}} \sum_{\mathbf{k}}^{\text{BZ}}. \tag{3.36}$$

We proceed by splitting the real space integrals into integrals over all unit cells and thereafter use the Bloch theorem (equation (2.14)) and the identity (2.20) to pull out two structure factors

$$\begin{aligned}
& \langle i\mathbf{k}_1, j\mathbf{k}_2 | k\mathbf{k}_3, l\mathbf{k}_4 \rangle \\
& = \frac{1}{\Omega^2} \sum_{\mathbf{R}_1 \mathbf{R}_2} \int_{\Omega_{\text{cell}}} d\mathbf{r}_1 \int_{\Omega_{\text{cell}}} d\mathbf{r}_2 \varphi_{i\mathbf{k}_1}^*(\mathbf{r}_1 + \mathbf{R}_1) \varphi_{j\mathbf{k}_2}^*(\mathbf{r}_2 + \mathbf{R}_2) \\
& \quad \times \frac{1}{|\mathbf{r}_1 + \mathbf{R}_1 - \mathbf{r}_2 - \mathbf{R}_2|} \varphi_{k\mathbf{k}_3}(\mathbf{r}_1 + \mathbf{R}_1) \varphi_{l\mathbf{k}_4}(\mathbf{r}_2 + \mathbf{R}_2) \\
& = \frac{1}{\Omega^2} \sum_{\mathbf{R}_1 \mathbf{R}_2} \int_{\Omega_{\text{cell}}} d\mathbf{r}_1 \int_{\Omega_{\text{cell}}} d\mathbf{r}_2 \left[\frac{1}{\Omega} \sum_{\mathbf{G}} \sum_{\mathbf{k}}^{\text{BZ}} \frac{4\pi}{(\mathbf{k} - \mathbf{G})^2} e^{i(\mathbf{k} - \mathbf{G}) \cdot (\mathbf{r}_1 + \mathbf{R}_1 - \mathbf{r}_2 - \mathbf{R}_2)} \right] \\
& \quad \times e^{i(\mathbf{k}_3 - \mathbf{k}_1) \cdot \mathbf{R}_1} e^{i(\mathbf{k}_4 - \mathbf{k}_2) \cdot \mathbf{R}_2} \varphi_{i\mathbf{k}_1}^*(\mathbf{r}_1) \varphi_{j\mathbf{k}_2}^*(\mathbf{r}_2) \varphi_{k\mathbf{k}_3}(\mathbf{r}_1) \varphi_{l\mathbf{k}_4}(\mathbf{r}_2) \\
& = \frac{1}{\Omega_{\text{cell}}} \int_{\Omega_{\text{cell}}} d\mathbf{r}_1 \frac{1}{\Omega_{\text{cell}}} \int_{\Omega_{\text{cell}}} d\mathbf{r}_2 \frac{1}{\Omega} \sum_{\mathbf{G}} \sum_{\mathbf{k}}^{\text{BZ}} \frac{4\pi}{(\mathbf{k} - \mathbf{G})^2} e^{i(\mathbf{k} - \mathbf{G}) \cdot (\mathbf{r} - \mathbf{r}')} \\
& \quad \times \delta_{\mathbf{k}T(\mathbf{k}_1 - \mathbf{k}_3)} \delta_{\mathbf{k}T(\mathbf{k}_4 - \mathbf{k}_2)} \varphi_{i\mathbf{k}_1}^*(\mathbf{r}_1) \varphi_{j\mathbf{k}_2}^*(\mathbf{r}_2) \varphi_{k\mathbf{k}_3}(\mathbf{r}_1) \varphi_{l\mathbf{k}_4}(\mathbf{r}_2),
\end{aligned} \tag{3.37}$$

where $T(\mathbf{q})$ is a function that maps \mathbf{q} to the first Brillouin zone, i.e.

$$\mathbf{q} = \mathbf{k} - \mathbf{G} \rightarrow T(\mathbf{q}) := \mathbf{k}. \tag{3.38}$$

Furthermore, we introduce a bracket notation that indicates integration over the unit cell

$$\langle i\mathbf{k}_1 | j\mathbf{k}_2 \rangle_{\Omega_{\text{cell}}} := \frac{1}{\Omega_{\text{cell}}} \int_{\Omega_{\text{cell}}} d\mathbf{r} \varphi_{i\mathbf{k}_1}^*(\mathbf{r}) \varphi_{j\mathbf{k}_2}(\mathbf{r}) \quad (3.39)$$

and carry out the sum over \mathbf{k} to finally obtain

$$\begin{aligned} & \langle i\mathbf{k}_1, j\mathbf{k}_2 | k\mathbf{k}_3, l\mathbf{k}_4 \rangle \\ &= \frac{1}{\Omega} \delta_{T(\mathbf{k}_1 - \mathbf{k}_3)T(\mathbf{k}_4 - \mathbf{k}_2)} \sum_{\mathbf{G}} \frac{4\pi}{|T(\mathbf{k}_1 - \mathbf{k}_3) - \mathbf{G}|^2} \\ & \times \langle i\mathbf{k}_1 | e^{i[T(\mathbf{k}_1 - \mathbf{k}_3) - \mathbf{G}] \cdot \mathbf{r}} | k\mathbf{k}_3 \rangle_{\Omega_{\text{cell}}} \langle j\mathbf{k}_2 | e^{-i[T(\mathbf{k}_4 - \mathbf{k}_2) - \mathbf{G}] \cdot \mathbf{r}} | l\mathbf{k}_4 \rangle_{\Omega_{\text{cell}}} . \end{aligned} \quad (3.40)$$

We find that the two-electron integrals vanish unless the crystal momentum conservation is fulfilled

$$\mathbf{k}_1 + \mathbf{k}_2 = \mathbf{k}_3 + \mathbf{k}_4 + \mathbf{G}, \quad (3.41)$$

which is manifest in the Kronecker delta. This eliminates one sum over the BZ in equation (3.34), i.e. we can fix $\mathbf{k}_4 = T(\mathbf{k}_1 + \mathbf{k}_2 - \mathbf{k}_3)$.

3.5 Goldstone diagrams

We can represent MP perturbation theory graphically via Goldstone diagrams. Figure 3.1 depicts the diagrammatic representation of the MP2 energy.

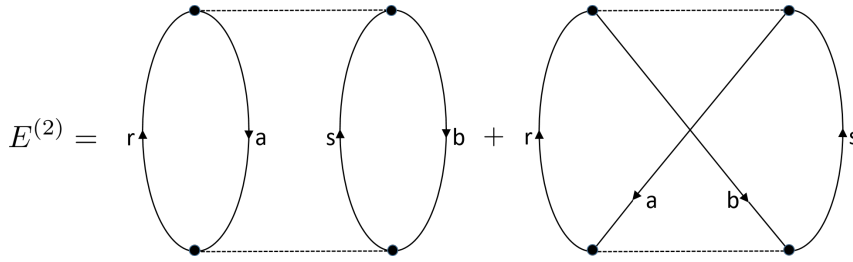


FIGURE 3.1: Diagrammatic representation of the MP2 energy. Left: direct diagram, right: exchange diagram. The upgoing lines labeled a, b, \dots indicate holes, whereas the downgoing lines labeled r, s, \dots indicate particles. The horizontal dashed lines represent the Coulomb interaction. Both diagrams have a global left/right symmetry and are thus multiplied by $1/2$.

The general rules for evaluating Goldstone diagrams read [see 27, chapter 6]

- (i) Each interaction line contributes a matrix factor

$$\langle \text{label-left in, label-right in} | \text{label-left out, label-right out} \rangle$$

to the numerator.

- (ii) Each pair of adjacent interaction lines contributes the denominator factor

$$\sum \varepsilon_{\text{hole}} - \sum \varepsilon_{\text{particle}}$$

where the sums run over the labels of all hole and particle lines crossing an imaginary horizontal line separating the two adjacent interaction lines.

- (iii) The overall sign of the expression is $(-)^{h+l}$, where h and l are the number of hole lines and closed loops, respectively.
- (iv) Sum the expression over all particle and hole indices.
- (v) Diagrams which have a mirror plane perpendicular to the plane of the paper are multiplied by a factor of $1/2$.
- (vi) For closed shell systems, a summation over spin orbitals is equal to 2^l times a summation over spatial orbitals, i.e.

$$\sum^N = 2^l \sum^{N/2}.$$

We have introduced the denominations “hole” and “particle” for occupied and unoccupied orbitals respectively. This picture corresponds to a physical interpretation of the excited determinants, which we have defined by moving electrons from occupied to unoccupied orbitals. The number of closed loops l can be easily determined by following the particle/hole lines along the direction that is indicated by the arrows, e.g. there are two loops for the direct MP2 diagram and one for the exchange diagram respectively.

3.5.1 Linked-cluster theorem

Especially for solids, it is important that a perturbation series is “size consistent”, i.e. its application to N independent units gives N times the correlation energy of the single unit. However, some terms in a Rayleigh-Schrödinger perturbation series scale as N^2 , not as N . In the mid 1950s, K.A. Brueckner was able to show, that up to 6th order in the perturbation series, the N^2 terms all cancel and conjectured, that this should be true for all orders. Shortly after, J. Goldstone proved that the N^2 terms are represented by unlinked diagrams, and that such diagrams never appear in the final result for a correlation energy. Hence, Goldstone verified Brueckner’s conjecture, which is now called the “linked-cluster theorem” (see Szabo and Ostlund [27, chapter 6] and references cited therein).

3.6 Random phase approximation

To derive the MP2 approximation for the correlation energy, we have included all terms (or equivalently all connected Goldstone diagrams) up to second order in the MP perturbation series. Analogously, we can derive higher order approximations (MP3, MP4, ...) by including all third, fourth, ... order diagrams. As we will see, it is also possible to sum up certain

“ring diagrams”, depicted in figure 3.2, up to infinite order. This is called the “random phase approximation” (RPA). We can apply the Goldstone rules to evaluate the RPA correlation energy, which yields

$$E_{\text{corr}}^{\text{RPA}} = \frac{1}{2} \sum_{ab}^{\text{occ}} \sum_{rs}^{\text{unocc}} \frac{\langle ab|rs\rangle \langle rs|ab\rangle}{\varepsilon_a + \varepsilon_b - \varepsilon_r - \varepsilon_s} + \sum_{abc}^{\text{occ}} \sum_{rst}^{\text{unocc}} \frac{\langle ac|rt\rangle \langle bt|sc\rangle \langle rs|ab\rangle}{(\varepsilon_a + \varepsilon_c - \varepsilon_r - \varepsilon_t)(\varepsilon_a + \varepsilon_b - \varepsilon_r - \varepsilon_s)} + \dots \quad (3.42)$$

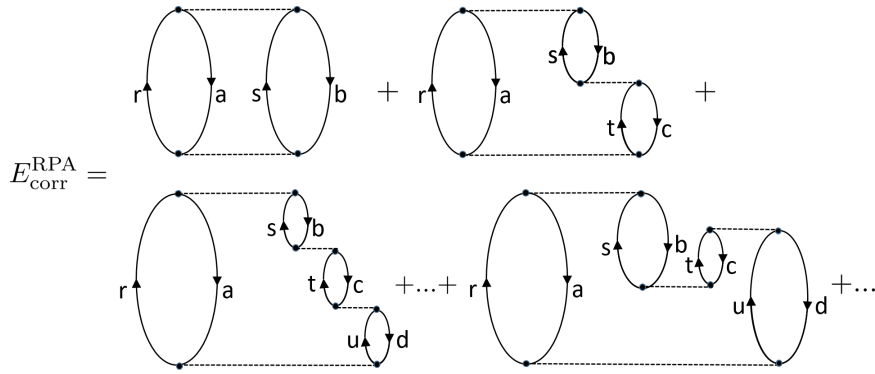


FIGURE 3.2: Diagrammatic representation of the RPA correlation energy, see Mattock [31, chapter 10]. Each n -th order RPA diagram has n rings, up to $n = 3$ there is only one distinct diagram. The leading RPA term is the direct MP2 diagram, compare figure 3.1.

In the following, we will derive a closed expression for $E_{\text{corr}}^{\text{RPA}}$ along the lines of Hummel [32]. We will not discuss the underlying principles of quantum field theory, but treat the derivation rather as an elaborate rewriting of $E_{\text{corr}}^{\text{RPA}}$.

We begin by expressing the energy denominator in the direct MP2 - term as

$$\begin{aligned} \frac{1}{\varepsilon_a + \varepsilon_b - \varepsilon_r - \varepsilon_s + i\eta} &= -i \int_{-\infty}^0 dt e^{\eta t} e^{-i(\varepsilon_a + \varepsilon_b - \varepsilon_r - \varepsilon_s)t} \\ &= -i \int_{t' > t} dt dt' \delta(t') e^{\eta t} e^{-i(\varepsilon_a + \varepsilon_b - \varepsilon_r - \varepsilon_s)(t-t')}, \end{aligned} \quad (3.43)$$

where we have added an infinitesimally small positive number η to render the integral convergent. By defining the “free propagator”

$$G_0(\mathbf{x}t; \mathbf{x}'t') := \begin{cases} -\frac{1}{\Omega} \sum_a^{\text{occ}} \varphi_a(\mathbf{x}) \varphi_a^*(\mathbf{x}') e^{(-i\varepsilon_a + \eta)(t-t')} & \text{for } t \leq t' \\ +\frac{1}{\Omega} \sum_r^{\text{unocc}} \varphi_r(\mathbf{x}) \varphi_r^*(\mathbf{x}') e^{(-i\varepsilon_r - \eta)(t-t')} & \text{otherwise,} \end{cases} \quad (3.44)$$

we can rewrite the direct MP2 - term as

$$\begin{aligned}
E_d^{(2)} &= \frac{-i}{2} \sum_{ab}^{\text{occ}} \sum_{rs}^{\text{unocc}} \int_{t_1 > t_3} dt_1 dt_3 \delta(t_1) e^{\eta(t_3 - t_1)} e^{-i(\varepsilon_a + \varepsilon_b - \varepsilon_r - \varepsilon_s)(t_3 - t_1)} \\
&\quad \times \frac{1}{\Omega^2} \int d\mathbf{x}_1 d\mathbf{x}_2 \varphi_a^*(\mathbf{x}_1) \varphi_b^*(\mathbf{x}_2) \frac{1}{|\mathbf{x}_1 - \mathbf{x}_2|} \varphi_r(\mathbf{x}_1) \varphi_s(\mathbf{x}_2) \\
&\quad \times \frac{1}{\Omega^2} \int d\mathbf{x}_3 d\mathbf{x}_4 \varphi_r^*(\mathbf{x}_3) \varphi_s^*(\mathbf{x}_4) \frac{1}{|\mathbf{x}_3 - \mathbf{x}_4|} \varphi_a(\mathbf{x}_3) \varphi_b(\mathbf{x}_4) \\
&= -i \int_{t_1 > t_3} dt_1 dt_3 \int d\mathbf{x}_1 d\mathbf{x}_2 d\mathbf{x}_3 d\mathbf{x}_4 \delta(t_1) \frac{1}{|\mathbf{x}_1 - \mathbf{x}_2|} \frac{1}{|\mathbf{x}_3 - \mathbf{x}_4|} \\
&\quad \times G_0(\mathbf{x}_1 t_1, \mathbf{x}_3 t_3) G_0(\mathbf{x}_3 t_3, \mathbf{x}_1 t_1) G_0(\mathbf{x}_2 t_1, \mathbf{x}_4 t_3) G_0(\mathbf{x}_4 t_3, \mathbf{x}_2 t_1).
\end{aligned} \tag{3.45}$$

To make the expression more symmetric, we extend the t_3 - integration to $[-\infty, \infty]$ and introduce additional “time” integrals $\int dt_2 dt_4$. To compensate, we have to include a factor $1/2$ and two delta functions

$$\begin{aligned}
(-i)E_d^{(2)} &= \frac{1}{4} \int dt_1 dt_2 dt_3 dt_4 \int d\mathbf{x}_1 d\mathbf{x}_2 d\mathbf{x}_3 d\mathbf{x}_4 \\
&\quad \times \delta(t_1) \frac{(-i)\delta(t_1 - t_2)}{|\mathbf{x}_1 - \mathbf{x}_2|} \frac{(-i)\delta(t_3 - t_4)}{|\mathbf{x}_3 - \mathbf{x}_4|} \\
&\quad \times G_0(\mathbf{x}_1 t_1, \mathbf{x}_3 t_3) G_0(\mathbf{x}_3 t_3, \mathbf{x}_1 t_1) G_0(\mathbf{x}_2 t_2, \mathbf{x}_4 t_4) G_0(\mathbf{x}_4 t_4, \mathbf{x}_2 t_2).
\end{aligned} \tag{3.46}$$

We proceed by introducing the “free particle polarizability” $\chi_0(\mathbf{x}t, \mathbf{x}'t')$

$$\chi_0(\mathbf{x}t, \mathbf{x}'t') = \chi_0(\mathbf{x}, \mathbf{x}', t - t') := iG_0(\mathbf{x}t, \mathbf{x}', t') G_0(\mathbf{x}'t', \mathbf{x}t) \tag{3.47}$$

and switch to the frequency domain

$$\chi_0(\mathbf{x}, \mathbf{x}', \omega) = \int d(t - t') e^{i\omega(t - t')} \chi_0(\mathbf{x}, \mathbf{x}', t - t'), \tag{3.48}$$

which simplifies the expression for $E_d^{(2)}$ significantly, as we can use up all the delta functions

$$\begin{aligned}
E_d^{(2)} &= \frac{i}{4} \int d\mathbf{x}_1 d\mathbf{x}_2 d\mathbf{x}_3 d\mathbf{x}_4 \frac{1}{|\mathbf{x}_1 - \mathbf{x}_2|} \frac{1}{|\mathbf{x}_3 - \mathbf{x}_4|} \int dt_1 dt_2 dt_3 dt_4 \\
&\quad \times \int \frac{d\omega}{2\pi} \frac{d\omega'}{2\pi} e^{-\omega(t_1 - t_3)} e^{-i\omega'(t_4 - t_2)} \delta(t_1 - t_2) \delta(t_3 - t_4) \\
&\quad \times \chi_0(\mathbf{x}_1, \mathbf{x}_3, \omega) \chi_0(\mathbf{x}_4, \mathbf{x}_2, \omega') \\
&= \frac{i}{4} \int \frac{d\omega}{2\pi} \int d\mathbf{x}_1 d\mathbf{x}_2 d\mathbf{x}_3 d\mathbf{x}_4 \\
&\quad \times \chi_0(\mathbf{x}_1, \mathbf{x}_3, \omega) \frac{1}{|\mathbf{x}_3 - \mathbf{x}_4|} \chi_0(\mathbf{x}_4, \mathbf{x}_2, \omega) \frac{1}{|\mathbf{x}_2 - \mathbf{x}_1|}.
\end{aligned} \tag{3.49}$$

By using the shorthand notations

$$\begin{aligned}\text{Tr}\{A(\mathbf{x}, \mathbf{x}', \omega)\} &= \text{Tr}\{A(\omega)\} := \int d\mathbf{x} A(\mathbf{x}, \mathbf{x}, \omega) \\ (AB)(\mathbf{x}, \mathbf{x}'', \omega) &:= \int d\mathbf{x}' A(\mathbf{x}, \mathbf{x}', \omega) B(\mathbf{x}', \mathbf{x}'', \omega),\end{aligned}\tag{3.50}$$

we finally obtain

$$E_d^{(2)} = \frac{i}{4} \int \frac{d\omega}{2\pi} \text{Tr} \{(\chi_0(\omega)\mathbf{V})^2\}.\tag{3.51}$$

The third order contribution to $E_{\text{corr}}^{\text{RPA}}$ can still be evaluated fairly easily, as there is only one Goldstone diagram. The crucial step is the extension of the time intervals to $[-\infty, \infty]$, see equation (3.46). Symbolically, we obtain

$$\int_{t_1 > t_2 > t_3} dt_1 dt_2 dt_3 = \frac{1}{6} \int_{-\infty}^{\infty} dt_1 dt_2 dt_3,\tag{3.52}$$

hence the third order contribution is given by

$$E_{\text{corr}}^{\text{RPA},(3)} = \frac{i}{6} \int \frac{d\omega}{2\pi} \text{Tr}\{(\chi_0(\omega)\mathbf{V})^3\}.\tag{3.53}$$

For higher orders, we have to sum up all Goldstone diagrams of that order. In general, the n -th order contribution is given by [see 32]

$$E_{\text{corr}}^{\text{RPA},(n)} = \frac{i}{2n} \int \frac{d\omega}{2\pi} \text{Tr}\{(\chi_0(\omega)\mathbf{V})^n\}.\tag{3.54}$$

We can use the Taylor expansion of $\ln(1-x)$

$$\ln(1-x) = -x - \frac{x^2}{2} - \frac{x^3}{3} - \dots,\tag{3.55}$$

to sum up all diagrams up to infinite order

$$\begin{aligned}E_{\text{corr}}^{\text{RPA}} &= \frac{i}{2} \int \frac{d\omega}{2\pi} \text{Tr} \left\{ \sum_{n=2}^{\infty} \frac{1}{n} (\chi_0(\omega)\mathbf{V})^n \right\} \\ &= -\frac{i}{2} \int \frac{d\omega}{2\pi} \text{Tr} \{ \ln(\mathbf{1} - \chi_0(\omega)\mathbf{V}) - \chi_0(\omega)\mathbf{V} \}.\end{aligned}\tag{3.56}$$

In practical calculations, we can handle the poles of χ_0 (located close to the real axis) by switching to imaginary frequencies, i.e.

$$E_{\text{corr}}^{\text{RPA}} = \frac{1}{2} \int \frac{d\omega}{2\pi} \text{Tr} \{ \ln(\mathbf{1} - \chi_0(i\omega)\mathbf{V}) - \chi_0(i\omega)\mathbf{V} \}.\tag{3.57}$$

For spin restricted periodic systems, the RPA correlation energy be written as [see 33]

$$E_{\text{corr}}^{\text{RPA}} = \int \frac{d\omega}{2\pi} \sum_{\mathbf{k}} \sum_{\mathbf{G}}^{\text{BZ}} \left\{ (\ln [\mathbf{1} - \chi_0(\mathbf{k}, i\omega)\mathbf{V}])_{\mathbf{G}\mathbf{G}} - \chi_{0\mathbf{G}\mathbf{G}}(\mathbf{k}, i\omega) \frac{4\pi}{(\mathbf{k} - \mathbf{G})^2} \right\}. \quad (3.58)$$

The Fourier representation of χ_0 is given by

$$\chi_{0\mathbf{G}\mathbf{G}'}(\mathbf{k}, \omega) = \frac{1}{\Omega_{\text{cell}}} \sum_{mn}^{\text{all}} \sum_{\mathbf{k}'}^{\text{BZ}} 2(f_{m\mathbf{k}'+\mathbf{k}} - f_{n\mathbf{k}'}) \times \frac{\langle m\mathbf{k}'+\mathbf{k} | e^{i(\mathbf{k}-\mathbf{G})\cdot\mathbf{r}} | n\mathbf{k}' \rangle_{\Omega_{\text{cell}}} \langle n\mathbf{k}' | e^{-i(\mathbf{k}-\mathbf{G})\cdot\mathbf{r}} | m\mathbf{k}'+\mathbf{k} \rangle_{\Omega_{\text{cell}}}}{\varepsilon_{m\mathbf{k}'+\mathbf{k}} - \varepsilon_{n\mathbf{k}'} - \omega - i\eta}, \quad (3.59)$$

where $f_{n\mathbf{k}}$ is 1 for occupied and 0 for unoccupied states .

The RPA can also be approached from a density functional theory (DFT) point of view. Through the “adiabatic-connection fluctuation-dissipation theorem” (ACFDT), it is possible to derive an exact expression for the correlation energy that depends on the polarizability of the interacting system, which is generally unknown. However, it can be related to the ground state polarizability through the ACFDT version of the random phase approximation. This yields an expression for $E_{\text{corr}}^{\text{RPA}}$ that is equivalent to equation (3.57), with the exception that the spin-orbitals that constitute χ_0 are the DFT orbitals, i.e. they minimize the DFT-, not the HF ground state energy, see Hummel [32] and Harl [33]. In the course of her thesis, Harl also discusses the implementation of the ACFDT-RPA expression in VASP.

Chapter 4

Pseudization of the $e^- - e^-$ interaction

In this chapter we apply the revised RRKJ method as discussed in section 2.7 to construct a pseudo-potential for the classical electron-electron interaction. As the repulsive Coulomb potential

$$V(r) = \frac{1}{r} \quad (4.1)$$

does not have any bound states, we use the normalization condition (2.84) throughout. In the following we discuss critical details of the implementation, such as numerical methods used and the choice of important parameters such as the reference energy E_{ref} .

4.1 Two-particle interaction

In contrast to the pseudo-potentials discussed before, the Born-Oppenheimer approximation is not applicable. Therefore, we have to solve a two-particle Schrödinger equation with the interaction potential $V(\mathbf{r}_1 - \mathbf{r}_2)$. Analog to the classical case, we can decouple the two-particle problem by coordinate transformation [see 34, pp. 89-90]. This yields two independent one-particle (time-independent) Schrödinger equations, one for the center of mass coordinates $M\mathbf{R} = m_1\mathbf{r}_1 + m_2\mathbf{r}_2$, where $M := m_1 + m_2$ is the total mass, and another for the relative coordinates $\mathbf{r} := \mathbf{r}_1 - \mathbf{r}_2$. The first describes a free particle of mass M

$$-\frac{1}{2M}\nabla_{\mathbf{R}}^2\Psi_{\mathbf{R}}(\mathbf{R}) = E_{\mathbf{R}}\Psi_{\mathbf{R}}(\mathbf{R}) \quad (4.2)$$

the second a particle of the reduced mass μ in the external potential V

$$\left[-\frac{1}{2\mu}\nabla_{\mathbf{r}}^2 + V(\mathbf{r})\right]\Psi_{\mathbf{r}}(\mathbf{r}) = E_{\mathbf{r}}\Psi_{\mathbf{r}}(\mathbf{r}) \quad (4.3)$$

$$\mu := \frac{m_1 m_2}{m_1 + m_2}.$$

As $\mu = m_e/2$ for the two-electron system, the radial Schrödinger equation of interest is [1],[2]

$$\left[-\frac{d^2}{dr^2} + \frac{l(l+1)}{r^2} + V(r) \right] \phi_l(r) = E\phi_l(r). \quad (4.4)$$

Furthermore, E can be interpreted as the kinetic energy of the separated electrons in the center of mass frame, where $E_{\mathbf{R}} = 0$.

4.2 Numerov algorithm

The Numerov algorithm is a fourth order integration method for problems of the type

$$\frac{d^2}{dt^2}x(t) = f(t)x(t), \quad (4.5)$$

such as the radial Schrödinger equation. The integration scheme consists of two steps and reads

$$\begin{aligned} x(t) &= \frac{1}{1 - \frac{(\Delta t)^2}{12}f(t)}w(t) \\ w(t + \Delta t) &= 2w(t) - w(t - \Delta t) + (\Delta t)^2f(t)x(t) \end{aligned} \quad (4.6)$$

The derivation is straightforward [see 17, pp. 573-574]: We expand $x(t + \Delta t)$ and $x(t - \Delta t)$ around $t = 0$ up to order six in t and add the equations to obtain

$$x(\Delta t) + x(-\Delta t) - 2x(0) = (\Delta t)^2f(0)x(0) + \frac{(\Delta t)^4}{12}x^{(4)}(0) + \mathcal{O}(\Delta t)^6 \quad (4.7)$$

We can make use of the form of equation (4.5) to replace the fourth derivative by a central difference scheme of second derivatives

$$x^{(4)} = \frac{f(\Delta t)x(\Delta t) - 2f(0)x(0) + f(-\Delta t)x(-\Delta t)}{(\Delta t)^2}. \quad (4.8)$$

We introduce

$$w(t) = \left(1 - \frac{(\Delta t)^2}{12}f(t) \right) x(t) \quad (4.9)$$

and rewrite equation (4.7) as

$$w(\Delta t) + w(-\Delta t) - 2w(0) = (\Delta t)^2f(0)x(0) + \mathcal{O}((\Delta t)^6), \quad (4.10)$$

yielding a sixth order expression for $x(t)$. However, the integration error over a fixed interval t scales only as $(\Delta t)^4$ (see Thijssen [17, p. 574] and references cited therein).

4.2.1 Boundary conditions

We use the Numerov algorithm whenever we need to integrate the radial Schrödinger equation (4.4), both for the Coulomb and the pseudo-potential. To initialize the algorithm, we need $\phi(0)$ and $\phi(\Delta r)$. For a regular potential, i.e. a potential that fulfills

$$\lim_{r \rightarrow 0} r^2 V(r) = 0, \quad (4.11)$$

we can neglect everything but the kinetic and centrifugal term for small r (and $l \neq 0$) and obtain

$$\frac{d^2}{dr^2} \phi(r) = \frac{l(l+1)}{r^2} \phi(r), \quad (4.12)$$

with general solution

$$\phi(r) = c_1 r^{l+1} + c_2 r^{-l}. \quad (4.13)$$

The second term is unphysical (there are fundamental objections beyond the singularity at $r = 0$ [see 15, pp. 210-211]) and can be neglected, leaving us with

$$\phi(r) \propto r^{l+1}. \quad (4.14)$$

The proportionality constant determines the norm of the wave function and can thus be set arbitrarily, since we enforce normalization at the end. Thus, we obtain

$$\phi(0) = 0; \quad \phi(\Delta r) = r^{l+1}. \quad (4.15)$$

4.3 Construction of the pseudo-potential

For each angular quantum number up to $l = l_{\max}$, we solve the radial Schrödinger equation for the Coulomb potential at $E = E_{\text{ref}}$ numerically as described above and store the value of the wave functions ϕ_l and their derivatives at $r = r_c$ (we discuss the truncation w.r.t. l as well as appropriate choices for the reference energy and the cutoff radius later on). Second, we construct the pseudo wave function by determining the parameters in the expansion (2.98). The q_i can be easily calculated by finding the first n roots of

$$f(q) = \frac{\frac{d}{dr} j_l(qr)}{j_j(qr)} \Big|_{r=r_c} - \left(\frac{\frac{d}{dr} \phi_l(r)}{\phi_l(r)} - \frac{1}{r} \right) \Big|_{r=r_c}, \quad (4.16)$$

compare equations (2.94),(2.75). We found that for relevant values of r_c and E_{ref} , it is always possible to find parameters α_i that fulfill the normalization condition, hence we choose $n = 3$ throughout. If we insert the expansion (2.98) into equation (2.95), the conditions on the α_i read

$$\begin{aligned} \text{(i)} \quad & \sum_i \alpha_i j_j(q_i r_c) r_c = \phi(r_c) \\ \text{(ii)} \quad & \sum_i \alpha_i [2j_j'(q_i r_c) q_i + j_j''(q_i r_c) q_i^2 r_c] = \phi''(r_c) \\ \text{(iii)} \quad & \sum_{i,j} 4\pi \int_0^{r_c} dr r^2 \alpha_j j_l(q_j) \alpha_i j_l(q_i r_c) = 1. \end{aligned} \quad (4.17)$$

We treat this problem by linearizing equation III

$$\sum_{ij} a_j A_{ij} a_i = 1 \rightarrow \alpha_j^{(n-1)} A_{ij} \alpha_i^{(n)} = 1 \quad (4.18)$$

and solving the resulting linear problem iteratively (the A_{ij} are integrals over spherical Bessel functions, see appendix A). We start with a random set $\alpha_i^{(0)}$ that fulfills the normalization condition and iterate until

$$\sum_{ij} a_j^{(n)} A_{ij} \alpha_i^{(n)} = 1. \quad (4.19)$$

Before each iteration step, normalization must be enforced. The convergence of this iterative scheme is very fast throughout (the number of iterations needed is $\lesssim 5$ for all relevant test cases).

Finally, we invert the Schrödinger equation to obtain the pseudo-potential

$$V_l^{\text{ps}}(r) = E_{\text{ref}} - \frac{l(l+1)}{r^2} + \frac{\phi_l^{\text{ps}''}(r)}{\phi_l^{\text{ps}}(r)}. \quad (4.20)$$

Figures (4.1) and (4.2) depict the typical form of the pseudo wave functions ϕ_l^{ps} and pseudo-potentials V_l^{ps} respectively.

4.4 Analysis of the scaling behavior

We can take advantage of the fact that the V_l can be optimized separately: Since $q_3^2/2\mu$ can be interpreted as a cutoff-energy E_c that determines convergence in Fourier space, we choose the cutoff-radii such that q_3 is approximately the same for all l (otherwise we would typically obtain V_l^{ps} that are unnecessarily hard for higher l). From the ansatz

$$r_{cl} = \sigma^l r_c, \quad (4.21)$$

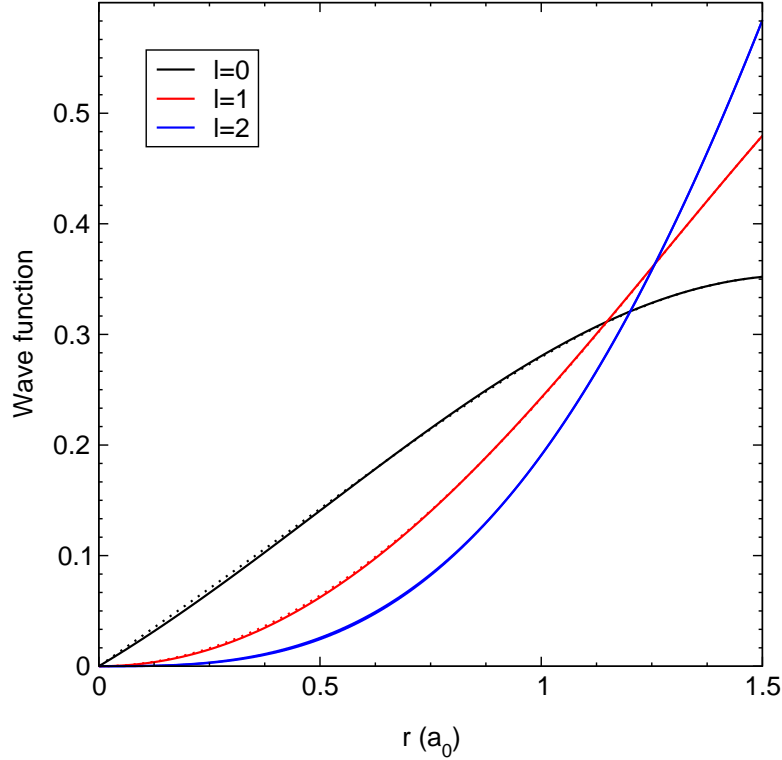


FIGURE 4.1: The pseudo wave functions ϕ_l^{ps} (dashed lines) are norm conserving and join the original wave functions ϕ_l (solid lines) smoothly at $r = r_c$. The cutoff radius was set to $1.5 a_0$ for all l and the reference energy was set to $2 E_h$.

we determine $\sigma \approx 1.14$ for $l_{\text{max}} = 2$. Since the repulsive Coulomb potential allows only scattering state solutions with a continuous energy spectrum, the choice for the reference energy is not as obvious as it is for bound states. Using dimensional analysis, we assess $q_c \propto r_c^{-1}$ from the form of the spherical Bessel functions. This means that the reference energy has to scale as

$$E_{\text{ref},l} \propto \frac{1}{r_{cl}^2}, \quad (4.22)$$

if we want to optimize the low energy scattering states ($E \ll E_c$). This ansatz is solidified by calculations that show the correct scaling behavior of E_{ref} , which is depicted in figures 4.3 and 4.4. To avoid singularities in the pseudo-potentials, E_{ref} must be located in the first branch of the logarithmic derivatives, since the branch cuts indicate nodes of the wave function.

4.5 Fourier space representation

As we have already seen, the form factor $V_{\mathbf{G}\mathbf{G}'}^{\text{loc}}$ of a local potential depends only on $\mathbf{G} - \mathbf{G}'$

$$V_{\mathbf{G}\mathbf{G}'}^{\text{loc}} = \frac{1}{\Omega_{\text{cell}}} \int d\mathbf{r} e^{-i(\mathbf{G}-\mathbf{G}')\cdot\mathbf{r}} V^{\text{loc}}(\mathbf{r}). \quad (4.23)$$

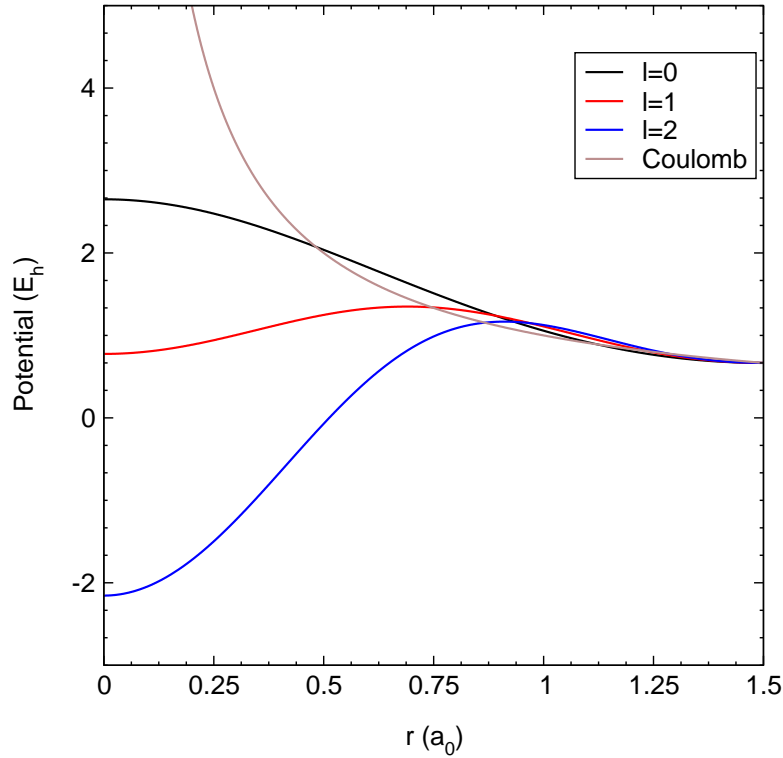


FIGURE 4.2: The pseudo-potential components V_l^{ps} are continuous at $r = r_c$. As r_c gets smaller, the pseudo-potential gets harder and the pseudo-wave functions converge towards their original counterparts. The same parameters as in figure 4.1 were used.

We can use the spherical symmetry of V^{loc} to efficiently evaluate the components via sine transform [4]

$$\begin{aligned}
 V_{\mathbf{G}\mathbf{G}'}^{\text{loc}} &= \frac{1}{\Omega_{\text{cell}}} \int_0^\infty dr r^2 V^{\text{loc}}(r) \int_0^{2\pi} d\phi \int_{-1}^1 d \cos \theta e^{-i|\mathbf{G}-\mathbf{G}'|r \cos \theta} \\
 &= \frac{1}{\Omega_{\text{cell}}} 2\pi \int_0^\infty dr r^2 V^{\text{loc}}(r) \frac{1}{-i|\mathbf{G}-\mathbf{G}'|r} \left(e^{-i|\mathbf{G}-\mathbf{G}'|r} - e^{i|\mathbf{G}-\mathbf{G}'|r} \right) \\
 &= \frac{1}{\Omega_{\text{cell}}} \frac{4\pi}{|\mathbf{G}-\mathbf{G}'|} \int_0^\infty dr r \sin(|\mathbf{G}-\mathbf{G}'|r) V^{\text{loc}}(r).
 \end{aligned} \tag{4.24}$$

For a semi-local potential such as the pseudo-potential, however, the components depend in general on the magnitudes of $\mathbf{k} - \mathbf{G}$ and $\mathbf{k} - \mathbf{G}'$ as well as the angle γ between them. To derive the corresponding expression for the l -th component of $V_{\mathbf{G}\mathbf{G}'}^{\text{ps}}$, we insert equations (2.70) and (2.37) to expand the pseudo-potential and the plane waves

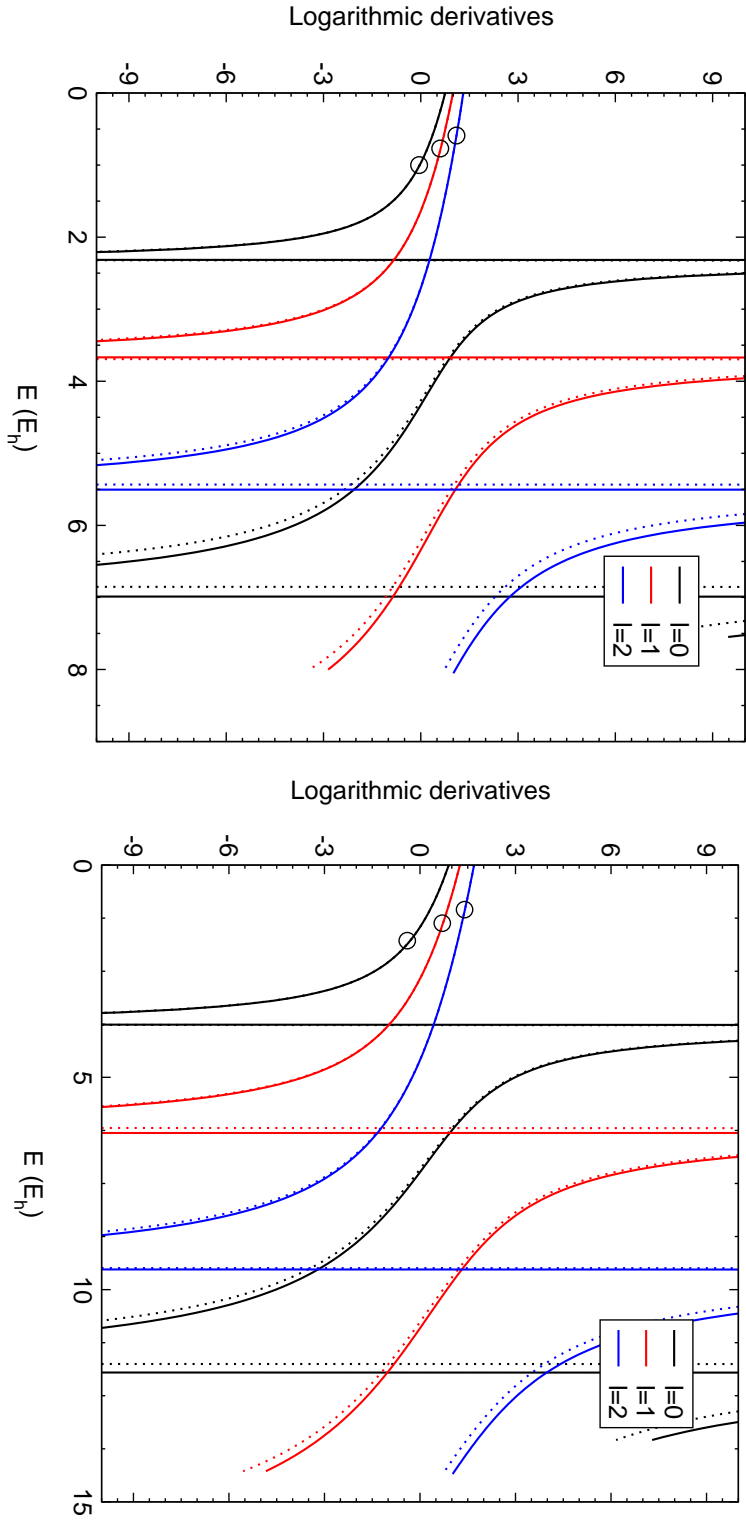


FIGURE 4.3: Depicted are the logarithmic derivatives for energies up to $E = 2E_c$ for various cutoff radii, where E_{ref} was set to $4/r_{cl}^2$ (indicated by circles). As the graphs are at least approximately similar, the assessed scaling for the reference energies is viable. The norm-conservation condition guarantees that the x_l^{ps} (dashed lines) agree with the x_l (solid lines) up to first order in E around the reference energies. For all l , the logarithmic derivatives are evaluated at $r = r_{c2}$, where $r_{c0} = 2.0 a_0$ (left) and $1.5 a_0$ (right) respectively.

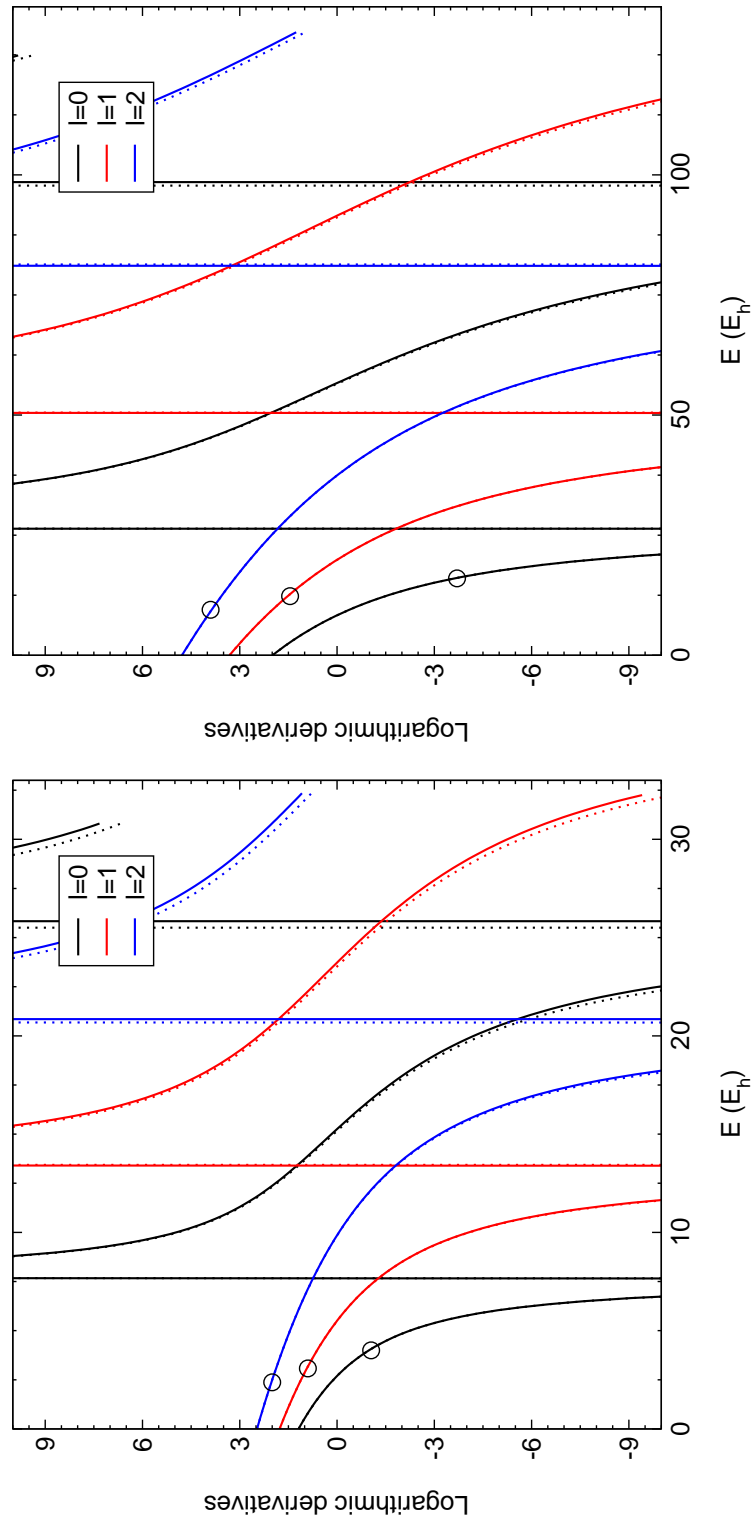


FIGURE 4.4: Same as figure 4.3, with $r_{c0} = 1.0 a_0$ (left) and $0.5 a_0$. (right) respectively.

$$\begin{aligned}
V_{l,\mathbf{G}\mathbf{G}'}^{\text{ps}} &= \frac{1}{\Omega_{\text{cell}}} \int d\mathbf{r} e^{-i(\mathbf{k}-\mathbf{G})\cdot\mathbf{r}} V_l(r) \mathcal{P}_l e^{i(\mathbf{k}-\mathbf{G}')\cdot\mathbf{r}} \\
&= \frac{1}{\Omega_{\text{cell}}} \int dr \left[4\pi \sum_{l'm'} i^{l'} Y_{l'}^{m'*}(\theta_{\mathbf{G}}, \phi_{\mathbf{G}}) Y_{l'}^{m'}(\theta, \phi) j_{l'}(|\mathbf{k}-\mathbf{G}|r) \right]^* \\
&\quad \times V_l^{\text{ps}} \mathcal{P}_l \left[4\pi \sum_{l''m''} i^{l''} Y_{l''}^{m''*}(\theta_{\mathbf{G}'}, \phi_{\mathbf{G}'}) Y_{l''}^{m''}(\theta, \phi) j_{l''}(|\mathbf{k}-\mathbf{G}'|r) \right] \\
&= \frac{1}{\Omega_{\text{cell}}} (4\pi)^2 \sum_{l'm'm} (-i)^{l'} i^l \int d\mathbf{r} V_l(r) j_{l'}(|\mathbf{k}-\mathbf{G}|r) j_l(|\mathbf{k}-\mathbf{G}'|r) \\
&\quad \times Y_l^m(\theta_{\mathbf{G}}, \phi_{\mathbf{G}}) Y_l^{m*}(\theta, \phi) Y_l^{m*}(\theta_{\mathbf{G}'}, \phi_{\mathbf{G}'}) Y_l^m(\theta, \phi) \\
&= \frac{1}{\Omega_{\text{cell}}} (4\pi)^2 \sum_m Y_l^{m*}(\theta_{\mathbf{G}'}, \phi_{\mathbf{G}'}) Y_l^m(\theta_{\mathbf{G}}, \phi_{\mathbf{G}}) \\
&\quad \times \int_0^\infty dr r^2 V_l^{\text{ps}}(r) j_l(|\mathbf{k}-\mathbf{G}|r) j_l(|\mathbf{k}-\mathbf{G}'|r),
\end{aligned} \tag{4.25}$$

where we have used equations (2.61) and (2.62). By invoking the spherical harmonic addition theorem [see 18, p. 798]

$$P_l(\cos(\gamma)) = \frac{4\pi}{2l+1} \sum_m Y_l^{m*}(\theta_{\mathbf{G}'}, \phi_{\mathbf{G}'}) Y_l^m(\theta_{\mathbf{G}}, \phi_{\mathbf{G}}), \tag{4.26}$$

where the P_l are Legendre polynomials, we finally obtain

$$\begin{aligned}
V_{l,\mathbf{G}\mathbf{G}'}^{\text{ps}} &= \frac{1}{\Omega_{\text{cell}}} (2l+1) 4\pi P_l(\cos(\gamma)) \\
&\quad \times \int_0^\infty dr r^2 V_l^{\text{ps}}(r) j_l(|\mathbf{k}-\mathbf{G}|r) j_l(|\mathbf{k}-\mathbf{G}'|r).
\end{aligned} \tag{4.27}$$

In constructing the full pseudo-potential via equation (2.70), it is convenient to subtract a local potential

$$V^{\text{ps}} = \sum_l V_l^{\text{ps}} \mathcal{P}_l = V^{\text{loc}} + \sum_l (V_l^{\text{ps}} - V^{\text{loc}}) \mathcal{P}_l, \tag{4.28}$$

where V^{loc} is in principle any function that has the correct $1/r$ - tail, such that the integrals in equation (4.27) need only be evaluated over a finite domain [35].

4.5.1 Local approximation

In practice, the sum over l is truncated after $l = l_{\text{max}}$, which implies the approximation

$$\sum_{l=l_{\text{max}}}^{\infty} (V_l^{\text{ps}} - V^{\text{loc}}) \approx 0. \tag{4.29}$$

However, since V is a pseudo-potential, only its scattering properties matter, and we can replace this requirement by the much weaker approximation

$$\begin{aligned} x_l^{\text{ps}}(r_{cl}) - x_l^{\text{loc}}(r_{cl}) &\approx 0 && \text{for } l > l_{\text{max}}, \\ \text{or equivalently } x_l(r_{cl}) - x_l^{\text{loc}}(r_{cl}) &\approx 0 && \text{for } l > l_{\text{max}}. \end{aligned} \quad (4.30)$$

Oftentimes the local potential is chosen to be the pseudo-potential component with the highest l , i.e.

$$V^{\text{loc}} = V_{l_{\text{max}}}^{\text{ps}}. \quad (4.31)$$

In figure 4.5, we show that already the local approximation ($l_{\text{max}} = 0$), is viable. Apart from simplicity, the major advantage of the local approximation is a substantial reduction in computation cost, since we need not evaluate any integrals of the type of equation (4.27).

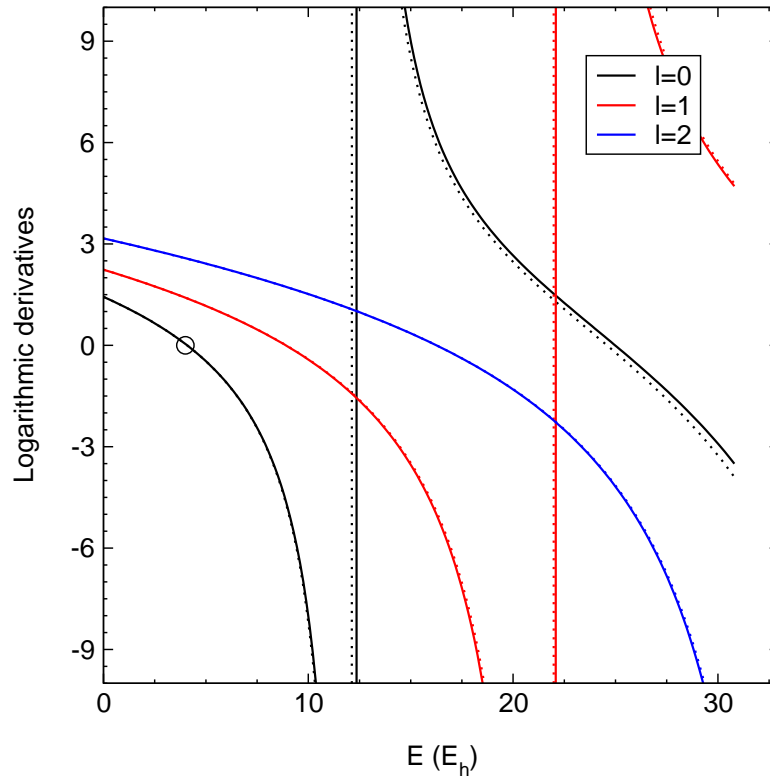


FIGURE 4.5: Depicted are the $x_l(r_c)$ (solid lines) versus the $x_l^{\text{loc}}(r_c)$ (dashed lines) at $r = r_c$. The local approximation $V^{\text{loc}} = V_0^{\text{ps}}$ is valid, as the local potential reproduces the scattering properties of the Coulomb potential very well also for higher l channels. The cutoff radius was set to $1.0 a_0$ and the reference energy was set to $4.0 E_h$.

We are then left with integrals of the form

$$V_{\mathbf{G}\mathbf{G}'}^{\text{ps}}(|\mathbf{G} - \mathbf{G}'|) = \frac{1}{\Omega_{\text{cell}}} \frac{4\pi}{|\mathbf{G} - \mathbf{G}'|} \int_0^\infty dr r \sin(|\mathbf{G} - \mathbf{G}'|r) V_0^{\text{ps}}(r), \quad (4.32)$$

which we evaluate by subtracting the singular Coulomb-potential, whose Fourier transform is given by [8, chapter 17]

$$V(q) = \int d\mathbf{r} e^{-i\mathbf{q}\cdot\mathbf{r}} \frac{1}{r} = \frac{4\pi}{q^2}. \quad (4.33)$$

This relation follows from the fact that the Coulomb potential obeys the Poisson equation

$$\begin{aligned} \nabla^2 V(\mathbf{r}) &= -4\pi\delta^3(\mathbf{r}) \\ \nabla^2 \int \frac{d\mathbf{q}}{(2\pi)^3} e^{i\mathbf{q}\cdot\mathbf{r}} V(\mathbf{q}) &= -4\pi\delta^3(\mathbf{r}) \\ \int \frac{d\mathbf{q}}{(2\pi)^3} e^{i\mathbf{q}\cdot\mathbf{r}} \frac{q^2}{4\pi} V(\mathbf{q}) &= \delta^3(\mathbf{r}) \\ \rightarrow V(q) &= \frac{4\pi}{q^2}. \end{aligned} \quad (4.34)$$

Thus, we obtain

$$\begin{aligned} V_{\mathbf{G}\mathbf{G}'}^{\text{ps}}(|\mathbf{G} - \mathbf{G}'|) &= \frac{1}{\Omega_{\text{cell}}} \frac{4\pi}{|\mathbf{G} - \mathbf{G}'|} \int_0^\infty dr r \sin(|\mathbf{G} - \mathbf{G}'| r) \left(V_0^{\text{ps}}(r) - \frac{1}{r} \right) \\ &+ \frac{1}{\Omega_{\text{cell}}} \frac{4\pi}{|\mathbf{G} - \mathbf{G}'|^2} \\ &= \frac{1}{\Omega_{\text{cell}}} \frac{4\pi}{|\mathbf{G} - \mathbf{G}'|} \int_0^{r_c} dr r \sin(|\mathbf{G} - \mathbf{G}'| r) \left(V_0^{\text{ps}}(r) - \frac{1}{r} \right) \\ &+ \frac{1}{\Omega_{\text{cell}}} \frac{4\pi}{|\mathbf{G} - \mathbf{G}'|^2} \\ &:= \Delta V(|\mathbf{G} - \mathbf{G}'|) + \frac{4\pi}{|\mathbf{G} - \mathbf{G}'|^2}. \end{aligned} \quad (4.35)$$

Figure 4.6 depicts the typical Fourier space behavior of the pseudo-potentials. Since the α_3 -component is typically very small (see figure 4.7), the Fourier space convergence is largely determined by q_2 .

4.5.2 Analysis of the asymptotic behavior

In the limit $q := |\mathbf{G} - \mathbf{G}'| \rightarrow 0$, $\Delta V(q)$ is finite since $\Delta V(r)$ is regular

$$\lim_{q \rightarrow 0} \Delta V(q) = \frac{4\pi}{\Omega_{\text{cell}}} \int_0^{r_c} dr r^2 \Delta V(r). \quad (4.36)$$

We can use partial integration to study how $V(q)$ depends on the discontinuity of V_0^{ps} in the high frequency limit [36]

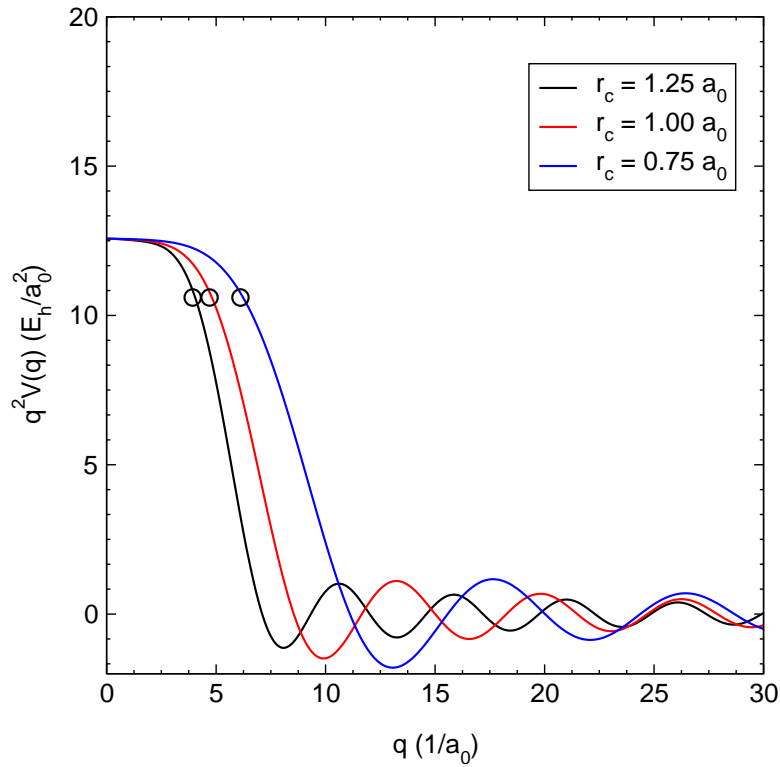


FIGURE 4.6: The potentials cut off rapidly at $q \approx q_2$ (indicated by circles) and exhibit high frequency oscillations. The reference energy was set to $4.0 E_h$ for each potential.

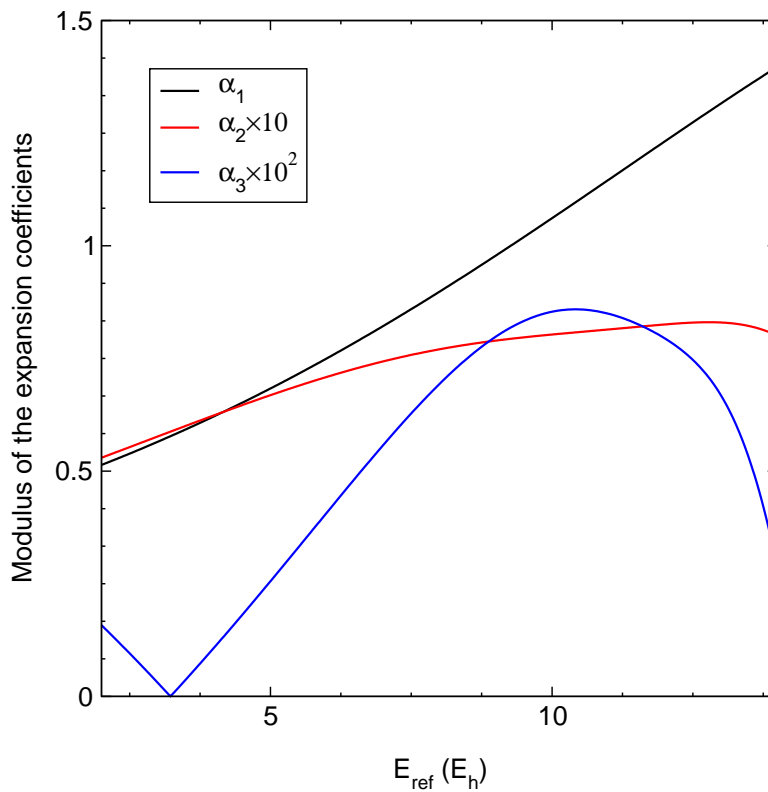


FIGURE 4.7: The expansion coefficient of the third spherical Bessel function α_3 is typically very small. The cutoff radius was set to $1.0 a_0$.

$$\begin{aligned}
\Delta V(q) &= \frac{1}{\Omega_{\text{cell}}} \frac{4\pi}{q} \int_0^\infty dr \Delta V(r) r \sin(qr) \\
&= -\frac{1}{\Omega_{\text{cell}}} \frac{4\pi}{q^2} \Delta V(r) r \cos(qr) \Big|_{r=0}^\infty \\
&\quad + \frac{1}{\Omega_{\text{cell}}} \frac{4\pi}{q^2} \int_0^\infty dr [\Delta V'(r) r + \Delta V] \cos(qr) \\
&= -\frac{1}{\Omega_{\text{cell}}} \frac{4\pi}{q^2} + \frac{1}{\Omega_{\text{cell}}} \frac{4\pi}{q^3} \sin(qr) [\Delta V' r + \Delta V] \Big|_{r=0}^\infty \\
&\quad - \frac{1}{\Omega_{\text{cell}}} \frac{4\pi}{q^3} \int_0^\infty dr \left[\frac{d}{dr} (\Delta V'(r) \theta(r_c - r)) r + 2\Delta V'(r) \right] \sin(qr) \\
&= -\frac{1}{\Omega_{\text{cell}}} \frac{4\pi}{q^2} + \frac{1}{\Omega_{\text{cell}}} \frac{4\pi}{q^3} \Delta V'(r_c) r_c \sin(qr_c) + \mathcal{O}(1/q^4).
\end{aligned} \tag{4.37}$$

We find that first term exactly cancels the Coulomb term, and the two boundary terms vanish since V_0^{ps} and $V_0^{\text{ps}'}$ are finite at the origin. Thus, the high frequency oscillations are in leading order caused by the mismatch of the first derivative at the cutoff radius. Figure 4.8 compares the asymptotic behavior of the pseudo-potentials with the prediction derived above.

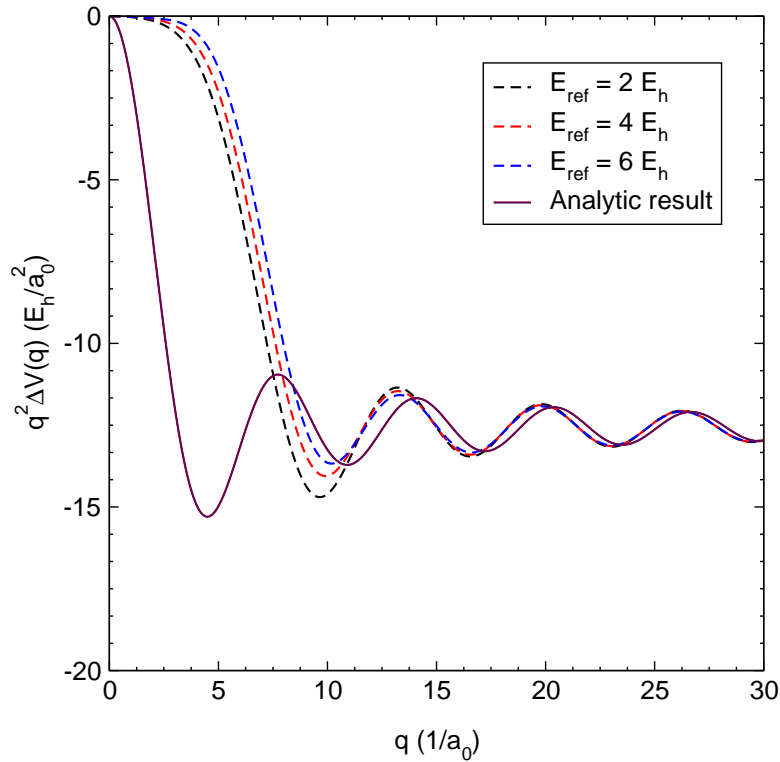


FIGURE 4.8: Depicted are various pseudo-potentials with $r_c = 1.0 a_0$ and different reference energies versus the third order analytic predictions ($\Delta V(r_c)$ does not change significantly enough to distinguish the lines).

4.6 Maximum reference energy rule

Given a set cutoff radius, it is possible to choose E_{ref} such that α_3 , the component of the third spherical Bessel function, vanishes, which is depicted in figure 4.9. This is remarkable insofar, as it effectively means that we can eliminate this “surplus” degree of freedom to obtain norm conservation.

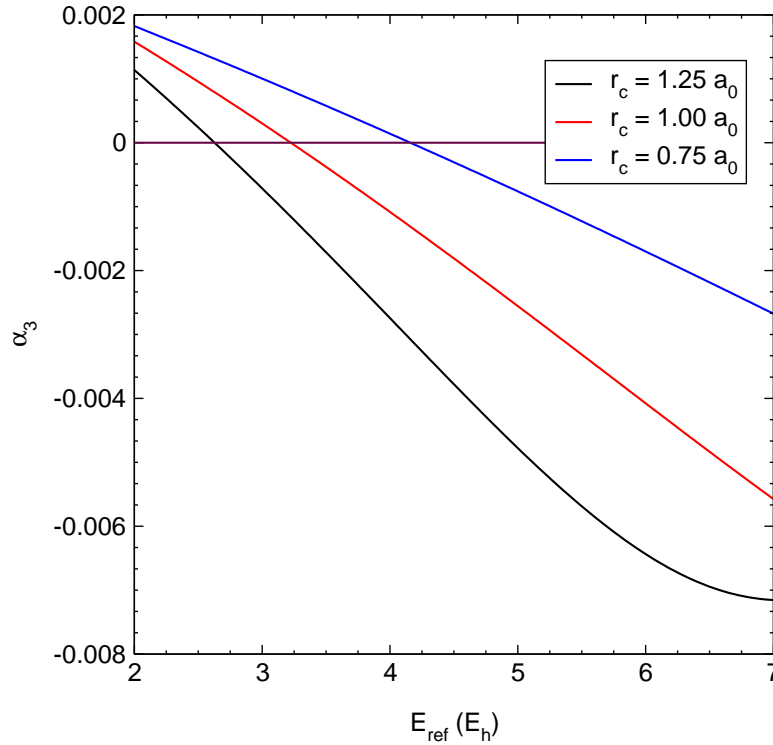


FIGURE 4.9: It is consistently possible to find a reference energy for which α_3 vanishes. This reference energy is located in the middle of the first branch of the logarithmic derivatives.

Similarly, we can choose E_{ref} such that the third derivative of the pseudo wave function and the original wave function match at the cutoff radius. In figure 4.10, we show that this is exactly achievable only at nodes of the wave function.

This can be understood by differentiating the inverted Schrödinger equation (4.20)

$$\begin{aligned}
 V_0^{\text{ps}'}(r) &= \frac{\phi_0^{\text{ps}'''}(r)}{\phi_0^{\text{ps}}(r)} - \frac{\phi_0^{\text{ps}''}(r)\phi_0^{\text{ps}'}(r)}{\phi_0^{\text{ps}}(r)^2} \\
 \Rightarrow \Delta\phi_0'''(r_c) &= \Delta V_0'(r_c)\phi_0(r_c),
 \end{aligned}
 \tag{4.38}$$

where we have used equation (2.90). Since $V'(r_c) = -1/r_c^2$ and $V_0^{\text{ps}'}(r_c) \approx 0$, which we will argue in the following, $\Delta\phi_0'''(r_c)$ can only vanish if $\phi_0(r_c)$ is equal to zero. To obtain an analytic expression for $V_0^{\text{ps}'}$, we assume that the first spherical Bessel function constitutes the main contribution to ϕ_0^{ps} and treat the rest as a small correction, which yields

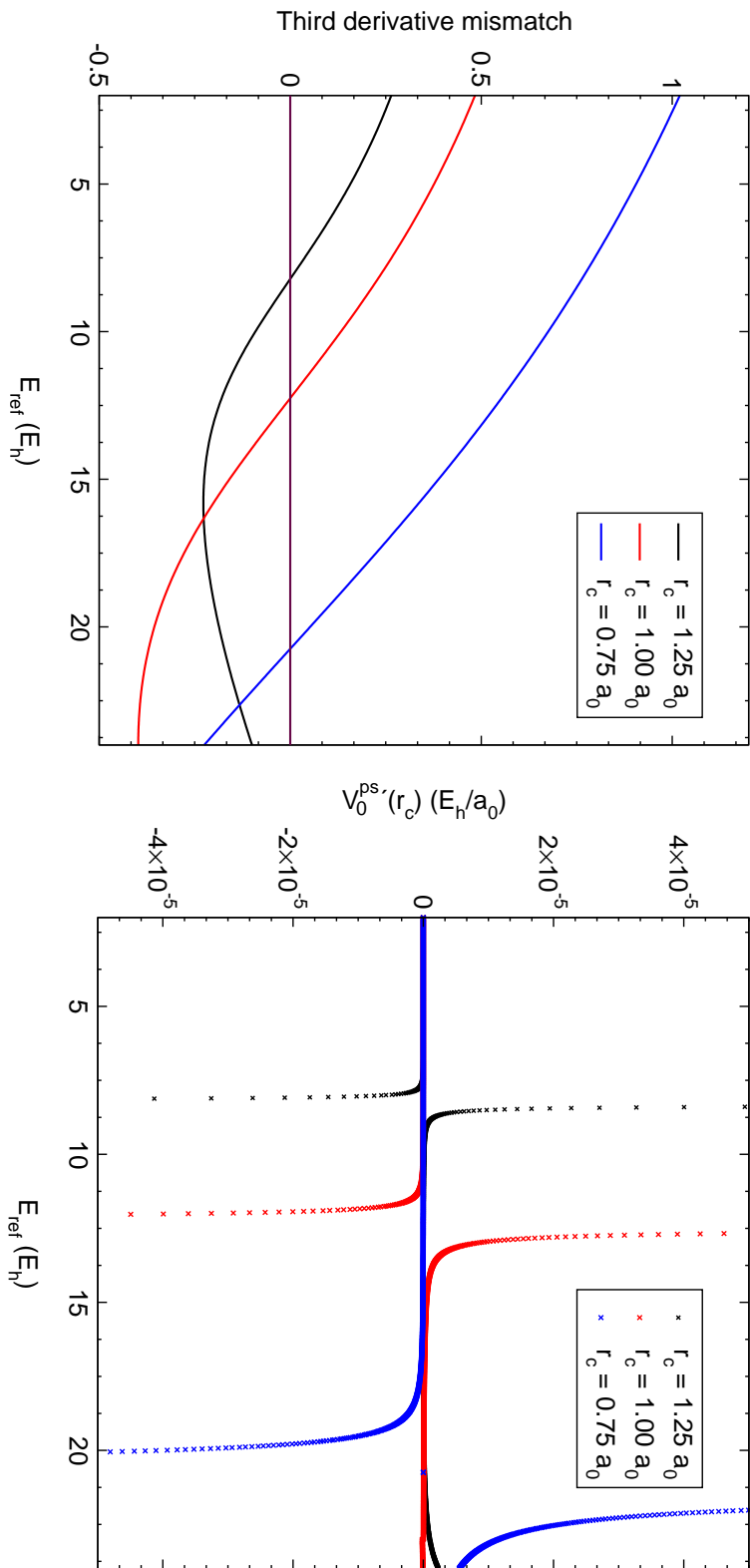


FIGURE 4.10: Left: It is possible to match also the third derivative. Shown is $\Delta\phi_0(r_c)$ for various cutoff radii. Right: The slope of the pseudo-potentials at $r = r_c$ is very small except for values of E_{ref} near the branch cuts, where V^{ps} is singular. $\Delta\phi_0(r_c)$ vanishes only for these reference energies.

$$\begin{aligned}
V_0^{\text{ps}'}(r) &\approx - \left\{ \frac{\alpha_1 \cos(q_1 r) q_1^2 + \sum_{i=2}^3 \alpha_i \cos(q_i r) q_i^2}{\alpha_1 \sin(q_1 r) q_1^{-1} + \sum_{i=2}^3 \alpha_i \sin(q_i r) q_i^{-1}} \right. \\
&\quad \left. - \frac{[\alpha_1 \sin(q_1 r) q_1 + \sum_{i=2}^3 \alpha_i \sin(q_i r) q_i][\alpha_1 \cos(q_1 r) + \sum_{i=2}^3 \alpha_i \cos(q_i r)]}{[\alpha_1 \sin(q_1 r) q_1^{-1} + \sum_{i=2}^3 \alpha_i \sin(q_i r) q_i^{-1}]^2} \right\} \\
&\approx 0 + \sum_{i=2}^3 \frac{\alpha_i}{\alpha_1} \left\{ \frac{\sin(q_i r) \cos(q_1 r) [q_1^4 - q_1^5/q_i]}{\sin^2(q_1 r)} \right. \\
&\quad \left. + \frac{\cos(q_i r) [q_1^3 - q_1 q_i^2]}{\sin(q_1 r)} \right\} + \dots,
\end{aligned} \tag{4.39}$$

where we have used the expansions

$$\frac{1}{1+x} \approx 1 - x + \mathcal{O}(x^2), \quad \frac{1}{(1+x)^2} \approx 1 - 2x + \mathcal{O}(x^2). \tag{4.40}$$

In figure 4.11, we compare this result with a numerical evaluation of $V_0^{\text{ps}'}$.

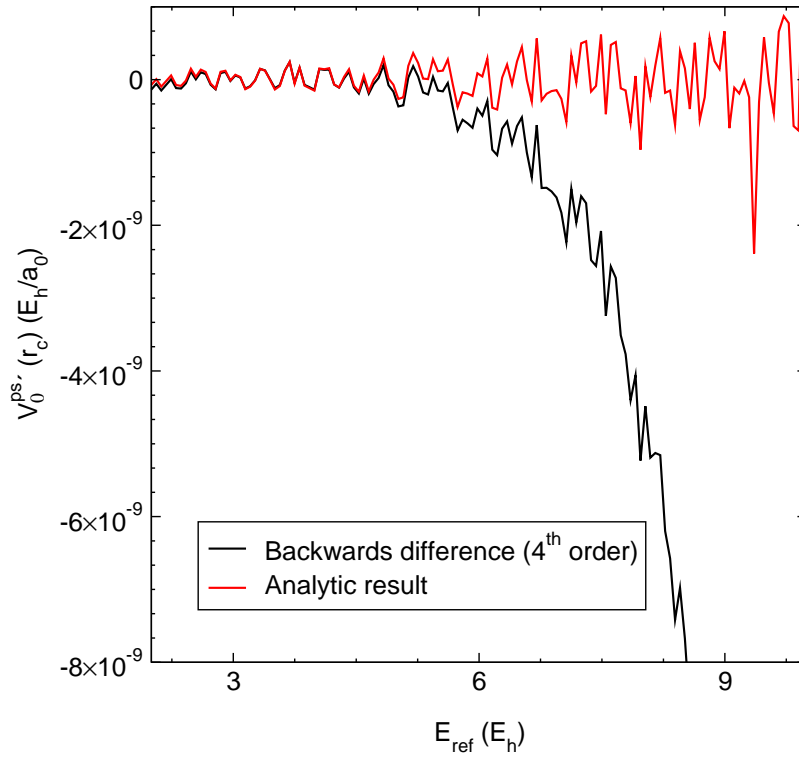


FIGURE 4.11: The first order series expansion shows good agreement for small reference energies. For large reference energies $\phi_0^{\text{ps}}(r_c)$ is small, rendering the expansion inapplicable. The cutoff radius was set to $1.0 a_0$.

By inserting $V_0^{\text{ps}'}(r_c) = 0$ in equation (4.37), we also obtain an explicit dependency for the amplitudes A of the high frequency oscillations on the cutoff radius

$$A(r_c) \approx \frac{1}{\Omega_{\text{cell}}} \frac{4\pi}{q^3} \frac{1}{r_c}. \tag{4.41}$$

To sum up, it is not possible to match the third derivatives exactly due to the form of ϕ_0 . Nevertheless, figure 4.10 shows that it is approximately achievable by choosing E_{ref} slightly to the left of the first branch cut. Furthermore, this “maximum reference energy rule” is also supported by the fact that the logarithmic derivatives are better reproduced for energies beneath E_{ref} , which is depicted in figure 4.12. A similar observation was made by Prendergast *et al.* [1], who used a HSC-type pseudo-potential to study the effect of the electron-electron cusp on configuration interaction energies.

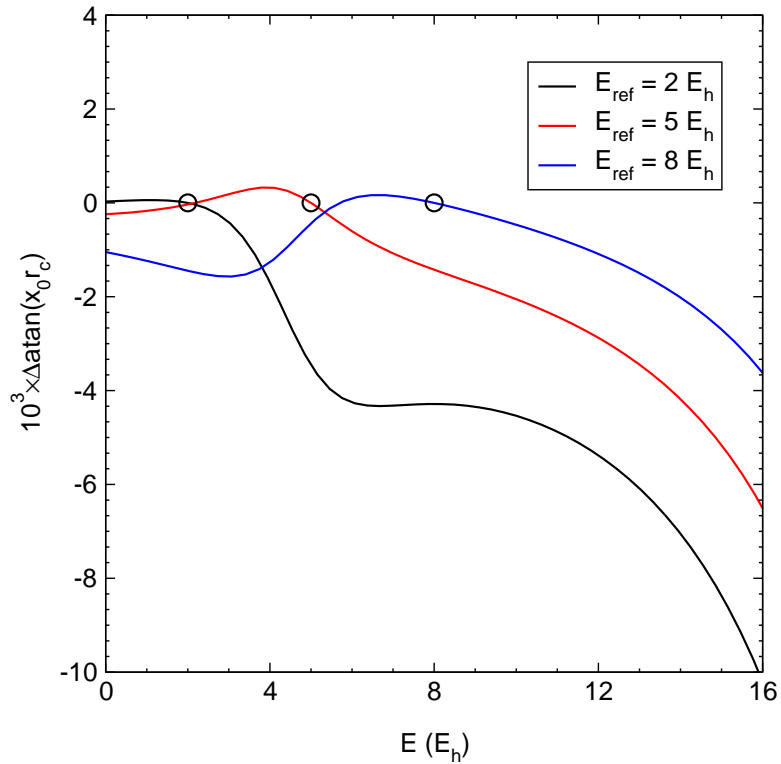


FIGURE 4.12: To fairly compare the scattering properties at different energies, we take the atan of the dimensionless quantity $x_0 r_c$. We find that the pseudo-potentials perform better for energies below E_{ref} . The extrema at $E = E_{\text{ref}}$ that we expect from norm conservation are slightly shifted, as $\Delta \dot{x}_0(r_c)$ is not exactly zero. This error is likely due to numerical inaccuracies in the construction of the pseudo-potential, amounts for intermediate r_c to $\lesssim 10^{-3} a_0^{-1} E_h^{-1}$ and vanishes for $r_c \rightarrow 0$. The cutoff radius was set to $1.0 a_0$.

Chapter 5

Correlation energies for Jellium

The natural test system for the electron-electron interaction is the homogeneous electron gas (“Jellium”). We obtain the many-body Hamiltonian for Jellium by replacing the nuclei in the Born-Oppenheimer Hamiltonian (3.3) by a homogeneous positive background charge

$$H_{\text{MB}} = \sum_{i=1}^N -\frac{1}{2} \nabla_i^2 + \sum_{i<j} \frac{1}{|\mathbf{r}_i - \mathbf{r}_j|} - \sum_{i=1}^N \int d\mathbf{r} \frac{n}{|\mathbf{r}_i - \mathbf{r}|} + \frac{1}{2} \int d\mathbf{r} d\mathbf{r}' \frac{n^2}{|\mathbf{r} - \mathbf{r}'|}, \quad (5.1)$$

where $n = N/\Omega$ is the average electron density [37]. The system is entirely characterized by n or equivalently by the standard density parameter r_s (also called “Wigner-Seitz radius”)

$$\frac{4\pi}{3} r_s^3 = \frac{\Omega}{N}, \quad r_s = \left(\frac{3}{4\pi n} \right)^{1/3}, \quad (5.2)$$

that is a measure for the average distance between electrons. For elemental solids, r_s typically ranges from 1 a_0 to 6 a_0 [see 14, p. 101]. Since the solutions are homogeneous, the background terms exactly cancel the Hartree energy

$$E_H := \frac{1}{2} \int d\mathbf{r} d\mathbf{r}' n(\mathbf{r}) n(\mathbf{r}') n(\mathbf{r}) := \langle \Psi | \sum_i \delta(\mathbf{r} - \mathbf{r}_i) | \Psi \rangle, \quad (5.3)$$

where $n(\mathbf{r})$ is the electron density. Within the spin restricted HF approximation, we can apply the first of the Slater-Condon rules (C.3) to immediately reobtain the expression of the Hartree energy that we derived in chapter 3.

$$n(\mathbf{r}) = \frac{2}{\Omega} \sum_i \varphi_i^*(\mathbf{r}) \varphi_i(\mathbf{r}) E_H = 2 \sum_{ij}^{\text{occ}} (ij|ij), \quad (5.4)$$

5.1 Simple cubic lattice

For the sake of simplicity, we simulate the Jellium system in a simple cubic (sc) unit cell. Furthermore, the high symmetry of the sc-lattice is advantageous, as we will see in the following. The direct and reciprocal lattice vectors of the simple cubic lattice are

$$a_{ij} = a\delta_{ij}, \quad b_{ij} = \frac{2\pi}{a}\delta_{ij}, \quad (5.5)$$

where a is the lattice constant and a_{ij} is the j -th component of the lattice vector \mathbf{a}_i (the same applies to b_{ij}). We sample the first Brillouin zone on a linear mesh centered at the Γ - point

$$\mathbf{k} = T(\mathbf{b}_1 \frac{n_1}{N_1} + \mathbf{b}_2 \frac{n_2}{N_2} + \mathbf{b}_3 \frac{n_3}{N_3}), \quad n_i = 0, \dots, N_i - 1. \quad (5.6)$$

Due to symmetry, some of these k -points are equivalent, i.e. we can reduce sums over the first Brillouin zone to its irreducible part (IBZ)

$$\sum_{\mathbf{k}}^{\text{BZ}} \rightarrow \sum_{\mathbf{k}}^{\text{IBZ}} w_{\mathbf{k}}, \quad (5.7)$$

where the $w_{\mathbf{k}}$ are the weights for each point in the IBZ [14, chapter 4].

For MP2 calculations, we have to consider that the MP2 energies diverge unless there is some sort of band gap, see equation (3.34). For metallic systems like Jellium, it is therefore important to find certain “magic numbers” N_i , that create a finite gap through shell filling effects. If each unit cell contains two electrons, this is achievable for $3 \times 3 \times 3$ k -points, see table 5.1. All following calculations use the $3 \times 3 \times 3$ k -point mesh to sample the IBZ.

| k -point in the IBZ [$2\pi/3a$] | weight |
|-------------------------------------|--------|
| (0,0,0) | 1 |
| (1,0,0) | 6 |
| (1,1,0) | 12 |
| (1,1,1) | 8 |

TABLE 5.1: Since we assume spin degeneracy, the energy eigenstates $\varepsilon_{n\mathbf{k}}$ can be doubly occupied. Therefore, the two electrons exactly fill up all $2 \times 3^3 = 54$ states in the lowest band.

5.2 Electron - nucleus scattering

To preliminarily test the performance of our pseudo-potentials outside a particular theory for the electron-electron interaction, we pseudize the electron-nucleus interaction. By rewriting the radial Schrödinger equation for the electron-electron interaction (4.4) as

$$\left[-\frac{1}{2} \frac{d^2}{dr^2} + \frac{l(l+1)}{2r} + \frac{V}{2} \right] \phi_l(r) = E' \phi_l(r), \quad (5.8)$$

where $E' = E/2$, we obtain an alternative interpretation of this problem as interaction between an electron and a nucleus with charge $Z = -1/2$. We therefore construct a somewhat artificial test system that is essentially sc-H, except that the H-atoms have a repulsive charge of $Z = -1/2$ and that we put in two electrons instead of one. Furthermore, we add compensating background charge to maintain charge neutrality. We pseudize the electron-nucleus interaction by replacing the Coulomb form factor

$$\frac{1}{2} \frac{4\pi}{q^2} \rightarrow \frac{1}{2} V_0^{\text{ps}}(q), \quad (5.9)$$

where the cutoff radius should be small enough that the pseudo-spheres do not overlap. In practice, the replacement is achieved by evaluating $\Delta V(q)$ on a linear mesh and interpolating to required values of q . We use natural cubic splines to perform the interpolation, see Press *et al.* [38, chapter 3]. Figure 5.1 compares the resulting band structure, obtained by a standard DFT calculation, to the original one.

5.3 Pseudization of MP perturbation theory

In the following, we will develop a pseudized MP perturbation theory for Jellium. We start by replacing the electron-electron interactions in the Jellium many-body Hamiltonian (5.1) by a local pseudo-potential V_0^{ps}

$$\begin{aligned} H_{\text{MB}}^{\text{ps}} &= \sum_{i=1}^N -\frac{1}{2} \nabla_i^2 + \sum_{i<j} V_0^{\text{ps}}(|\mathbf{r}_i - \mathbf{r}_j|) \\ &\quad - \sum_{i=1}^N \int d\mathbf{r} \frac{n}{|\mathbf{r}_i - \mathbf{r}|} + \frac{1}{2} \int d\mathbf{r}_1 d\mathbf{r}_2 \frac{n^2}{|\mathbf{r}_1 - \mathbf{r}_2|}. \end{aligned} \quad (5.10)$$

Since the correction $\Delta V(q)$ is finite, the background terms still cancel the Hartree energy, which given is solely by its $\mathbf{G} = \mathbf{0}$ - term in reciprocal space. To show this, we evaluate the Jellium Hartree energy in a small sphere of radius q_s around $\mathbf{G} = \mathbf{0}$ and take the limit $q_s \rightarrow 0$

$$\begin{aligned} E_H^{\text{ps}} &= \int d\mathbf{r}_1 d\mathbf{r}_2 n^2 V_0^{\text{ps}}(|\mathbf{r}_1 - \mathbf{r}_2|) \\ &= \lim_{q_s \rightarrow 0} \int_{q < q_s} \frac{d\mathbf{q}}{(2\pi)^3} \left[\frac{4\pi}{q^2} + \Delta V(q) \right] e^{i\mathbf{q} \cdot (\mathbf{r}_1 - \mathbf{r}_2)} \int d\mathbf{r}_1 d\mathbf{r}_2 n^2 \\ &\approx E_H + \lim_{q_s \rightarrow 0} \int_0^{q_s} \frac{dq}{(2\pi)^3} 4\pi q^2 \Delta V(q) \int d\mathbf{r}_1 d\mathbf{r}_2 n^2 = E_H. \end{aligned} \quad (5.11)$$

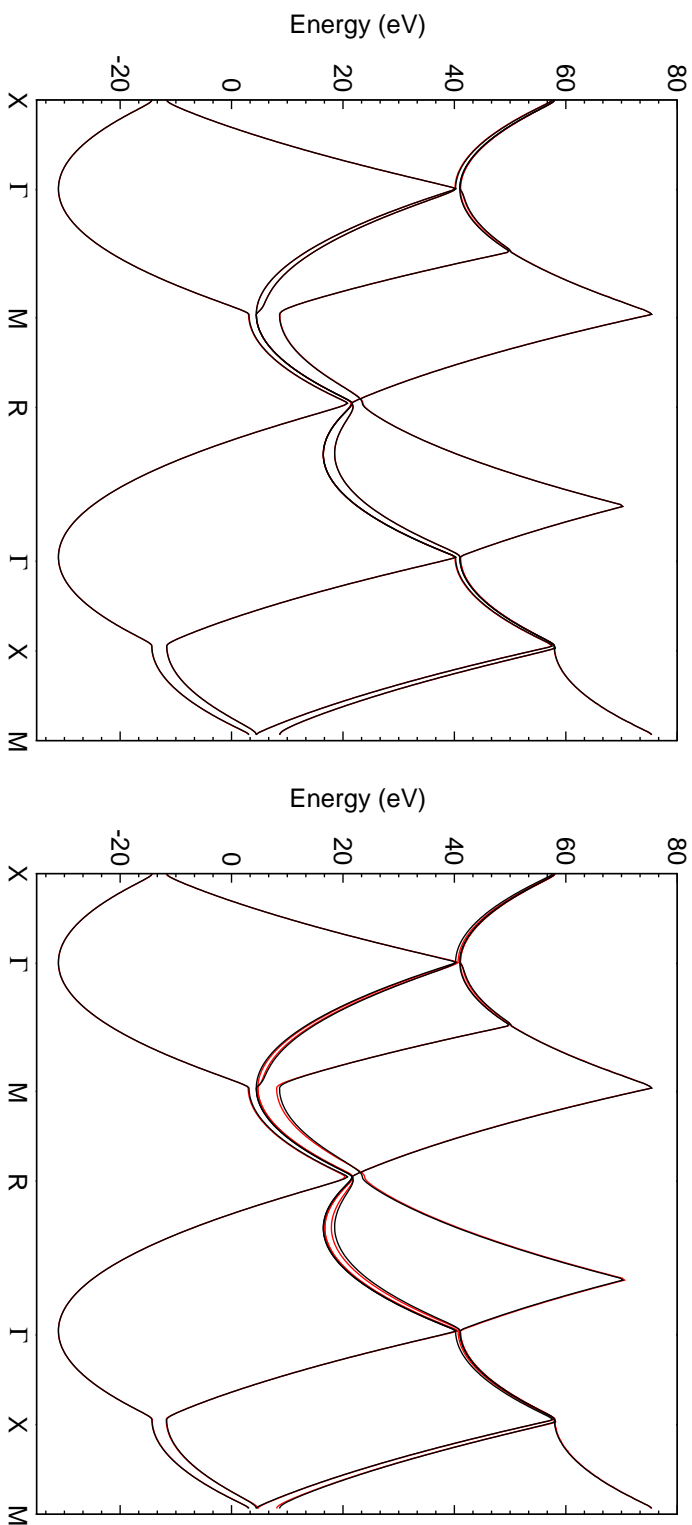


FIGURE 5.1: Depicted is the original band structure of the test system (black lines) versus the band structure of the pseudoized system (red lines). For a pseudo-potential with $r_c = 1.0a_0$ and $E_{\text{ref}} = 12.0E_h$ (left), the band structures agree well, whereas the higher bands deviate for a softer pseudo-potential with $r_c = 1.5a_0$ and $E_{\text{ref}} = 5.5E_h$ (right). The lattice constant was set to approx. $2.73 a_0$, i.e. the pseudo-spheres overlap for the softer pseudo-potential.

In the derivation, we have assumed that the lattice volume is large, so that we can approximate the sum over all \mathbf{G} by an integral, but finite, so that the correction does not diverge.

5.3.1 Hartree-Fock groundstate energies

Since E_H^{ps} is also canceled by the background terms, the pseudized electron-electron interaction still reduces to the exchange term within Hartree-Fock. Therefore, we can obtain a consistent pseudized HF-theory by simply replacing the exchange operator

$$-\sum_j^{\text{occ}} K_j^{\text{ps}} \varphi_i := -\sum_j^{\text{occ}} \frac{1}{\Omega} \int d\mathbf{r}_2 \varphi_j^*(\mathbf{r}_2) V_0^{\text{ps}}(|\mathbf{r}_1 - \mathbf{r}_2|) \varphi_i(\mathbf{r}_2) \varphi_j(\mathbf{r}_1) \quad (5.12)$$

or equivalently by replacing the form factor in the Fourier representation. So far, we have not achieved much since the HF-theory for Jellium is even analytically solvable in the thermodynamic limit $N, \Omega \rightarrow \infty, n = \text{const}$ [8, chapter 17]. The solutions are plane waves as in the non-interacting case. We can prove this by showing that plane waves are eigenfunctions of the exchange operator

$$\begin{aligned} \sum_{q_j < k_F} K_j e^{i\mathbf{q}_j \cdot \mathbf{r}_1} &= \sum_{q_j < k_F} \frac{1}{\Omega} \int d\mathbf{r}_2 e^{-i\mathbf{q}_j \cdot \mathbf{r}_2} \frac{1}{|\mathbf{r}_1 - \mathbf{r}_2|} e^{i\mathbf{q}_i \cdot \mathbf{r}_2} e^{i\mathbf{q}_j \cdot \mathbf{r}_1} \\ &\approx \sum_{q_j < k_F} \frac{1}{\Omega} \int \frac{d\mathbf{q}'}{(2\pi)^3} \frac{4\pi}{q'^2} e^{i(\mathbf{q}_j + \mathbf{q}') \cdot \mathbf{r}_1} \int d\mathbf{r}_2 e^{i(\mathbf{q}_i - \mathbf{q}_j - \mathbf{q}') \cdot \mathbf{r}_2} \\ &= \sum_{q_j < k_F} \frac{1}{\Omega} \int \frac{d\mathbf{q}'}{(2\pi)^3} \frac{4\pi}{q'^2} e^{i(\mathbf{q}_j + \mathbf{q}') \cdot \mathbf{r}_1} (2\pi)^3 \delta(\mathbf{q}_i - \mathbf{q}_j - \mathbf{q}') \quad (5.13) \\ &= \frac{1}{\Omega} \sum_{q_j < k_F} \frac{4\pi}{|\mathbf{q}_i - \mathbf{q}_j|^2} e^{i\mathbf{q}_i \cdot \mathbf{r}_1} \\ &\approx \int_{q' < k_F} \frac{d\mathbf{q}'}{(2\pi)^3} \frac{4\pi}{|\mathbf{q}_i - \mathbf{q}'|} e^{i\mathbf{q}_i \cdot \mathbf{r}_1}, \end{aligned}$$

where the Fermi wave vector k_F is the radius of the sphere that encloses the occupied states in reciprocal space

$$\frac{4\pi}{3} k_F^3 := \frac{(2\pi)^3}{\Omega} N, \quad k_F = \frac{(9\pi/4)^{1/3}}{r_s}. \quad (5.14)$$

By adding the kinetic energy, we obtain thus for the orbital energies ε_i

$$\varepsilon_i = \frac{q_i^2}{2} - \int_{q < k_F} \frac{d\mathbf{q}'}{(2\pi)^3} \frac{4\pi}{|\mathbf{q}_i - \mathbf{q}'|}, \quad (5.15)$$

which yields for the HF ground state energy

$$E_{\text{HF}} = \sum_{q_i < k_F} 2 \frac{q_i^2}{2} - \int_{q < k_F} \frac{d\mathbf{q}'}{(2\pi)^3} \frac{4\pi}{|\mathbf{q}_i - \mathbf{q}'|}, \quad (5.16)$$

compare equation (3.23). We can replace the sum by an integral to obtain a simple expression for the Jellium HF ground state energy per electron [see 8, chapter 17]

$$\frac{E_{\text{HF}}}{N} = \frac{3}{5} E_F - \frac{3k_F}{4\pi}, \quad (5.17)$$

where $E_F := k_F^2/2$ is the Fermi energy.

Although the HF ground state is thus not of theoretical interest, we can use it to gauge the pseudo-potentials. Lloyd-Williams *et al.* [2], who developed pseudo-potentials for the electron-electron interaction in CID and DMC calculations, proposed to optimize the pseudo-potentials for $E < 2E_F$, since only wave vectors below k_F are occupied in the ground state. However, from our discussion of the maximum energy rule, see section 4.6, we expect that it can prove beneficial to choose the reference energy higher than that. Figure 5.2 shows that the maximum reference energy rule works well for $r_c \gtrsim r_s$, whereas for smaller cutoff radii the maximum reference energy is too far away from $2E_F$. Then, the optimum value for E_{ref} lies between $E_{\text{ref}}^{\text{max}}(r_s)$ and $E_{\text{ref}}^{\text{max}}(r_c)$. In all following calculations, we use pseudo-potentials that are optimized for $E_F = 1 E_h$, see figure 5.2.

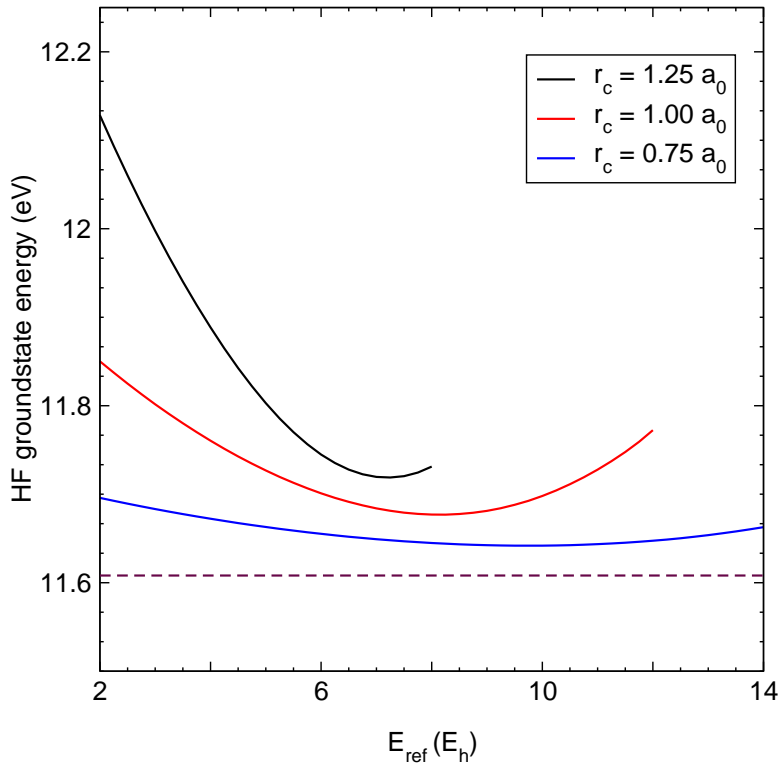


FIGURE 5.2: Depicted is the convergence of the HF ground state energies for Jellium w.r.t. the reference energy calculated using $3 \times 3 \times 3$ k -points. The dashed line indicates the ground state energy obtained by the original Coulomb potential. The lattice volume was chosen such that $E_F = 1 E_h$, which corresponds to $r_s \approx 1.36 a_0$.

5.3.2 MP2 correlation energies

The pseudized Fock operator has eigenvectors φ_i^{ps} with eigenvalues $\varepsilon_i^{\text{ps}}$. To obtain the pseudized MP perturbation series, we partition the pseudized many-body Hamiltonian as

$$H_{\text{MB}}^{\text{ps}} = H_0^{\text{ps}} + (H_{\text{MB}}^{\text{ps}} - H_0^{\text{ps}}), \quad (5.18)$$

where H_0^{ps} is the pseudized HF Hamiltonian constructed from the φ_i^{ps} . Analog to the derivation in chapter 3, the pseudized MP2 energy per unit cell is given by

$$\begin{aligned} E^{(2),\text{ps}} = & \\ & \frac{2}{N_{\text{cell}}} \sum_{\mathbf{k}_1 \dots \mathbf{k}_4}^{\text{BZ}} \sum_{ab}^{\text{occ}} \sum_{rs}^{\text{unocc}} \frac{(a\mathbf{k}_1, b\mathbf{k}_2 | r\mathbf{k}_3, s\mathbf{k}_4)^{\text{ps}} (r\mathbf{k}_3, s\mathbf{k}_4 | a\mathbf{k}_1, b\mathbf{k}_2)^{\text{ps}}}{\varepsilon_{a\mathbf{k}_1}^{\text{ps}} + \varepsilon_{b\mathbf{k}_2}^{\text{ps}} - \varepsilon_{r\mathbf{k}_3}^{\text{ps}} - \varepsilon_{s\mathbf{k}_4}^{\text{ps}}} \\ & - \frac{1}{N_{\text{cell}}} \sum_{\mathbf{k}_1 \dots \mathbf{k}_4}^{\text{BZ}} \sum_{ab}^{\text{occ}} \sum_{rs}^{\text{unocc}} \frac{(a\mathbf{k}_1, b\mathbf{k}_2 | r\mathbf{k}_3, s\mathbf{k}_4)^{\text{ps}} (r\mathbf{k}_3, s\mathbf{k}_4 | b\mathbf{k}_2, a\mathbf{k}_1)^{\text{ps}}}{\varepsilon_{a\mathbf{k}_1}^{\text{ps}} + \varepsilon_{b\mathbf{k}_2}^{\text{ps}} - \varepsilon_{r\mathbf{k}_3}^{\text{ps}} - \varepsilon_{s\mathbf{k}_4}^{\text{ps}}}, \end{aligned} \quad (5.19)$$

where the pseudized two-electron integrals are obtained by replacing the spatial orbitals and the form factor in equation (3.40) by their pseudized counterparts.

In principle, it is possible to choose a smaller cutoff energy $E_{\text{max}}^{\text{aux}}$ for the two-electron integrals than for the basis set. For the Coulomb potential, the error in the MP2 energy can be approximated as

$$E^{(2)}(E_{\text{max}}^{\text{aux}}) - E^{(2)}(E_{\text{max}}^{\text{aux}} = \infty) \approx E_{\text{max}}^{\text{aux} - 3/2} \quad \text{for } E_{\text{max}}^{\text{aux}} \text{ large}, \quad (5.20)$$

which can be used to estimate $E^{(2)}(E_{\text{max}}^{\text{aux}} = \infty)$ via extrapolation (see Schäfer *et al.* [29] and references cited therein). Since the pseudo-potentials cut off rapidly in Fourier space, the pseudized MP2 energies converge much faster. This is depicted in figure 5.3.

Although there is some error cancellation between the direct and the exchange term, the relative errors for the MP2 energies are about one order of magnitude greater than the respective errors for the HF energies. The main source of the errors is the fact that electrons of opposite spin can be located at the same place. Thus, the pseudo-potentials (with r_c fixed) are more accurate for smaller densities, as the probability that two electrons are inside a sphere of radius r_c is higher for larger densities. Figure 5.4 depicts the performance of the pseudo-potentials for different density parameters r_s .

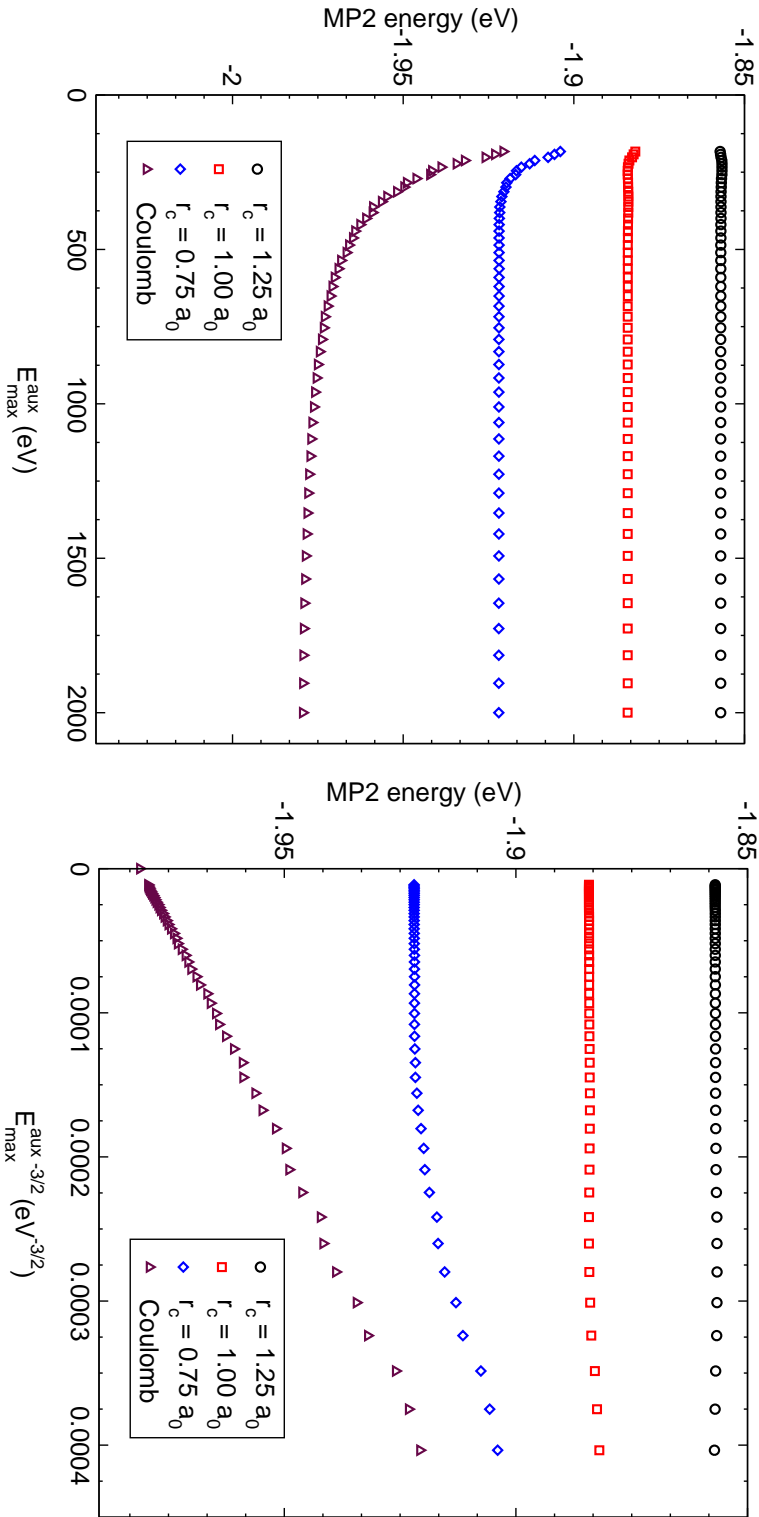


FIGURE 5.3: Left: As the pseudo-potentials cut off faster in Fourier space as r_c increases (see figure 4.6), the convergence is faster for larger r_c . There are small oscillations that stem from the fact that the slope of $V^{\text{ps}}(r)$ is discontinuous at $r = r_c$, see section 4.5. Right: For high cutoff energies, the Coulomb correlation energies scale linearly with E_{\max}^{aux} , which is used to extrapolate to $E_{\max}^{\text{aux}} = \infty$. The density parameter was the same as in figure 5.2, from which we take the optimal values for E_{ref} as well. The basis set cutoff energy was set to 2000 eV and a $3 \times 3 \times 3$ k -point mesh was used.

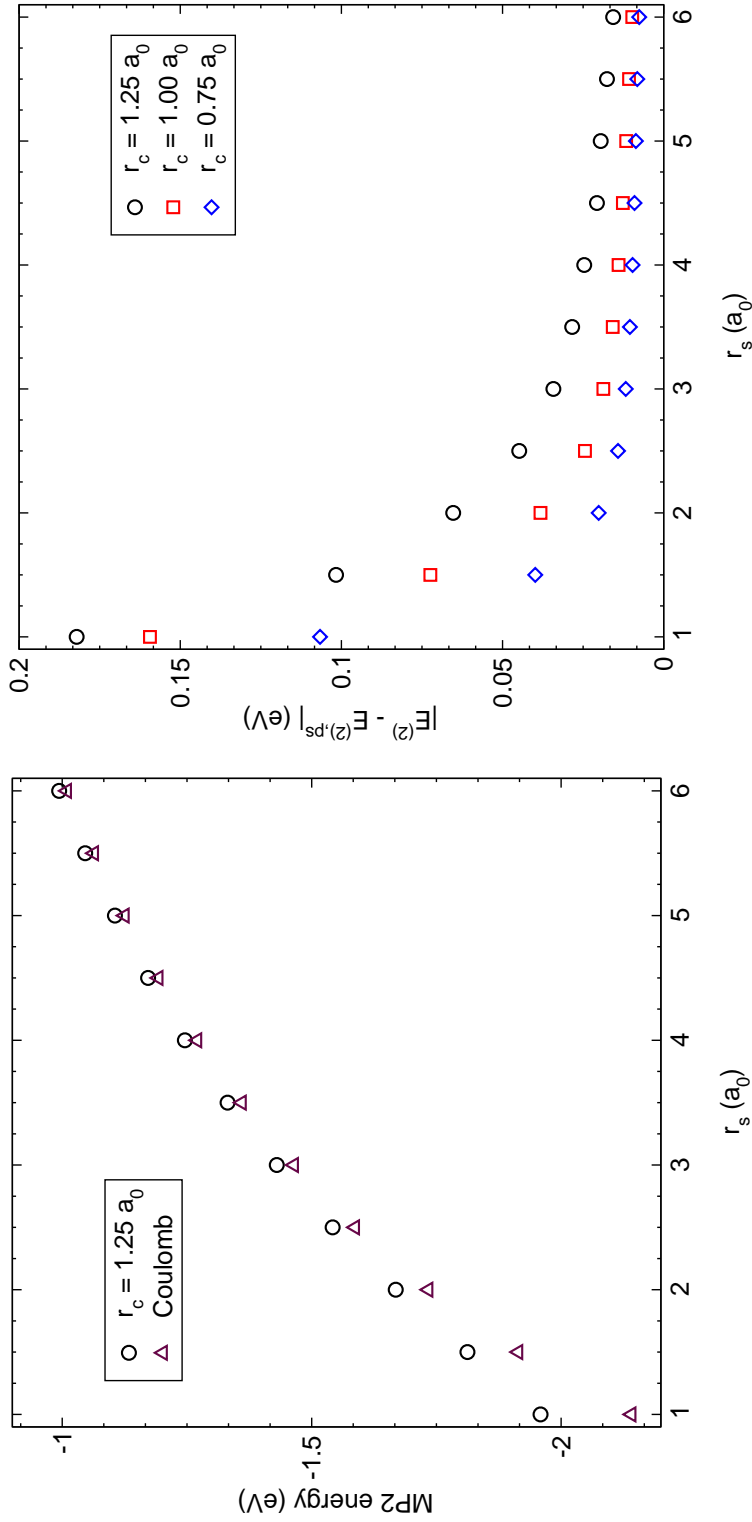


FIGURE 5.4: Depicted is the performance of the pseudo-potentials for various densities. Left: For the sake of readability, we show $E^{(2),ps}$ only for $r_c = 1.25$, right: differences between original and pseudized MP2 energies, all calculated using $3 \times 3 \times 3$ k -points. The pseudo-potentials were identical for all r_s and the reference energies for the pseudization were chosen so as to optimize the HF energies at $r_s \approx 1.36 a_0$ (compare figure 5.2) For the Coulomb potential, we show the extrapolated values. The cutoff energies were set to $E_{\max} = E_{\max}^{\text{aux}} = 1000(a_0/r_s)^2$ eV to keep the basis set size error approx. constant (≈ 0.01 eV error for the extrapolated MP2 energies).

5.4 Pseudization of ACFDT-RPA

We can obtain an alternative version of pseudized MP perturbation theory by partitioning the pseudized many-body Hamiltonian such that the zeroth order term is the original HF Hamiltonian

$$H_{\text{MB}}^{\text{ps}} = H_{\text{HF}} + (H_{\text{MB}}^{\text{ps}} - H_{\text{HF}}). \quad (5.21)$$

On the one hand, this version is convenient since we need not alter the ground state calculation. On the other hand, this complicates the expressions for the correlation energies (e.g. Brillouin's theorem does no longer apply). However, we can remedy this large disadvantage by introducing the following approximation

$$\sum_{i < j} V(|\mathbf{r}_i - \mathbf{r}_j|) |\Psi_0\rangle \approx \sum_{i < j} V^{\text{ps}}(|\mathbf{r}_i - \mathbf{r}_j|) |\Psi_0\rangle. \quad (5.22)$$

This approximation goes beyond mere pseudization, since a pseudo-potential reproduces the original eigenvalues only if it acts on the pseudo-wave function and not on the original wave function. For Jellium, the approximation is certainly valid, since plane waves are solutions for both the original and the pseudized HF ground state (only the eigenvalues change under pseudization). In general, this approximation is applicable for small cutoff radii, as the Ψ^{ps} approaches Ψ as $r_c \rightarrow 0$. Then, the pseudized MP2 energy can be obtained simply by replacing the form factor in equation (3.40). We can obtain this result also by applying the approximation (5.22) directly in the original series expansion (3.22)

We use the DFT analogon of this approximate method to obtain pseudized ACFDT-RPA correlation energies, i.e. we replace only the form factor in the DFT version of equation (3.58). As before, the cutoff energy for the correlation energies can be chosen smaller than E_{max} . Again, we can use extrapolation for the Coulomb potential, since the RPA correlation energies obey the asymptotic error behavior (5.20) as well [see 33]. Figures 5.5 and 5.6 show that the pseudo-potentials perform similarly as in the MP2 case.

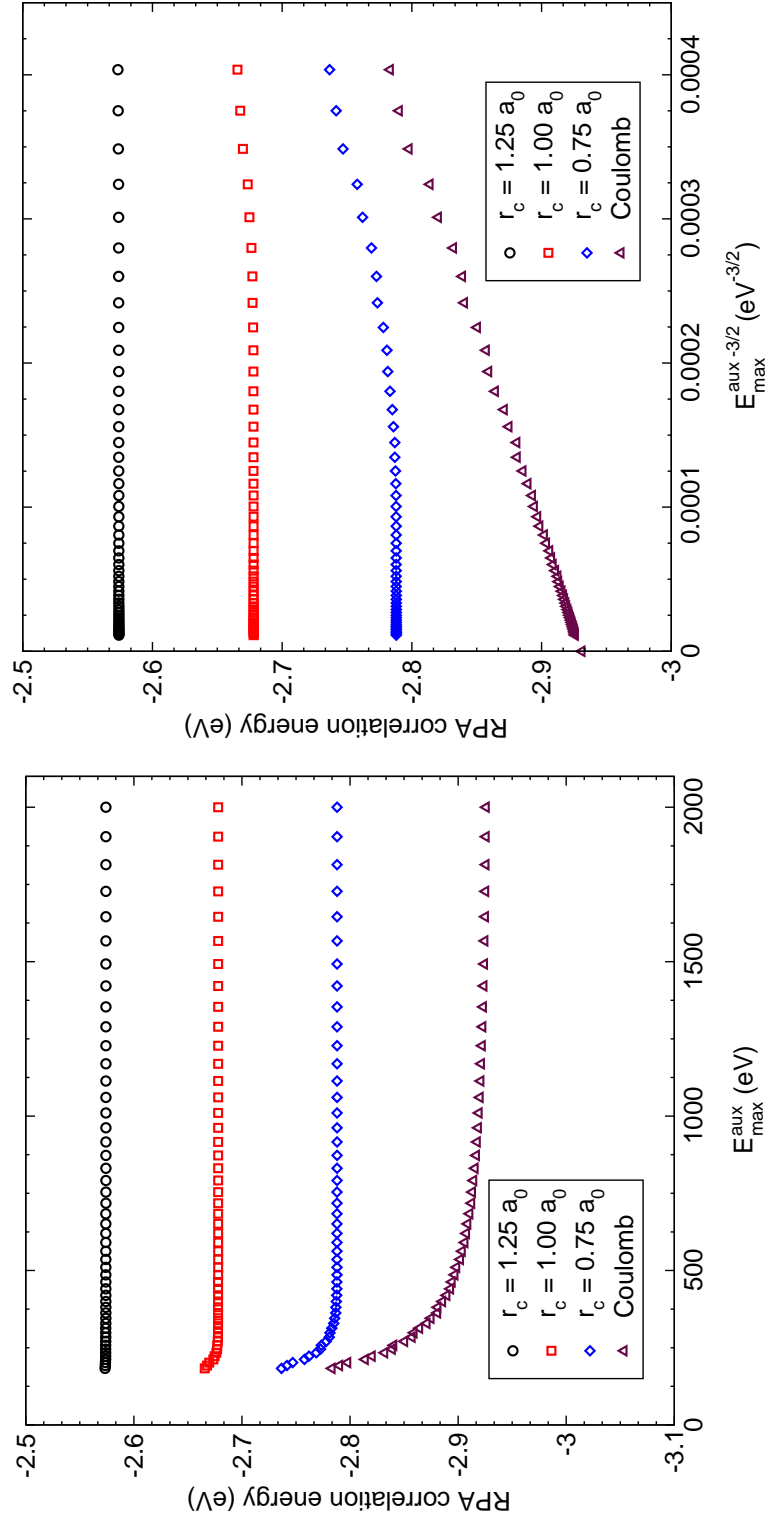


FIGURE 5.5: Depicted is the convergence of the RPA correlation energies w.r.t. E_{\max}^{aux} (left) and $E_{\max}^{\text{aux}-3/2}$ (right) respectively. Again, for the Coulomb potential we can extrapolate to $E_{\max}^{\text{aux}} = \infty$. The same parameters as in figure 5.3 were used.

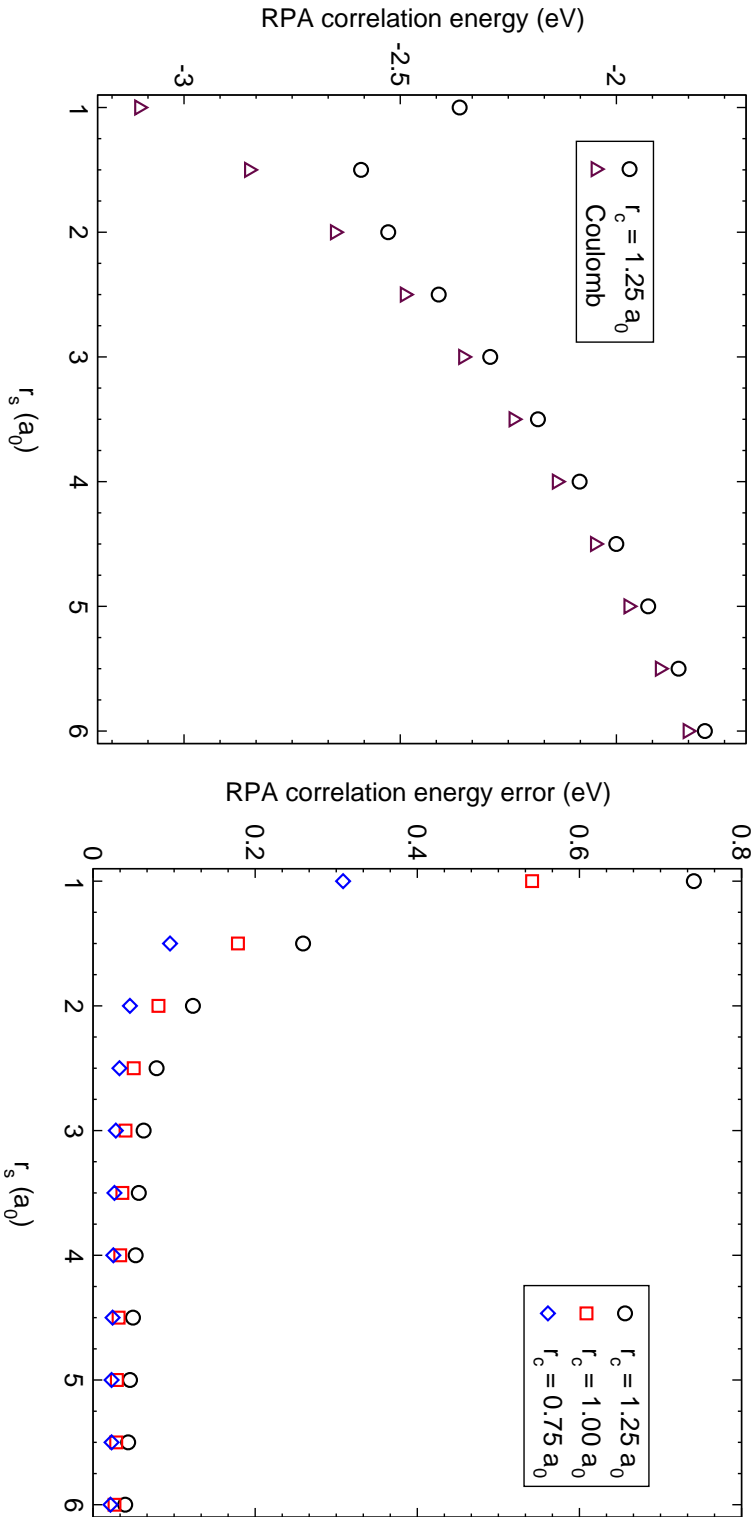


FIGURE 5.6: Depicted are RPA correlation energies for different densities (left) and the respective errors $|E_{\text{corr}}^{\text{RPA,ps}} - E_{\text{corr}}^{\text{RPA}}|$ (right). The “outliers” at $r_s = 1 a_0$ are caused by the fact that the reference energies are not optimal (they were chosen such that the HF energies at $r_s \approx 1.36 a_0$ are reproduced best, see figure 5.2). The basis set size error for the extrapolated RPA correlation energies was approx. 0.01 eV. The same parameters as in figure 5.4 were used.

Chapter 6

Summary and conclusion

We have constructed norm conserving pseudo-potentials for the electron-electron interaction using the revised RRKJ method. The construction is straightforward and reliable for all relevant cutoff radii and reference energies. Furthermore, we have shown that the local approximation is very good, which substantially simplifies the Fourier representation. On the negative side, the discontinuous first derivatives of the pseudo-potentials cause high frequency oscillations. For the construction of the pseudo-potentials, two parameters have to be set: (i) the cutoff radius r_c that determines the accuracy and hardness of the pseudo-potentials and (ii) the reference energy E_{ref} at which the pseudization is performed. We have found that the following rule is a good basis for the optimization of E_{ref} : For a given value of r_c , E_{ref} is chosen such that the innermost node of the radial wave function is located slightly outside the core region.

We have developed pseudized MP2 and ACFDT-RPA theories for Jellium and implemented them in VASP. To obtain MP2 energies, it is sufficient to replace the form factors in the exchange and the MP2 terms. For ACFDT-RPA calculations, we have replaced only the correlation term at the cost of an additional approximation. Future work is required to evaluate the quality of this approximation for other materials. In both cases, we have found that the convergence w.r.t the cutoff energy $E_{\text{max}}^{\text{aux}}$ is much faster than for the bare Coulomb potential. Furthermore, the effect of the high frequency oscillations is small and can be mostly neglected.

The pseudo-potentials reproduce well the scattering properties of the Coulomb potential, which we have demonstrated by comparing the logarithmic derivatives and band structures for a periodic lattice of positive ions. However, the relative errors in the correlation energies are large for intermediate cutoff radii $r_c \lesssim r_s$. For smaller cutoff radii the errors diminish, but so does the gain in convergence speed. This is certainly disappointing, but possibly it is feasible to better handle correlation effects by treating the residual errors via a local density approximation. Finally, future work would investigate pseudized theories for ferro-magnetic systems ($\sum_{\text{spin}} = 1$). Since the errors are due to the fact that electrons of opposite spin can be located at the same place, we expect that the pseudo-potentials will perform better there.

Appendix A

Spherical Bessel functions

The radial Schrödinger equation for a free particle of mass μ is

$$r^2 \frac{d^2 R_l(r)}{dr^2} + 2r \frac{dR_l(r)}{dr} + [q^2 r^2 - l(l+1)] R_l(r) = 0, \quad (\text{A.1})$$

$$q = \sqrt{2\mu E}.$$

compare equation (2.36). The substitutions $R_l(r) = Z_l(r)/r^{-1/2}$ and $x = qr$ yield

$$x^2 \frac{d^2 Z_l(x)}{dx^2} + x \frac{dZ_l(x)}{dx} + \left[x^2 - \left(l + \frac{1}{2} \right)^2 \right] Z_l(x) = 0, \quad (\text{A.2})$$

which is the Bessel equation of order $l + \frac{1}{2}$, whose general solution is a linear combination of Bessel functions J and Neumann functions Y , hence [18, pp. 426-427]

$$R_l(x) = \frac{A}{\sqrt{x}} J_{l+1/2}(x) + \frac{B}{\sqrt{x}} Y_{l+1/2}(x). \quad (\text{A.3})$$

It is useful to include an additional normalization factor to define the spherical Bessel functions j_l and spherical Neumann functions n_l

$$j_l(x) := \sqrt{\frac{\pi}{2x}} J_{l+1/2}(x) \quad (\text{A.4})$$

$$n_l(x) := \sqrt{\frac{\pi}{2x}} Y_{l+1/2}(x)$$

Through the Rayleigh formulas [18, section 14.7]

$$j_l(x) = (-1)^l x^l \left[\frac{1}{x} \frac{d}{dx} \right]^l \left(\frac{\sin(x)}{x} \right) \quad (\text{A.5})$$

$$n_l(x) = -(-1)^l x^l \left[\frac{1}{x} \frac{d}{dx} \right]^l \left(\frac{\cos(x)}{x} \right),$$

we obtain explicit expressions for the first few j_l and n_l

$$\begin{aligned}
j_0(x) &= \frac{\sin(x)}{x} \\
j_1(x) &= \frac{\sin(x)}{x^2} - \frac{\cos(x)}{x} \\
j_2(x) &= \left(\frac{3}{x^2} - \frac{1}{x}\right) \sin(x) - \frac{3}{x^2} \cos(x) \\
n_0(x) &= -\frac{\cos(x)}{x} \\
n_1(x) &= -\frac{\cos(x)}{x^2} - \frac{\sin(x)}{x} \\
n_2(x) &= -\left(\frac{3}{x^2} - \frac{1}{x}\right) \cos(x) - \frac{2}{x^2} \sin(x).
\end{aligned} \tag{A.6}$$

For higher l they can also be constructed via a recurrence relation

$$f_{l-1}(x) + f_{l+1}(x) = \frac{2l+1}{x} f_l(x), \tag{A.7}$$

where f_l is either a spherical Bessel function or a spherical Neumann function. Another recurrence relations allows us to evaluate their first derivatives

$$l f_{l-1}(x) + (l+1) f_{l+1}(x) = (2l+1) f'_l(x), \tag{A.8}$$

and higher derivatives by differentiation on both sides [18, section 14.7]. At the origin, the j_l are finite whereas the n_l are singular

$$\begin{aligned}
j_l(x) &\xrightarrow{x \rightarrow 0} \frac{x^l}{(2l+1)!!} \\
n_l(x) &\xrightarrow{x \rightarrow 0} -\frac{(2l-1)!!}{x^{l+1}},
\end{aligned} \tag{A.9}$$

compare equation (4.13). The asymptotic behavior for large x is

$$\begin{aligned}
j_l(x) &\xrightarrow{x \rightarrow \infty} \frac{1}{x} \sin\left(x - \frac{l\pi}{2}\right) \\
n_l(x) &\xrightarrow{x \rightarrow \infty} -\frac{1}{x} \cos\left(x - \frac{l\pi}{2}\right).
\end{aligned} \tag{A.10}$$

A.1 Spherical Bessel transform

The j_l fulfill the following orthogonality relations over a finite interval $[0, r_c]$

$$\begin{aligned}
A(q, q') &= \int_0^{r_c} dr r^2 j_l(qr) j_l(q'r) \\
&= \frac{r_c^2}{q^2 - q'^2} \left(j_l(qr_c) \frac{d}{dr} j_l(q'r) - j_l(q'r) \frac{d}{dr} j_l(qr_c) \right),
\end{aligned} \tag{A.11}$$

which follows from the corresponding property of the J_l [18, p. 661]. The (pseudo) wave function can be expressed as a series of spherical Bessel functions with the correct boundary conditions

$$\begin{aligned} \phi_l(r) &= \sum_i \phi_{li} j_l(q_i r) r \quad \text{for } r \leq r_c \\ \left. \frac{d}{dr} (\ln j_l(q_i r) r) \right|_{r=r_c} &= x_l(r_c), \end{aligned} \quad (\text{A.12})$$

where the coefficients are given by

$$\phi_{li} = \int_0^{r_c} dr \phi_l(r) j_l(q_i r) r / A(q_i, q_i). \quad (\text{A.13})$$

Hence, the kinetic energy can be evaluated as

$$E_l^{\text{kin}} = \int_0^{r_c} dr \phi_l(r) \left[-\frac{1}{2} \frac{d^2}{dr^2} + \frac{l(l+1)}{2r^2} \right] \phi_l(r) = \sum_i \phi_{li}^2 q_i^2 A(q_i, q_i), \quad (\text{A.14})$$

where we have used equation (A.1). In the limit $r_c \rightarrow \infty$ we obtain the orthonormality relations [4]

$$qq' \frac{2}{\pi} \int_0^\infty dr j_l(qr) j_l(q'r) r^2 = \delta(q - q'), \quad (\text{A.15})$$

and the series (A.12) becomes an integral transform

$$\bar{\phi}_l(q) = \sqrt{\frac{2}{\pi}} \int_0^\infty dr \phi_l(r) j_l(qr) qr. \quad (\text{A.16})$$

From equation (A.15) we can obtain that the Bessel transform is involutory

$$\phi_l(r) = \sqrt{\frac{2}{\pi}} \int_0^\infty dq \bar{\phi}_l(q) j_l(qr) qr, \quad (\text{A.17})$$

as well as norm conserving

$$\int_0^\infty dr r^2 \phi_l(r)^2 = \int_0^\infty dq q^2 \bar{\phi}_l(q)^2 = 1. \quad (\text{A.18})$$

Analog to equation (A.13), the corresponding expression for the kinetic energy is

$$E_l^{\text{kin}} = \int_0^\infty dr \phi_l(r) \left[-\frac{1}{2} \frac{d^2}{dr^2} + \frac{l(l+1)}{2r^2} \right] \phi_l(r) = \frac{1}{2} \int_0^\infty dq q^2 \bar{\phi}_l(q)^2. \quad (\text{A.19})$$

Appendix B

Scattering theory

Let us consider an incoming particle of mass μ moving forward in the z -direction that scatters off some potential V , that goes to zero for large r . In this asymptotic limit, the outgoing solution of the Schrödinger equation

$$\left[-\frac{1}{2\mu}\nabla^2 + V(\mathbf{r}) \right] \Psi(\mathbf{r}) = E\Psi(\mathbf{r}) \quad (\text{B.1})$$

generally consists of two parts that describe an incident particle and a radially outgoing scattered particle respectively [34, chapter 18]

$$\Psi(\mathbf{r}) \xrightarrow{r \rightarrow \infty} A[e^{iqz} + r^{-1}f(\theta, \phi)e^{iqr}], \quad q = \sqrt{2\mu E}. \quad (\text{B.2})$$

If V is spherically symmetric, it is possible to obtain an analytic solution for the scattering amplitude $f(\theta, \phi)$ by matching the solution of the radial Schrödinger equation to the asymptotic result (B.2). We will discuss this “method of partial waves” for potentials of finite range and the Coulomb potential following Schiff [34, chapters 19,21], Sakurai and Napolitano [15, chapter 6] and Taylor [39, chapters 11,14].

B.1 Finite range potentials

For the sake of simplicity, we mostly concentrate on the special case of elastic scattering off a real, spherically symmetric, regular, local potential that vanishes for $r \geq r_c$. Square wells and the muffin-tin potentials discussed in section 2.3 are examples of this form. Since the problem is independent of ϕ , we can expand Ψ into Legendre polynomials

$$\Psi(r, \theta) = \sum_l (2l+1)i^l R_l(r) P_l(\cos(\theta)), \quad (\text{B.3})$$

which follows from the general spherical harmonic expansion (2.35) by keeping only the Y_l^0 functions, which do not depend on ϕ [18, section 15.5]

$$Y_l^0 = \sqrt{\frac{2l+1}{4\pi}} P_l(\cos(\theta)). \quad (\text{B.4})$$

Analogously, the plane wave expansion (2.37) reduces to

$$e^{iqz} = \sum_l (2l+1) i^l j_l(qr) P_l(\cos(\theta)), \quad (\text{B.5})$$

compare also equation (4.26). Furthermore, the general solution for $r \geq r_c$ is given by equation (A.3), since the potential vanishes in that region. We rewrite this as

$$R_l(r) = A_l [\cos(\delta_l) j_l(kr) - \sin(\delta_l) n_l(kr)], \quad (\text{B.6})$$

where the δ_l are real as we assume V is real.

To obtain the scattering amplitude $f(\theta)$, we insert the above results in equation (B.1). In the asymptotic limit, we can use the expansions (A.10) yielding

$$\begin{aligned} & \sum_l (2l+1) i^l A_l (qr)^{-1} \sin\left(qr - \frac{l\pi}{2} + \delta_l\right) P_l(\cos(\theta)) \\ &= \sum_l (2l+1) i^l (qr)^{-1} \sin\left(qr - \frac{l\pi}{2}\right) P_l(\cos(\theta)) + r^{-1} f(\theta) e^{iqr}, \end{aligned} \quad (\text{B.7})$$

where we have used the identity

$$\sin(x+y) = \sin(x) \cos(y) + \cos(x) \sin(y). \quad (\text{B.8})$$

We proceed by writing the sines in complex exponential form and comparing the coefficients for the e^{iqr} and e^{-iqr} parts

$$\begin{aligned} e^{iqr} &: \sum_l (2l+1) i^l A_l (qr)^{-1} e^{-i\left(\frac{l\pi}{2} - \delta_l\right)} P_l(\cos(\theta)) \\ &= \sum_l (2l+1) i^l (qr)^{-1} e^{-i\frac{l\pi}{2}} P_l(\cos(\theta)) + 2ir^{-1} f(\theta) \\ e^{-iqr} &: \sum_l (2l+1) i^l A_l (qr)^{-1} e^{i\left(\frac{l\pi}{2} - \delta_l\right)} P_l(\cos(\theta)) \\ &= \sum_l (2l+1) i^l (qr)^{-1} e^{i\frac{l\pi}{2}} P_l(\cos(\theta)). \end{aligned} \quad (\text{B.9})$$

Finally, the second equation yields

$$A_l = e^{i\delta_l}, \quad (\text{B.10})$$

which we insert in the first equation to obtain the scattering amplitude

$$f(\theta) = \frac{1}{2iq} \sum_l (2l+1) \left(e^{2i\delta_l} - 1 \right) P_l(\cos(\theta)). \quad (\text{B.11})$$

The coefficients of f in the Legendre expansion are called “partial wave amplitudes”

$$\begin{aligned} f(\theta) &=: \sum_l (2l+1) f_l(\delta_l) P_l(\cos(\theta)) \\ f_l(\delta_l) &= \frac{1}{2iq} \left(e^{2i\delta_l} - 1 \right) = \frac{e^{i\delta_l} \sin(\delta_l)}{q}. \end{aligned} \quad (\text{B.12})$$

B.1.1 Phase shifts

We find that f is completely determined by the phase shifts δ_l , which constitute the phase difference between the R_l and the j_l in the asymptotic limit. There is a modulo π ambiguity in the definition of the δ_l , as f is invariant under

$$\delta_l \rightarrow \delta_l + n_l \pi, \quad n_l \text{ integer.} \quad (\text{B.13})$$

This ambiguity is usually removed by requiring that the phase shifts are a continuous function of q that goes to zero as $q \rightarrow \infty$. When we adopt this convention, the following heuristical argument holds true [see 39, chapter 11]: The δ_l will be negative for a repulsive potential, as the wave function is “pushed out” by V , whereas an attractive potential will “pull in” the wave function, resulting in positive δ_l .

To obtain an explicit expression for the δ_l , we match the core wave function to the free particle solution (B.6) at $r = r_c$. The boundary condition is that the logarithmic derivatives are continuous

$$\begin{aligned} L_l(r_c) &= \frac{q j_l'(qr_c) \cos(\delta_l) - q \sin(\delta_l) n_l'(qr_c)}{\cos(\delta_l) j_l(r_c) - \sin(\delta_l) n_l(r_c)} \\ \Rightarrow \tan(\delta_l) &= \frac{q j_l'(qr_c) - L_l(r_c) j_l(qr_c)}{q n_l'(qr_c) - L_l(r_c) n_l(qr_c)}. \end{aligned} \quad (\text{B.14})$$

We can distinguish three distinct limiting cases: (i) the R_l will approach the j_l as $V \rightarrow 0$, thus f and the δ_l (with our convention not just $\delta_l \bmod \pi$) vanish. (ii) the same argument can be applied in the high energy limit. (iii) for high values of l (with V and E fixed), the centrifugal wall will dominate the effective potential

$$V_{\text{eff}}(r) = V(r) + \frac{l(l+1)}{2\mu r^2} \quad (\text{B.15})$$

inside the core region, which effectively blocks the particle from “seeing” the potential. Thus, the δ_l approach $n_l \pi$ in the limit

$$\frac{q^2}{2\mu} \ll \frac{l(l+1)}{2\mu r_c^2} \approx \frac{l^2}{2\mu r_c^2} \Rightarrow l \gg qr_c, \quad (\text{B.16})$$

similar to the classical case, where the distance of closest approach is given by the impact parameter $b = l/q$.

B.1.2 Born approximation

We can generically obtain general solutions to the Schrödinger equation using the Green's function method

$$\begin{aligned}\Psi(\mathbf{r}) &= \Psi_0(\mathbf{r}) + 2\mu \int d\mathbf{r}' G(\mathbf{r} - \mathbf{r}') V(r') \Psi(\mathbf{r}') \\ [\nabla^2 + q^2]G(\mathbf{r}) &= \delta^3(\mathbf{r}),\end{aligned}\tag{B.17}$$

where Ψ_0 is a homogeneous solution of the Schrödinger equation and G is a Green's function with appropriate boundary conditions. Since we are interested in outgoing solutions of the type (B.2), we use

$$\Psi_0(\mathbf{r}) = e^{iqz}, \quad G(\mathbf{r} - \mathbf{r}') = -\frac{e^{iq|\mathbf{r}-\mathbf{r}'|}}{4\pi|\mathbf{r} - \mathbf{r}'|},\tag{B.18}$$

which yields the Lippmann-Schwinger equation

$$\begin{aligned}\Psi(\mathbf{r}) &= e^{iqz} - \frac{\mu}{2\pi} \int d\mathbf{r}' \frac{e^{iq|\mathbf{r}-\mathbf{r}'|}}{|\mathbf{r} - \mathbf{r}'|} V(r') \Psi(\mathbf{r}') \\ &\xrightarrow{r \rightarrow \infty} e^{iqz} - \frac{\mu}{2\pi} \frac{e^{iqr}}{r} \int d\mathbf{r}' e^{-i\mathbf{q}\cdot\mathbf{r}'} V(r') \Psi(\mathbf{r}'),\end{aligned}\tag{B.19}$$

where we have used

$$|\mathbf{r} - \mathbf{r}'| = r \left(1 - \frac{2\hat{\mathbf{r}} \cdot \mathbf{r}'}{r} + \frac{r'^2}{r^2} \right)^{1/2} \xrightarrow{r \rightarrow \infty} r - \hat{\mathbf{r}} \cdot \mathbf{r}',\tag{B.20}$$

and introduced $\mathbf{q} = q\hat{\mathbf{r}}$. By comparing this result with equation (B.2), we obtain a general expression for the scattering amplitude

$$f(\theta) = -\frac{\mu}{2\pi} \int d\mathbf{r}' e^{-i\mathbf{q}\cdot\mathbf{r}'} V(r') \Psi(\mathbf{r}').\tag{B.21}$$

If we assume that the potential is a weak scatterer, it will not alter the wave function significantly. We can therefore approximate the scattering amplitude by

$$f(\theta) \approx -\frac{\mu}{2\pi} \int d\mathbf{r}' e^{-i\mathbf{q}\cdot\mathbf{r}'} V(r') e^{i\mathbf{q}'\cdot\mathbf{r}'},\tag{B.22}$$

where $\mathbf{q}' = q\hat{\mathbf{z}}$. We find that in this (first order) Born approximation, the scattering amplitude is proportional to the Fourier representation of V . By expanding the plane waves in spherical harmonics and using that $|\mathbf{q}| = |\mathbf{q}'|$ as well as the fact that θ is the angle between \mathbf{q} and \mathbf{q}' , we obtain

$$\begin{aligned}
f(\theta) &= -2\mu \sum_l (2l+1) P_l(\cos(\theta)) \int dr r^2 V(r) j_l(qr)^2 \\
&\Rightarrow f_l(\theta) = -2\mu \int_0^\infty dr r^2 V(r) j_l(qr)^2,
\end{aligned} \tag{B.23}$$

compare equations (4.25) and (4.27). We find that the f_l are real within the Born approximation. By comparing this with the general result (B.12), we obtain that the Born approximation is valid, if the $\delta_l \bmod \pi$ are small and the f_l thus close to the real axis. Hence, we can use the Born approximation in the limiting cases (i)-(iii) that we discussed earlier. In particular, we can study the low energy limit of the f_l in the Born approximation

$$f_l(q) \xrightarrow{q \rightarrow 0} -a_l q^{2l}, \tag{B.24}$$

where we have used equation (A.9) to expand the j_l . The constants a_l are called “scattering lengths”. We find, that the f_l rapidly vanish for high values of l , and for very small energies, only the $l = 0$ wave contributes to the scattering amplitude

$$f(q) = \sum_l (2l+1) f_l(q) P_l(\cos(\theta)) \xrightarrow{q \rightarrow 0} -a_0. \tag{B.25}$$

By inserting the above expansion for f_l in equation (B.12), we obtain the low energy limit for the phase shifts

$$\begin{aligned}
\sin(\delta_l) &\xrightarrow{q \rightarrow 0} -a_l q^{2l+1} \\
\delta_l(q) &\xrightarrow{q \rightarrow 0} n_l \pi - a_l q^{2l+1}.
\end{aligned} \tag{B.26}$$

Levinson’s theorem [see 39, chapter 12] states that the n_l equal the number of bound states. It is possible that an attractive potential has a zero energy resonance for $l = 0$, which relates to a divergence of a_0 . In this case, the above result needs to be modified to

$$\delta_0(0) = (n_0 + \frac{1}{2})\pi. \tag{B.27}$$

We can interpret a_0 as the r -intercept of the exterior wave function if we extend it to smaller values of r

$$\begin{aligned}
\lim_{q \rightarrow 0} \phi_0(qr) &= \lim_{q \rightarrow 0} A_0 q^{-1} \sin(qr + \delta_0) = A_0(r - a_0) \\
-\frac{1}{2\mu} \frac{d^2}{dr^2} \phi_0(r) &= 0.
\end{aligned} \tag{B.28}$$

We obtain from equation (B.26) that a_0 is always positive for attractive potentials. For an attractive potential, the wave function is “pulled in” more and more as the potential strength increases until it develops a bound state, i.e. the wave function develops a node. The scattering length is therefore

small and negative for weak attractive potentials, becomes more negative as V increases in strength until it diverges (resonance) and gets finally positive (bound state).

B.1.3 Scattering approach to pseudo-potentials

In section 2.5, we demanded that the pseudo-potential has the same logarithmic derivatives as the original potential at $r = r_c$ for some reference energy. Since the logarithmic derivatives are related to the phase shifts via equation (B.14), we can replace this requirement by demanding instead that V^{ps} has the same phase shifts modulo π as V

$$\delta_l^{\text{ps}}(r_c) \bmod \pi = \delta_l(r_c) \bmod \pi. \quad (\text{B.29})$$

In particular, we can choose pseudo-potentials with $|\delta_l^{\text{ps}}(r_c)| \leq \pi$, hence pseudo-potentials that don't have bound states. This is exactly the approach of the OPW-method as discussed in section 2.4.

B.2 Coulomb potential

The Coulomb potential differs from the potentials discussed above as its range is infinite. Thus, the solution of the radial Schrödinger equation

$$\left[\frac{d^2}{dr^2} + \frac{l(l+1)}{r^2} - \frac{2\mu Z_1 Z_2}{r} + q^2 \right] \phi_l(r) = 0 \quad (\text{B.30})$$

never reaches the free particle limit. Rather, it can be expressed by a linear combination of regular and irregular solutions of the confluent hypergeometric equation [see 18, section 18.6], which we denote as F_l and G_l respectively. These functions have the asymptotic form [see 39, p. 267]

$$\begin{aligned} F_l(qr) &\xrightarrow{r \rightarrow \infty} \sin \left(qr - \gamma \ln(2pr) - \frac{l\pi}{2} + \sigma_l \right) \\ G_l(qr) &\xrightarrow{r \rightarrow \infty} -\cos \left(qr - \gamma \ln(2qr) - \frac{l\pi}{2} + \sigma_l \right) \\ \gamma &= \frac{\mu Z_1 Z_2}{q}, \quad \sigma_l = \arg(\Gamma(l+1+i\gamma)), \end{aligned} \quad (\text{B.31})$$

where γ is a strength parameter and σ_l is called ‘‘Coulomb phase shift’’.

Let us consider distorted Coulomb potentials that differ from the pure Coulomb potential only for $r \leq r_c$, e.g. our pseudo-potentials for the electron-electron interaction. Analog to equation (B.6), we write the distorted wave function for $r \geq r_c$ as

$$\phi_l(r) = A_l [\cos(\nu_l) F_l(qr) - \sin(\nu_l) G_l(qr)], \quad (\text{B.32})$$

where the ν_l are the additional phase shifts introduced by V^{ps} , as we can see by comparing the asymptotic expansions of the ϕ_l and the F_l

$$\phi_l(r) \xrightarrow{r \rightarrow \infty} A_l \sin \left(qr - \gamma \ln(2pr) - \frac{l\pi}{2} + \sigma_l + \nu_l \right). \quad (\text{B.33})$$

To calculate the ν_l , we match the distorted wave function to the pure Coulomb wave function. The boundary condition is once again that the logarithmic derivatives agree at $r = r_c$

$$\begin{aligned} x_l(r_c) &= \frac{qF'_l(qr_c) \cos(\nu_l) - q \sin(\nu_l)G'_l(qr_c)}{\cos(\nu_l)F_l(r_c) - \sin(\delta_l)G_l(r_c)} \\ \Rightarrow \tan(\nu_l) &= \frac{qF'_l(qr_c) - x_l(r_c)F_l(qr_c)}{qG'_l(qr_c) - x_l(r_c)G_l(qr_c)}. \end{aligned} \quad (\text{B.34})$$

Just as in the finite range case, the ν_l are negligible for $l \gg qr_c$.

Appendix C

Hartree-Fock approximation

This appendix serves as complementary material to our discussion of the HF approximation (chapter 3). We will state the Slater-Condon rules and derive the HF equations closely following Szabo and Ostlund [27].

C.1 Slater-Condon rules

The Slater-Condon rules allow us to evaluate matrix elements of the type $\langle K | \mathcal{O} | L \rangle$, where $|K\rangle$ is a reference determinant (e.g. the HF ground state) that occupies the spin orbitals χ_m, χ_n, \dots and $|L\rangle$ is a determinant built from the same set of spin orbitals

$$\begin{aligned} |K\rangle &= \frac{1}{\sqrt{N!}} \sum_{\sigma} (-1)^{\sigma} \chi_m(x_{\sigma(1)}) \chi_n(x_{\sigma(2)}) \dots \chi_k(x_{\sigma(N)}) \\ |L\rangle &= \frac{1}{\sqrt{N!}} \sum_{\sigma'} (-1)^{\sigma'} \chi_{m'}(x_{\sigma'(1)}) \chi_{n'}(x_{\sigma'(2)}) \dots \chi_{k'}(x_{\sigma'(N)}). \end{aligned} \quad (\text{C.1})$$

We assume that the determinants are in maximum coincidence (i.e. we have exchanged the columns of $|L\rangle$, such that it differs from $|K\rangle$ by the minimal amount). We need to distinguish between one and two particle operators \mathcal{O} and cases where $|L\rangle$ that differ from $|K\rangle$ by 0,1,2... spin orbitals, i.e.

$$\begin{aligned} \text{case 1: } \{m', n', \dots, k'\} &= \{m, n, \dots, k\} \\ \text{case 2: } \{m', n', \dots, k'\} &= \{p, n, \dots, k\} \\ \text{case 3: } \{m', n', \dots, k'\} &= \{p, q, \dots, k\}. \end{aligned} \quad (\text{C.2})$$

The derivations are straightforward, but rather lengthy, so we shall only quote the results. The matrix elements for the one particle operators are non-vanishing only for $|L\rangle$, that differ by maximally one spin orbital from $|K\rangle$

$$\begin{aligned}
\text{case 1: } \langle K | \sum_{i=1}^N h(x_i) | K \rangle &= \sum_m^{\text{occ}} \langle \chi_m | h | \chi_m \rangle \\
\text{case 2: } \langle K | \sum_{i=1}^N h(x_i) | L \rangle &= \langle \chi_m | h | \chi_p \rangle \\
\text{else: } \langle K | \sum_{i=1}^N h(x_i) | L \rangle &= 0,
\end{aligned} \tag{C.3}$$

where \sum^{occ} indicates summation over all orbitals occupied in $|K\rangle$. In the same way, only $|L\rangle$ that differ by maximally two spin orbitals are relevant for the two-particle operators

$$\begin{aligned}
\text{case 1: } \langle K | \sum_{i<j}^N \frac{1}{|\mathbf{r}_i - \mathbf{r}_j|} | K \rangle &= \frac{1}{2} \sum_{mn}^{\text{occ}} \langle mn || mn \rangle \\
\text{case 2: } \langle K | \sum_{i<j}^N \frac{1}{|\mathbf{r}_i - \mathbf{r}_j|} | L \rangle &= \sum_n^{\text{occ}} \langle mn || pn \rangle \\
\text{case 3: } \langle K | \sum_{i<j}^N \frac{1}{|\mathbf{r}_i - \mathbf{r}_j|} | L \rangle &= \langle mn || pq \rangle \\
\text{else: } \langle K | \sum_{i<j}^N \frac{1}{|\mathbf{r}_i - \mathbf{r}_j|} | L \rangle &= 0.
\end{aligned} \tag{C.4}$$

C.2 Derivation of the Hartree-Fock equations

By setting $|K\rangle = |\Psi_0\rangle$, we can apply the Slater-Condon rules to obtain the HF ground state energy

$$E_{\text{HF}} = \sum_a^{\text{occ}} \langle a | h | a \rangle + \frac{1}{2} \sum_{ab}^{\text{occ}} \langle ab || ab \rangle. \tag{C.5}$$

To find the optimal χ_a , we use functional variation to minimize $E_{\text{HF}}[\chi_a]$

$$\begin{aligned}
\mathcal{L}[\chi_a] &= E_{\text{HF}}[\chi_a] - \sum_{ab}^N [\varepsilon_{ba} \langle \chi_a | \chi_b \rangle - \delta_{ab}] \\
\delta \mathcal{L} &= \mathcal{L}[\chi_a + \delta \chi_a] - \mathcal{L}[\chi_a] = 0,
\end{aligned} \tag{C.6}$$

where we have imposed the orthonormality of the χ_a with the help of Lagrange multipliers ε_{ba} . The matrix ε is Hermitian, since \mathcal{L} has to be real

$$\begin{aligned}
\mathcal{L}^*[\chi_a] &= E_{\text{HF}}[\chi_a] - \sum_{ab}^N \varepsilon_{ba}^* [\langle \chi_b | \chi_a \rangle - \delta_{ba}] \stackrel{!}{=} \mathcal{L}[\chi_a] \\
\Rightarrow \varepsilon_{ba}^* &= \varepsilon_{ab}.
\end{aligned} \tag{C.7}$$

In the evaluation of $\delta\mathcal{L}$, we keep only the first order terms

$$\begin{aligned}\delta\mathcal{L} &= \delta E_{\text{HF}} - \sum_{ab}^N \varepsilon_{ba} [\langle \delta\chi_a | \chi_b \rangle + \langle \chi_a | \delta\chi_b \rangle] \\ \delta E_{\text{HF}} &= \sum_a^N \langle \delta a | h | a \rangle + \langle a | h | \delta a \rangle \\ &\quad + \frac{1}{2} \sum_{ab}^N \langle \delta ab || ab \rangle + \langle a\delta b || ab \rangle + \langle ab || \delta ab \rangle + \langle ab || a\delta b \rangle.\end{aligned}\tag{C.8}$$

By using the identity (3.9) as well as the symmetries of the double sums, we can simplify the expression for $\delta\mathcal{L}$ to

$$\delta\mathcal{L} = \sum_a^N \langle \delta a | h | a \rangle + \sum_{ab}^N \langle \delta ab || ab \rangle - \sum_{ab}^N \varepsilon_{ba} \langle \delta\chi_a | \chi_b \rangle + \text{c.c.},\tag{C.9}$$

which we can rewrite using the definitions of the Coulomb and exchange operators (equation (3.13)) to obtain

$$\begin{aligned}\delta\mathcal{L} &= \sum_a^N \frac{1}{\Omega} \int d\mathbf{x}_1 \delta\chi_a^*(\mathbf{x}_1) \left\{ h(x_1) + \sum_b^N [J_b - K_b] \chi_a(\mathbf{x}_1) \right. \\ &\quad \left. - \sum_b^N \varepsilon_{ba} \chi_b(\mathbf{x}_1) \right\} + \text{c.c.},\end{aligned}\tag{C.10}$$

which implies that the spin orbitals have to fulfill the generalized eigenvalue problem

$$f |\chi_a\rangle = \sum_b^N \varepsilon_{ba} |\chi_b\rangle,\tag{C.11}$$

since the variation $\delta\chi_a$ is arbitrary. To obtain the canonical HF equations, we use the fact, that the χ_a are only uniquely determined up to a unitary transformation U

$$\begin{aligned}\chi'_a &= \sum_b^N \chi_b U_{ba} \\ U_{ab}^* &= U_{ba}^{-1},\end{aligned}\tag{C.12}$$

since the HF energy is invariant under such a transformation. This follows immediately from the fact, that the transformed determinant changes only by a phase factor

$$\begin{aligned}
\Psi'_0(\mathbf{x}_1, \dots, \mathbf{x}_N) &= \frac{1}{\sqrt{N!}} \sum_{\sigma} (-1)^{\sigma} \sum_b U_{b1} \chi_b(\mathbf{x}_{\sigma(1)}) \dots \sum_c U_{cN} \chi_c(\mathbf{x}_{\sigma(N)}) \\
&= \sum_{b\dots c} U_{b1} \dots U_{cN} \frac{1}{\sqrt{N!}} \sum_{\sigma} (-1)^{\sigma} \chi_b(\mathbf{x}_{\sigma(1)}) \dots \chi_c(\mathbf{x}_{\sigma(N)}) \quad (\text{C.13}) \\
&= \left[\sum_{\sigma} (-1)^{\sigma} U_{\sigma(1)1} \dots U_{\sigma(N)N} \right] \Psi_0(\mathbf{x}_1, \dots, \mathbf{x}_N) \\
&= \det(U) \Psi_0(\mathbf{x}_1, \dots, \mathbf{x}_N),
\end{aligned}$$

yielding

$$E'_{\text{HF}} = \langle \Psi'_0 | H_{\text{MB}} | \Psi'_0 \rangle = \langle \Psi_0 | e^{-i\phi} H_{\text{MB}} e^{i\phi} | \Psi_0 \rangle = E_{\text{HF}}. \quad (\text{C.14})$$

Since the Fock operator is invariant under the transformation (see equation (3.13)), the transformed HF equations read

$$f |\chi'_a\rangle = \sum_b \varepsilon'_{ba} |\chi'_b\rangle. \quad (\text{C.15})$$

We obtain the transformation behavior of the Lagrange multipliers writing them as elements of the Fock matrix

$$\langle \chi_c | f | \chi_a \rangle = \sum_b \varepsilon_{ba} \langle \chi_c | \chi_b \rangle = \varepsilon_{ca}, \quad (\text{C.16})$$

which yields in combination with equations (C.15) and (C.12)

$$\begin{aligned}
\varepsilon'_{ab} &= \langle \chi'_a | f | \chi'_b \rangle = \sum_{cd} U_{ac}^* U_{db} \langle \chi_c | f | \chi_d \rangle \\
&\Rightarrow \varepsilon' = U^\dagger \varepsilon U.
\end{aligned} \quad (\text{C.17})$$

Since ε is Hermitian, we can always find a U that diagonalizes it, hence we finally obtain the canonical HF equations by dropping the primes

$$f |\chi_a\rangle = \sum_b \varepsilon_b \delta_{ba} |\chi_b\rangle = \varepsilon_a |\chi_a\rangle. \quad (\text{C.18})$$

C.3 Brillouin's theorem

Brillouin's theorem states, that the HF ground state does not interact with singly excited determinants

$$\langle \Psi_0 | H_{\text{MB}} | \Psi_a^r \rangle = 0. \quad (\text{C.19})$$

On the one hand, we can evaluate the matrix element directly via the Slater-Condon rules

$$\langle \Psi_0 | H_{\text{MB}} | \Psi_a^r \rangle = \langle a | h | r \rangle + \sum_b^{\text{occ}} \langle ab || rb \rangle. \quad (\text{C.20})$$

On the other hand, we get the same expression as

$$\langle \chi_a | f | \chi_r \rangle = \langle a | h | r \rangle + \sum_b \langle ab || rb \rangle. \quad (\text{C.21})$$

Since the non-diagonal Fock matrix elements vanish

$$\langle \chi_i | f | \chi_j \rangle = \varepsilon_j \langle \chi_i | \chi_j \rangle = \delta_{ij} \varepsilon_j, \quad (\text{C.22})$$

and $a \neq r$ per definition, we obtain equation (C.19).

Bibliography

- [1] D. Prendergast, M. Nolan, C. Filippi, S. Fahy, and J. C. Greer, "Impact of electron–electron cusp on configuration interaction energies", *The Journal of Chemical Physics*, vol. 115, no. 4, pp. 1626–1634, 2001.
- [2] J. H. Lloyd-Williams, R. J. Needs, and G. J. Conduit, "Pseudopotential for the electron-electron interaction", *Phys. Rev. B*, vol. 92, no. 7, 2015.
- [3] A. M. Rappe, K. M. Rabe, E. Kaxiras, and J. D. Joannopoulos, "Optimized pseudopotentials", *Phys. Rev. B*, vol. 41, no. 2, pp. 1227–1230, 1990.
- [4] G. Kresse, "Ab initio molekular dynamik für flüssige metalle", PhD thesis, Technische Universität Wien, 1993.
- [5] J. C. Phillips and L. Kleinman, "New method for calculating wave functions in crystals and molecules", *Phys. Rev.*, vol. 116, pp. 287–294, 2 1959.
- [6] E. Antončík, "Approximate formulation of the orthogonalized plane-wave method", *Journal of Physics and Chemistry of Solids*, vol. 10, no. 4, pp. 314–320, 1959.
- [7] F. Bloch, "Über die quantenmechanik der elektronen in kristallgittern", *Zeitschrift für Physik*, vol. 52, no. 7-8, pp. 555–600, 1929.
- [8] N. W. Ashcroft and D. N. Mermin, *Festkörperphysik*, 4th ed. Gruyter, de Oldenbourg, 2013, 1080 pp.
- [9] J. M. Ziman, *Principles of the theory of solids*, 2nd ed. Cambridge University Press (CUP), 1972.
- [10] V. Heine and D. Weaire, "Pseudopotential theory of cohesion and structure", in *Solid State Physics*, vol. 24, Elsevier BV, 1970, pp. 249–463.
- [11] V. Heine, "The pseudopotential concept", in *Solid State Physics*, vol. 24, Elsevier BV, 1970, pp. 1–36.
- [12] J. C. Slater, "Wave functions in a periodic potential", *Physical Review*, vol. 51, no. 10, pp. 846–851, 1937.
- [13] C. Herring, "A new method for calculating wave functions in crystals", *Physical Review*, vol. 57, no. 12, pp. 1169–1177, 1940.
- [14] R. M. Martin, *Electronic structure*. Cambridge University Press (CUP), 2004.
- [15] J. J. Sakurai and J. J. Napolitano, *Modern quantum mechanics*, 2nd ed. PEARSON, 2010, 528 pp.
- [16] T. Loucks, *Augmented plane wave method: A guide to performing electronic structure calculations*, ser. Frontiers in Physics: Lecture note and reprint series, A. Benjamin, 1967.
- [17] J. Thijssen, *Computational physics*. Cambridge University Press, 2007, 638 pp.
- [18] G. B. Arfken and H. J. Weber, *Mathematical methods for physicists*. Elsevier LTD, Oxford, 2012, 1205 pp.

- [19] M. L. Cohen and V. Heine, "The fitting of pseudopotentials to experimental data and their subsequent application", in *Solid State Physics*, vol. 24, Elsevier BV, 1970, pp. 37–248.
- [20] D. R. Hamann, "Generalized norm-conserving pseudopotentials", *Phys. Rev. B*, vol. 40, no. 5, pp. 2980–2987, 1989.
- [21] W. C. Topp and J. J. Hopfield, "Chemically motivated pseudopotential for sodium", *Phys. Rev. B*, vol. 7, no. 4, pp. 1295–1303, 1973.
- [22] D. R. Hamann, M. Schlüter, and C. Chiang, "Norm conserving pseudopotentials", *Phys. Rev. Lett.*, vol. 43, no. 20, pp. 1494–1497, 1979.
- [23] G. B. Bachelet, D. R. Hamann, and M. Schlüter, "Pseudopotentials that work: From h to pu", *Phys. Rev. B*, vol. 26, no. 8, pp. 4199–4228, 1982.
- [24] G. P. Kerker, "Non-singular atomic pseudopotentials for solid state applications", *Journal of Physics C: Solid State Physics*, vol. 13, no. 9, p. L189, 1980.
- [25] G. Kresse and J. Hafner, "Norm-conserving and ultrasoft pseudopotentials for first-row and transition elements", *Journal of Physics: Condensed Matter*, vol. 6, no. 40, pp. 8245–8257, 1994.
- [26] J. S. Lin, A. Qteish, M. C. Payne, and V. Heine, "Optimized and transferable nonlocal separable *ab initio* pseudopotentials", *Phys. Rev. B*, vol. 47, pp. 4174–4180, 8 1993.
- [27] A. Szabo and N. S. Ostlund, *Modern quantum chemistry*. Dover Publications Inc., 1996, 480 pp.
- [28] S. Suhai, "Quasiparticle energy-band structures in semiconducting polymers: Correlation effects on the band gap in polyacetylene", *Phys. Rev. B*, vol. 27, pp. 3506–3518, 6 1983.
- [29] T. Schäfer, B. Ramberger, and G. Kresse, "Quartic scaling mp2 for solids: A highly parallelized algorithm in the plane wave basis", *The Journal of Chemical Physics*, vol. 146, no. 10, p. 104 101, 2017.
- [30] J. Almlöf, "Elimination of energy denominators in möller—plesset perturbation theory by a laplace transform approach", *Chemical Physics Letters*, vol. 181, no. 4, pp. 319–320, 1991.
- [31] R. Mattuck, *A guide to feynman diagrams in the many-body problem*, 2nd ed., ser. Dover Books on Physics Series. Dover Publications, 1976.
- [32] F. A. Hummel, "Density functional theory applied to liquid metals and the adjacent pairs exchange correction to the random phase approximation", PhD thesis, Universität Wien, 2015.
- [33] J. Harl, "The linear response function in density functional theory: Optical spectra and improved description of the electron correlation", PhD thesis, Universität Wien, 2008.
- [34] L. I. Schiff, *Quantum mechanics*, 3rd ed. McGraw-Hill, 1968.
- [35] J. Ihm, A. Zunger, and M. L. Cohen, "Momentum-space formalism for the total energy of solids", *Journal of Physics C: Solid State Physics*, vol. 12, no. 21, p. 4409, 1979.
- [36] N. Troullier and J. L. Martins, "Efficient pseudopotentials for plane-wave calculations", *Phys. Rev. B*, vol. 43, pp. 1993–2006, 3 1991.
- [37] P. Ziesche and G. Lehmann, *Ergebnisse in der elektronentheorie der metalle - methoden, ideale und gestörte kristalle, messgrößen*. Berlin, Heidelberg: Springer, 1983.
- [38] W. H. Press, S. A. Teukolsky, W. T. Vetterling, and B. P. Flannery, *Numerical recipes in fortran (2nd ed.): The art of scientific computing*. New York, NY, USA: Cambridge University Press, 1992.

- [39] J. R. Taylor, *Scattering theory: Quantum theory on nonrelativistic collisions*. Wiley, 1972.